AN EFFICIENT NUMERICAL MODEL FOR SOLVING THE SINGLE ELECTRON

BAND STRUCTURE IN SI BASED ON THE SELF-CONSISTENT

PSEUDOPOTENTIAL METHOD

AN EFFICIENT NUMERICAL MODEL FOR SOLVING THE SINGLE

ELECTRON BAND STRUCTURE IN SI BASED ON THE SELF-CONSISTENT

PSEUDOPOTENTIAL METHOD

By

MOHAMMAD H SOBHANI, B.Sc.

A Thesis

Submitted to the School of Graduate Studies

in Partial Fulfillment of the Requirements

for the Degree

Master of Applied Science

McMaster University

Master of Applied Science (2008)   McMaster University

(Electrical and computer Engineering)   Hamilton, Ontario

TITLE: An Efficient Numerical Model for Solving the Single

                Electron Band Structure in Si Based on the

                Self-consistent Pseudopotential Method

AUTHOR: Mohammad H Sobhani, B.S. (Shiraz University, 2005)

SUPERVISORS: Professor X. Li

                Professor M. J. Deen

NUMBER OF PAGES: xviii, 203

To my wife, Vista, who completes me with love,

And to my mother, Masoumeh, who raised me with love.

Abstract

The electronic band structure of a semiconductor is an essential property to determine most of its optical characteristics. The complexity of the energy band structure calculations makes analytical calculations impossible. Any calculation leading to electronic band structures has to utilize numerical methods. In this thesis, two solvers were developed to calculate the energy band structure of 1D Kronig-Penney lattice, 3D diamond lattice-structure and silicon lattice.

In this thesis, many of the important methods of calculating the energy band structures were discussed. Through comparisons among different methods, we have determined that Self-Consistent Pseudopotential Method, SCPM, is the most suitable method for calculating the energy band structures when self-sufficiency and accuracy are of special importance. The SCPM is an iterative method which was utilized in this thesis by using efficient numerical methods. Instead of using conventional numerical methods such as Finite Difference Method or Finite Element Method which cause inefficiency, this thesis calculates the energy band structure by utilizing Orthogonal Plane-Wave expansion of the potentials.

The 1D electronic band structure solver was developed as a foundation for the implementation of the 3D electronic band structure solver. It uses a minimal number of Fourier coefficients to calculate the energy band structure of the 1D Lattices without compromising accuracy. The 3D electronic band structure solver development needs multiple changes and modifications to the 1D solver. As the

3D solver is essentially made using the 1D solver platform, it is also efficient and needs a minimal number of Fourier coefficients for accurate results. The 3D solver can be used for either Nearly Free Electron Method, NFEM, or SCPM calculations. The NFEM calculations were done on the diamond lattice structure. The results were shown to be the same as the benchmarks of [28, 80]. The silicon lattice energy band structure was also calculated with the 3D solver using SCPM with LDA. The results were in the same range as the four sets of data gathered from three benchmarks [58, 81, 82], showing good agreement. Based on the two comparisons made for the 3D solver, it was shown that it is a reliable and efficient program to calculate energy band structures of the 3D lattices.

Acknowledgements

First and foremost I shall offer my sincerest gratitude to my supervisor, Professor Li, who has supported me throughout my studies and thesis with his patience and knowledge whilst allowing me the room to work in my own way. I attribute the level of my master of applied science degree to his encouragement and effort. Without him this thesis, too, would not have been completed or written. One simply could not wish for a better or friendlier supervisor.

Professor Deen was extremely patient, advised me all the way, and gave me much of his precious time. I shall thank Professor Kumar and Professor Howlader for taking time to review this thesis. I must also thank the Electrical and computer Department for the scholarships they granted me.

I am especially grateful to the person who put up with a distracted and busy husband, my wife Vista. I am always thankful for her patience and for her passionate caring about me. My life has changed in the best ways by being with her and I want her to know that I am always grateful for that.

My mother and father, Masoumeh and Akbar, are the wonderful people who brought me to this world. I shall be forever indebted to them. They are present in all the important stages of my life. Whatever I am and will be is the result of the love they gave me. My brother, Hossein, always encouraged me to do my best.

My mother-in-law and father-in-law have always shown me their love and helpfulness. Throughout the writing of this thesis they have always given their moral support.

Ms. Cheryl Gies was always there to help me with any document or advice I may have needed. Her extraordinary passion for her job makes her one of the best administrative assistants that a department can have. I will be always thankful of all the things she did for me.

My friend, Mehdi Ranjbaran, has helped me very much in my studies from the time I have come to McMaster University. He has always put up with a distant and distracted friend.

Contents

List of Figures

List of Tables

List of Symbols and Acronyms

Symbols:

$\Psi(\vec{r},t)$ ....Wave Function

$\psi(\vec{r})$ ....Position-Dependant Part of Wave Function

$\Phi(t)$ ....Time-Dependant Part of Wave Function

E ....Energy

$\hbar$ ....Plank's Constant divided by 2π

$V(\vec{r})$ ....Potential Energy

$v(\vec{r})$ ....Potential

$\hat{x}$ ....x Direction Unit Vector

$\hat{y}$ ....y Direction Unit Vector

$\hat{z}$ ....z Direction Unit Vector

$\mathbb{Z}$ ....The Group of Integer Numbers

p ....Momentum

$\vec{k}$ ....Wave Vector

$\vec{r}$ ....Position Vector

E_{kin} ....Kinetic Energy

m_0 ....Mass of Electron

H ....Hamiltonian

ρ ....Charge Density

ε_0 ....Permittivity of Vacuum

V_{ion} ....Ion Potential Energy

$V_{Hartree}$ ....Hartree Potential Energy

V_{xc} ....Exchange and Correlation Potential Energy

V_{sc} ....Self-Consistent correction Potential Energy

r_c ....Cut-off Radius

Acronyms:

1D ....One Dimensional

3D ....Three Dimensional

APW ....Augmented Plane Wave

BCC ....Body-Centered Cubic

CMOS.............................Complementary Metal-Oxide Semiconductor

CPU ....Central Processing Unit

DFT ....Density Functional Theory

EPM ....Empirical Pseudopotential Method

FCC ....Face-Centered Cubic

FDM.............................Finite Difference Method

FEM.............................Finite Element Method

KKR ....Korringa, Kohn and Rostoker

LCAO ....Linear Combination of Atomic Orbitals

LDA ....Local Density Approximation

LMTO ....Linear Muffin-Tin Orbital

NFEM ....Nearly Free Electron Method

NLDA ....Non-Local Density Approximation

OPW ....Orthogonal Plane Wave

RMS ....Root Mean Square

RMSD.............................Root Mean Square Deviation

RMSE.............................Root Mean Square Error

SCPM.............................Self-Consistent Pseudopotential Method

XC ....Exchange and Correlation

Chapter 1: Introduction

1.1 Motivation

Looking at the materials in terms of conductivity, we have insulators, semiconductors, conductors and superconductors. Among these groups, semiconductors are perhaps the group that has attracted the most amount of attention to themselves. The property which causes the difference in insulators, semiconductors and conductors electrical conductivity is the energy gap in their electronic band structure. Electron behavior can be predicted in most conventional cases just by having the electronic band structure of the material being studied [1]. The most important difference in the electronic band structure of semiconductors that makes them perhaps the most important group of materials in terms of conductivity is their energy gaps. The energy gap in semiconductors is less than that of the conventional insulators and more than the energy gap of the conductor materials, which is zero or less than zero in most cases.

The energy band structure of a semiconductor has a very big impact on its behavior and basic characteristics. For instance, the fact that a semiconductor can effectively produce light depends on the alignment of the valence-band maximum and conduction band minimum. If they align, the semiconductor is said to have a direct band-gap and can effectively produce light with a frequency that is directly dependent on the band-gap energy. Semiconductor lasers have been

realized using the direct band gap materials, like the III-V materials [2]. If the valence and conduction band extremes do not align, the semiconductor has an indirect band-gap and cannot effectively produce light. So, to have a very good idea about the characteristics of any semiconductor it is very important to know its energy band structure.

To calculate the energy band structure for any material, one has to solve the Schrödinger equation for the material. Solving the Schrödinger equation directly (analytically) and without any numerical method is very complex and virtually impossible and impractical for a bulk material or any other complicated physical structure. Even for big atoms, the Schrödinger equation is solved numerically rather than analytically. Knowing the fact that it is impractical to solve this equation analytically, we have to look for a good method to simplify the real model that we have for the material and/or use a good numerical method that will ease solving the Schrödinger equation.

There are three major methods of calculating the electronic band structure of different materials: "The Pseudopotential Method", "The Tight-Binding Method", and the "k.p Method" [1]. The latter is only used to find the electronic band structure of materials for a small interval of wave vectors. This method is specially used for direct band-gap semiconductors and cannot be effectively used to calculate the energy band gap for all the materials because it calculates only a small interval of the electronic band structure around $k = 0$ or any other extreme point in the energy band structure, which doesn't give enough

information about the material being discussed in many cases. To calculate the complete electronic band structure of a material, we can either use the tight-binding or pseudopotential method. Based on what kind of information is more important in a given case, one can then decide which technique better suits the situation. To explain the pseudopotential method in a very brief manner, it can be said that pseudopotential method simplifies the real potential of the lattice under calculation and solves the Schrödinger equation using the simplified potential. On the other hand, the tight-binding method generates the crystalline lattice from the single atoms for which the Schrödinger equation is solved and calculates the solution of the material's Schrödinger equation based on the solution of the atoms that make up the lattice.

It should be noted that there is also a fourth method for calculating the band structure of crystalline materials which is called the nearly free electron method. This method however, only provides a whole picture of the energy band structure without any specifics or accuracy but can be useful in many cases. This method will be discussed later in this thesis as well.

As it is known, the world of photonics is an ever-expanding world which had led to many advances in human life. To expand this field even faster, the scientists and engineers are looking for a new material to use that is much cheaper than the exotic III-V and II-VI semiconductors and makes opto-electronics circuits integration much easier. As the CMOS technology is a standard technology that is widely used in making electronic integrated circuitry,

the researchers are now looking to find a new semiconductor material to be used in photonics and opto-electronics that is compatible with the CMOS technology. As a matter of fact, in the recent years, silicon itself has become the target for the researchers for usage in photonics industry. They are looking at changing some physical properties of silicon in order to change its electronic band structure and make it a direct band gap material.

In this research, we are introducing a solver which solves the electronic band structures of bulk materials. As a first step we will introduce a One Dimensional Lattice Electronic Band Structure Solver, which will have specific uses and will be a base to generate the Three Dimensional Lattice Electronic Band Structure Solver.

1.2 Background of Research

Pseudopotential was introduced in 1930's. Perhaps the first time it was used was by Fermi [3], who used it to calculate the energy shift of alkali spectral lines which arise from high energy electrons scattering levels by foreign gas atoms under pressure. Pseudopotential has been used in many different fields to solve many different problems. This method has been one of the most important methods, which has been extensively used in solid state physics to solve many different problems. This method is one of the very important tools that solid state physics has used in its history. Over time, pseudopotential approach has been used in many areas including: electronic structure, optical properties,

photoemission, electron-phonon coupling, and transport properties. The idea behind the theory stays the same in all the applications but the method of creating the pseudopotential varies in most cases [4].

For the pseudopotential method to be used for atoms, molecules, solids (in form of crystalline lattices, etc.), it had to be modified from the form that was used by Fermi. One of the first applications of pseudopotential is the one done by Hellman [5]. The applications of pseudopotential have been practiced by many researchers over the times and pseudopotential has always been improving through the time. There were relatively few publications on pseudopotential method and its applications in the next 25 years after Fermi. Most of the uses were just in atomic physics which Fermi was originally using the method in the field.

Pseudopotential method in the form used in solid state physics has been extensively worked on in the last 40 years. One of the widely used methods is called the empirical pseudopotential in which the pseudopotential was created using the experimental data that the researchers had from the material they were working on. It was shown that because of the Pauli law of exclusion, the valence electrons are strongly repulsed if they are getting near the core as all the bands near the core are filled with electrons. They also feel an attractive Coulomb force from the core protons. The studies showed that the net potential would be much lower near the core for the valence electrons [6, 7]. So the pseudopotential will

roughly look like what is seen in figure 1-1. The tail of the function is from the Coulomb force, but the core region potential is modified.

Empirical pseudopotential method was used in 1950's and 1960's for the first times. The first applications were on optical and photo emission spectra. After investigation of many crystals, it was seen that the theoretical results and the experimental data are in very good agreement and this method was proved to be productive and very helpful [4]. Over time, the inputs became the potentials of the lattice and the outcome of the method after applying the Schrödinger equation became the electronic band structure of the materials being inspected.
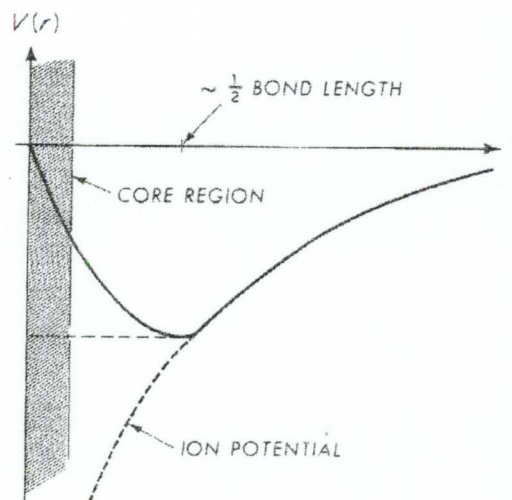
Figure 1-1. The whole picture of a typical pseudopotential showing its features [4].

The Empirical Pseudopotential Method (EPM) yielded accurate results on electronic band structure, density of states spectra but to a greater importance helped researchers get detailed charge density profiles of the semiconductors in detail [8].

Along with the development of the empirical method, the self-consistent method started developing too. The 1960's and 1970's were the years that this method was gaining ground and many different theories were being made and calculations were being done in this field [9-21]. Along with the calculations of energy bands being done in the first stages of this method, some new theories were being brought to improve the accuracy and efficiency of the method. In 1960, Allen, *et al.* [12] introduced some basis functions for the ab-initio methods and included ab-initio basis functions for LCAO and pseudopotential methods both, but the self-consistent pseudopotential method, gained a solid ground following the works of P. Hohenberg and W. Kohn [13] in 1964, and W. Kohn and L. J. Sham [14] in 1965. The works of Kohn and Sham [14] provided a theoretical basis for the self-consistent pseudopotential method which included the exchange and correlation potentials which are a part of this method in the recent days as well. In 1968, Goddard [16] introduced a new foundation for the use of the self-consistent pseudopotential approach for the electronic energy bands of metals. This foundation removed many of the past theoretical difficulties in utilizing the self-consistent method for metals. O'Keefe and Goddard later used this new foundation to calculate the energy band structure of Lithium [17] in 1969. Hamann, *et al.* [21] introduced the norm-conserving pseudopotentials in late 1970's. The band structures of some metals, insulating ions and also some semiconductors were also calculated during this period of time.

In the 1980's, many researchers focused on the different pseudopotentials and different algorithms to make the self consistent method more efficient. Among the studies done was the introduction of a pseudopotential that worked for all the elements of the periodic table by Bachelet, *et al.* [22] in 1982. An efficient iteration scheme was introduced by Kerker [23] to be utilized in Self-consistent calculations. This efficient scheme was adopted from other model calculation methods done before. In 1982, Yin and Cohen [24] provided the theory that illustrated why the self-consistent pseudopotential algorithms using the norm-conserving pseudopotentials lead to accurate energy band structures and other results.

One of the other important improvements of the types of pseudopotentials that were suitable for the self-consistent method was done by Vanderbilt [25] in the early 90's. The introduction of the soft and ultra soft pseudopotentials by Vanderbilt could improve the methods involving the plane-wave basis, because with the use of the soft pseudopotentials, a lower number of plane-wave basis terms will be needed to conduct the calculations. These kinds of pseudopotentials remove most of the high-frequency components of the pseudopotentials which are crucial to lowering the number of terms needed in the plane-wave basis methods. The self-consistent pseudopotential is an ever expanding method which is being refined even to the present time and has been used in calculating the energy band structure of many semiconductors in the past.

1.3 Outline of Thesis

This thesis consists of five chapters. After the introduction, the second chapter will be discussing the theory of pseudopotential method in general and the self-consistent pseudopotential method in more details. The second chapter will also contain a brief introduction to other methods of electronic band structure calculations. In chapter two the 1D Crystal Electronic Band Structure Solver will be introduced and discussed in details. This chapter is the first and most important step of the work as it is the major foundation of the 3D Crystal Electronic Band Structure Solver. It will be shown how the method can be used in solving the electronic band structure of any 1D crystalline material. Chapter four of this thesis will discuss how to transform the 1D Crystal Electronic Band Structure Solver to the 3D Crystal Electronic Band Structure Solver. Every aspect of the transformation will be discussed in detail and we will find the generalized 3D Crystal Electronic Band Structure Solver and the logic behind it. Finally, Chapter 5 will conclude the whole thesis and will propose some future research directions for the work.

1.4 Contribution of Thesis

The main contributions of this thesis can be summarized briefly as follows:

1. Starting pseudopotentials are always important in band structure calculations. Any new starting pseudopotential can be more useful than others in some cases. A new starting pseudopotential has been introduced in this thesis.

2. The Poisson equation has been solved analytically using the density function in the k-space without going from the k-space to the real space and going back to the k space. This saves time in the band structure calculations.

3. The solver utilizes the new calculation abilities of the newer generation of the CPUs in performing calculations. The solvers perform a large number of multiplications at the same time. This makes the calculation of the integrals in the solver much more efficient.

4. The solver solves the lattices accurately, with negligible or very small errors in both 1D and 3D cases.

Chapter 2: Theory of Pseudopotential Method

2.1 Introduction

In this chapter we will first have a brief look at quantum mechanics as it is playing a major part in understanding the pseudopotential method. As a matter of fact, the Schrödinger equation will be solved after utilizing the pseudopotential method. The next part in this chapter will be on the translational symmetry of the lattices and the Brillouin zones. A brief review of the other methods of finding the Electronic Band Structure of the crystalline lattices will be conducted. The details on the superior suitability of pseudopotential method for the case of this thesis will be discussed. The other methods that will be discussed are Nearly Free Electron or Empty Lattice Method, k.p Method and Tight-binding Method. After that a review of the Empirical Pseudopotential Method (EPM) will be conducted briefly and the Self-Consistent Pseudopotential Method will be discussed in more details. In the end of this chapter, a summary of the materials covered will be presented.

2.1.1 Introduction to Quantum Mechanics

In late 1920's, Heisenberg and Schrödinger developed a new kind of mechanics that is called quantum mechanics. They had different approaches to the problem. And they were working independently on the subject. Heisenberg used matrices to develop the new mechanics and his approach is now called

matrix mechanics. But the more important approach was Schrödinger's approach that uses a wave function to describe all of the properties of a particle in one function. It means that everything about a particle could be derived from that function. His approach is called wave mechanics. The two methods will give the same results in same situations. Closer looks to the methods show that they have the same basics and beyond the formulism, their approaches are the same. It is possible to show that the results of the matrix mechanics can be reduced to those of the wave mechanics. The wave mechanics is however easier to understand and manipulate as it involves less mathematical discussion and the solutions to some few simple problems are possible without much mathematical work compared to matrix mechanics [26, 27]. Some of the basics of the quantum mechanics theory are discussed in Appendix A. A brief review of Schrödinger equation is provided below.

2.1.1.2 The Schrödinger Wave Equation

The complete Schrödinger equation which results in a position and time dependent wave function is as follows:

$$(-\frac{\hbar^2}{2m})\nabla^2\Psi(\vec{r},t) + V(\vec{r},t)\Psi(\vec{r},t) = (-\frac{\hbar}{i})\frac{\partial\Psi(\vec{r},t)}{\partial t} \qquad (2\text{-}1)$$

where:

$$\nabla^2\Psi = \frac{\partial^2\Psi}{\partial x^2} + \frac{\partial^2\Psi}{\partial y^2} + \frac{\partial^2\Psi}{\partial z^2} \qquad (2\text{-}2)$$

Equation (2-1) can be reduced to the following for a one dimensional case:

$$\left(\frac{-\hbar^2}{2m}\right)\frac{\partial^2 \Psi(x,t)}{\partial x^2} + V(x,t)\Psi(x,t) = \left(\frac{-\hbar}{i}\right)\frac{\partial \Psi(x,t)}{\partial t} \qquad (2\text{-}3)$$

The wave functions of equations (2-1) and (2-3) are both time-dependent and position-dependent. When V is not a function of time, separation of variables can be done for the Schrödinger equation. The Schrödinger equation is then separated into two equations, one only dependent on time and the other only dependent on spatial variables. The wave function is separated to the multiplication of two functions as below:

$$\Psi(\vec{r},t) = \psi(\vec{r})\Phi(t) \qquad (2\text{-}4)$$

After some mathematical work, the variables can be separated to obtain the two equations; a time-dependent equation,

$$\frac{d\Phi(t)}{dt} + \left(\frac{iE}{\hbar}\right)\Phi(t) = 0 \qquad (2\text{-}5)$$

and a time-independent equation,

$$\nabla^2 \psi(\vec{r}) + \left(\frac{2m}{\hbar^2}\right)[E - V(\vec{r})]\psi(x) = 0 \qquad (2\text{-}6)$$

To obtain information about the system for which the Schrödinger equation is solved, both Ψ or ψ can be used because the solution to equation (2-5) is a plane wave which has an absolute value of one and for any property calculation the absolute value of the wave function plays the central role. As a result, as soon as the wave function, Ψ or ψ, is found for a given particle or system, we can calculate any desired property of that particle or system, like its average position, energy, and momentum, using the wave function. So it is

obvious that the most important part of any problem in quantum mechanics is to find the wave function for the system being discussed. It should be noted that any property of the system can be calculated using the quantum operators on the wave function that is calculated. A small list of some quantum operators can be seen in table (A-1) in appendix A.

It can be shown that the separation constant, E, in equations (2-5) and (2-6), is corresponding to the energy of the particle for particular solutions obtained. So for example, the wave function ψ_n is related to the particle energy E_n.

Equations (2-5) and (2-6) are the basis of quantum mechanics in the case of time-independent potentials. One can find the wave function of any system by solving the Schrödinger equation for that system. For electrons and other charged particles, the term $V(x)$ that is the potential term and our only bridge to reality in quantum mechanics, is the result of an electrostatic or magnetic field. (As we assumed the independency of $V(x)$ from time, so the fields should be static. More complicated problems should be solved using the time dependent Schrödinger equation.) [26, 27]

If we write the 3D time-independent Schrödinger equation in the following form, it will have a part which is called the Hamiltonian.

$$[-\frac{\hbar^2}{2m}\nabla^2 + V(r)]\psi(r) = E\psi(r) \qquad (2-7)$$

The first part of equation (2-7) which is also shown in equation (2-8) is called the Hamiltonian. Any system can be described completely by its Hamiltonian and by solving the Schrödinger equation using the Hamiltonian which is calculated for that system; all the properties of the system are known when using the right operators on the wave function.

$$H = -\frac{\hbar^2}{2m}\nabla^2 + V(r)$$
(2-8)

2.1.2 Translational Symmetry of Crystals and Brillouin Zones

Crystals by definition are the repetition of a structure in the space with defined periods in the space. For example, a simple cubic crystal lattice is a single atom that is being repeated in x, y, and z directions with the same period of "a" meters. So the most important translational symmetry that any crystal will have will be invariance under defined spatial translations. As an example, a simple cubic crystal will be invariant if it is translated by the vector $\vec{T} = m.a.\hat{x} + n.a.\hat{y} + p.a.\hat{z}$ where $m, n, p \in Z$ [28].

In a majority of crystals, we have other kinds of translational symmetries which we will group them into rotational symmetry category and reflection symmetry category. The more kinds of symmetry a crystal owns, the easier it is to calculate its energy band structure. Fortunately, semiconductor crystals often have high degrees of symmetry, mostly rotational, which will result in less complexity in the calculations of their energy band structure calculations.

One of the most important simplifications that one can get from the most basic translational symmetry which was talked about, is the Bloch theorem which can be used to greatly reduce the complexity of a crystal's energy band structure calculation. The theorem states that if the potential in the space, V, is periodic with the period $\vec{T} = a\hat{x} + b\hat{y} + c\hat{z}$ then we will have the following:

$$V(\vec{r} + \vec{T}) = V(\vec{r}) \Rightarrow \psi(\vec{r}) = e^{\pm i\vec{k}\cdot\vec{r}} u_k(\vec{r}) \quad \text{where } u_k(\vec{r} + \vec{T}) = u_k(\vec{r}) \tag{2-9}$$

It can be seen that $u_k(\vec{r})$ is periodic with the same period as $V(\vec{r})$. To understand the theorem better, we will prove it for a 1D crystal [29, 30]. So we will prove that if $V(x+a) = V(x)$ then we will have $\psi(x) = e^{\pm ikx} u_k(x)$ where $u_k(x+a) = u_k(x)$.

When a free electron is in a constant potential of V_0 with infinite boundaries in a 1D space, the Schrödinger equation is:

$$\frac{d\psi^2}{dx^2} + \frac{2m}{\hbar^2}[E - V_0]\psi = 0 \tag{2-10}$$

The solutions of this equation are plane waves of the type:

$$\psi(x) = e^{\pm ikx} \tag{2-11}$$

The kinetic energy of the electron will be the total energy minus its potential energy.

$$E_{kin} = E - V_0 = \frac{\hbar^2 k^2}{2m} = \frac{p^2}{2m} \tag{2-12}$$

16

k is the momentum of the electron divided by $\hbar$ as it is obvious from above. To find the complete solution we should solve the time-dependent equation too. And multiply the solution obtained from that equation by $\psi(x)$. It is known that the solution of the time-dependent equation is always $e^{-i\omega t}$ where $\omega = \dfrac{E}{\hbar}$. So equation (2-11) shows only the wave propagation along the x-axis without time-dependency.

Now we shall start the main problem which is solving the Schrödinger equation for an electron in a one-dimensional periodic potential. So the potential energy should be like below:

$$V(x+a) = V(x) \tag{2-13}$$

where 'a' is the period. The Schrödinger equation is

$$\frac{d\psi^2}{dx^2} + \frac{2m}{\hbar^2}[E - V(x)]\psi = 0 \tag{2-14}$$

There is a very important theorem that says there are solutions to this equation with a periodic potential. They are of the form

$$\psi(x) = e^{\pm ikx} u_k(x) \quad \text{where} \quad u_k(x+a) = u_k(x) \tag{2-15}$$

So the solutions are plane waves that are modulated by $u_k(x)$. This function has the same periodicity as that of the lattice. Although this theorem is known as the Floquet's theorem [31] in the theory of the differential equations and was proved before it is used in solid state physics, this theorem is known as the Bloch theorem in solid state physics as he was the first to use it in this field.

The functions of the type (2-15) are called Bloch functions. Before starting the proof of the theorem it should be noted that the Bloch functions has the following property:

$$\psi(x+a) = e^{ik(x+a)}u_k(x+a) = \psi(x)e^{ika} \tag{2-16}$$

Because $u_k(x+a) = u_k(x)$. So Bloch functions have the property that

$$\psi(x+a) = Q\psi(x) \quad \text{where} \quad Q = e^{\pm ika} \tag{2-17}$$

The problem is solved if we can show that the Schrödinger equation (2-14) has solutions with the property (2-16), because then the solutions will be in the form of Bloch functions. When the solution to the Schrödinger equation is the Bloch functions, it means that we have proved the Bloch theorem. Now we will go through the solution.

Suppose there are two independent real solutions to the Schrödinger equation, say $f(x)$ and $g(x)$. Since the Schrödinger equation is a second order differential equation it only has two independent solutions. All other solutions can be written as a linear combination of $f(x)$ and $g(x)$. So we can write $f(x+a)$ and $g(x+a)$ as linear combination of $f(x)$ and $g(x)$. It is obvious that $f(x+a)$ and $g(x+a)$ are also solutions to the Schrödinger equation. So we must have

$$f(x+a) = \alpha_1 f(x) + \alpha_2 g(x) \tag{2-18a}$$

$$g(x+a) = \beta_1 f(x) + \beta_2 g(x) \tag{2-18b}$$

It should be noted that the α's and β's must be real functions of E. Any general solution to the Schrödinger equation is of the form

18

$$\psi(x) = Af(x) + Bg(x) \qquad (2\text{-}19)$$

where A and B are arbitrary constants. According to (2-18), we must have

$$\psi(x + a) = (A\alpha_1 + B\beta_1)f(x) + (A\alpha_2 + B\beta_2)g(x) \qquad (2\text{-}20)$$

As we know the Bloch functions has the property (2-17). So we will choose A and B so that

$$A\alpha_1 + B\beta_1 = QA \qquad (2\text{-}21a)$$

$$A\alpha_2 + B\beta_2 = QB \qquad (2\text{-}21b)$$

where Q is a constant. If we find the answer to (2-21) equations, we have found a function $\psi(x)$ with the property

$$\psi(x + a) = Q\psi(x) \qquad (2\text{-}22)$$

Because equations (2-21a,b) have non-vanishing solutions for A and B only if the determinant of their coefficients is equal to zero, we will have the following equation for Q:

$$\begin{vmatrix} \alpha_1 - Q & \beta_1 \\ \alpha_2 & \beta_2 - Q \end{vmatrix} = 0 \qquad (2\text{-}23a)$$

or

$$Q^2 - (\alpha_1 + \beta_2)Q + \alpha_1\beta_2 - \alpha_2\beta_1 = 0 \qquad (2\text{-}23b)$$

Now, it can be shown that $\alpha_1\beta_2 - \alpha_2\beta_1 = 1$ in the following manner:

From equation (2-18) it can be shown that

$$\begin{vmatrix} f(x+a) & g(x+a) \\ f'(x+a) & g'(x+a) \end{vmatrix} = \begin{vmatrix} f(x) & g(x) \\ f'(x) & g'(x) \end{vmatrix} \cdot \begin{vmatrix} \alpha_1 & \alpha_2 \\ \beta_1 & \beta_2 \end{vmatrix} \tag{2-24}$$

If we multiply the Schrödinger equation for $g(x)$ by $f(x)$ and the equation for $f(x)$ by $g(x)$, by subtracting them we will find

$$0 = fg'' - gf'' = \frac{d(fg' - gf')}{dx} \tag{2-25}$$

So, as a matter of fact the so-called Wronskian in this case is a constant:

$$\begin{vmatrix} f(x) & g(x) \\ f'(x) & g'(x) \end{vmatrix} = const. \tag{2-26}$$

This result, together with equation (2-24), leads to the conclusion that $\alpha_1 \beta_2 - \alpha_2 \beta_1 = 1$. So instead of (2-23b) the following can be written:

$$Q^2 - (\alpha_1 + \beta_2)Q + 1 = 0 \tag{2-27}$$

It should be noted that $(\alpha_1 + \beta_2)$ is a real function of E. There are two roots for equation (2-27). So there are two wave functions that exhibit the property (2-22). Suppose the two roots are Q_1 and Q_2. We know from the equation that the product $Q_1 Q_2 = 1$. For a certain range of E, when $(\alpha_1 + \beta_2)^2 < 4$, the roots are complex, and as the product $Q_1 Q_2 = 1$ the roots will be complex conjugates. In such energy ranges the answers will be

$$Q_1 = e^{ika} \quad \text{and} \quad Q_2 = e^{-ika} \tag{2-28}$$

So the functions $\psi_1(x)$ and $\psi_2(x)$ will have the property (2-22). So they will obey the following equations

$$\psi_1(x+a) = e^{ika}\psi_1(x) \text{ and } \psi_2(x+a) = e^{-ika}\psi_2(x) \tag{2-29}$$

20

So the functions $\psi_1(x)$ and $\psi_2(x)$ are Bloch functions for the energy ranges that were discussed. In the other regions of E that correspond to $(\alpha_1 + \beta_2)^2 > 4$, Q_1 and Q_2 will be real and as we know their product will be 1. The solution to the Schrödinger equation with these roots will be

$$\psi_1(x) = e^{\mu \cdot x} u(x) \text{ and } \psi_2(x) = e^{-\mu \cdot x} u(x) \tag{2-30}$$

where μ is a real quantity. These solutions are mathematically right but they are not physically accepted in general. They cannot be the wave function of the electrons because they are not bounded. So there will be no energy states corresponding to the real roots. In other words, these energy states are forbidden. So it is shown that the energy spectrum of an electron in a periodic potential has allowed states as well as forbidden states.

If we write a total $\psi(x)$ for all different wave vector, k, values as a sum of Bloch functions, we will have equation (2-31). The constants, A_k, in equation (2-31) show how much each wave vector's eigen-function is contributing to the total eigen-function.:

$$\psi(x) = \sum_k A_k e^{ikx} u_k(x) \tag{2-31}$$

Let's assume that in the free electron case, the electron is not completely free, but just nearly free in a one dimensional lattice with period "a" and we assume for simplification that $V_0 \to 0$ in equation (2-10). The energy band structure is the diagram of the energies found from equation (2-10), or in general

any structure's Schrödinger equation, versus k. From equation (2-12), it is known that:

$$E = \frac{\hbar^2 k^2}{2m}$$ (2-32)

k can be any number in general and from that point of view the energy band structure of a free electron in a zero potential will be like figure 2-1a. This form of energy band structure diagram is called the extended zone scheme.
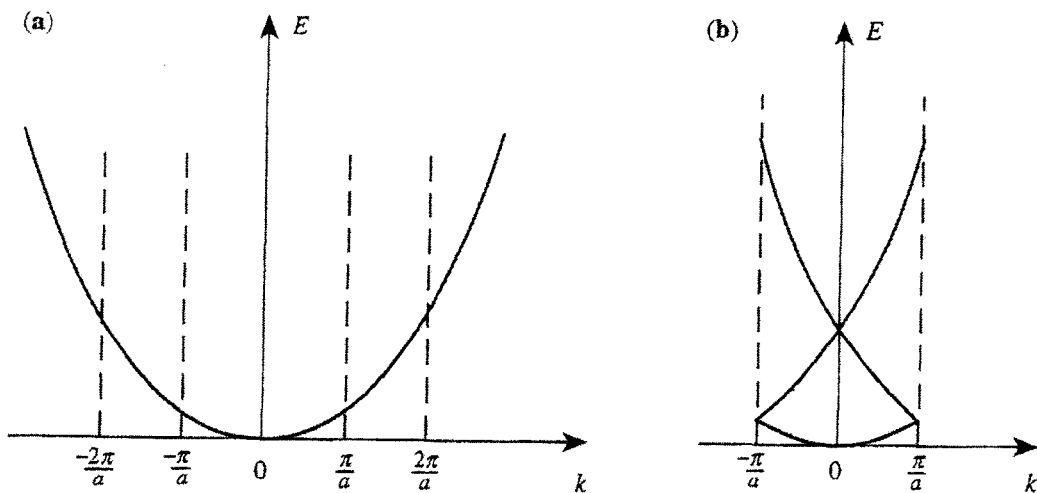
Figure 2-1. The energy band structure of a free electron. a) The extended zone scheme. b) The reduced zone scheme [28].

From equation (2-11), it can be seen that the wave function is not unique for different values of k and it is in fact periodic for k values with a period of $\frac{2\pi}{a}$. It is most conventional to draw the energy band structure diagram in the period of $[-\frac{\pi}{a}, \frac{\pi}{a}]$ when taking advantage of the periodicity of the lattice. The period of k from $[-\frac{\pi}{a}, \frac{\pi}{a}]$ is called the first Brillouin zone. Each other period after it is

respectively called the second, third, etc. Brillouin zone. A more general definition of Brillouin zones can be found in [32]. If we plot the energy band structure of a lattice in this way it is called the reduced zone scheme and it is shown in figure 2-1b. The reduced scheme is a better scheme in general because it is more compact and provides more understanding about the crystal being studied. If the electron gains enough energy to have a transition from a k value to any other value under the influence of any translationaly invariant operator like $\frac{2\pi}{a}$ (the lattice period), in a lattice, it is observed that the value of k is preserved after the process in this scheme but in the extended scheme the value of k is only conserved to a multiple of $\frac{2\pi}{a}$. Because of this property of the reduced zone scheme it is used almost everywhere in the literature. It should be noted that all the results introduced here for 1D are easily expandable to 3D cases.

We can also talk about the translational symmetries of the crystals in terms of primitive lattice vectors of $\mathbf{a}_1$, $\mathbf{a}_2$, and $\mathbf{a}_3$. As it was mentioned before in the start of this part (2.1.2), a crystal is a periodic structure that is formed by the repetition of a minimal set of atoms (the basic set) by the linear combinations of the lattice vectors. Here we will discuss the diamond lattice as an example. The structure of a unit cell of the silicon crystal is shown in figure 2-2. In this crystal structure, the basis set is made of two atoms. The other lattice points are then made by the translation of this basis set by the lattice vectors or by any linear

combination of them. This lattice which is made by such action is called the direct lattice.

The primitive lattice vectors of a face-centered cubic (FCC) crystal are shown in figure 2-3 and it should be noted that the primitive lattice vectors are not unique. If we show each lattice point of the diamond crystal structure by only one point we will then get an FCC crystal because the diamond crystal structure is essentially two FCC structures which are in each other with $(\frac{a}{4}, \frac{a}{4}, \frac{a}{4})$ offset. So the set of the primitive lattice vectors for the FCC crystal and the diamond crystal are essentially the same.
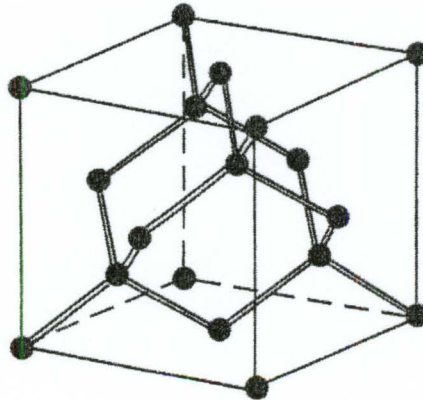
Figure 2-2. The crystal structure of silicon (the unit cell) [28]
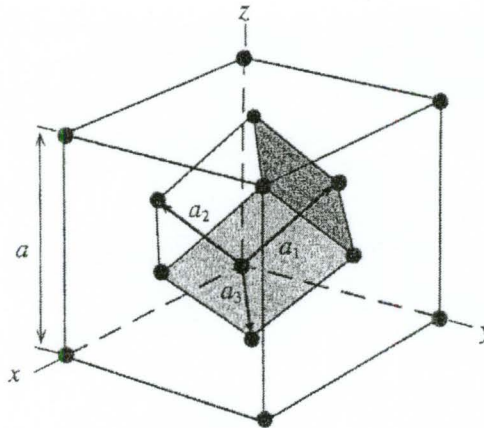
Figure 2-3. The FCC lattice or diamond lattice with only the lattice points (consisting of two atoms) shown with a set of primitive lattice vectors [28].

The lattice vectors in figure 2-3 are as follow:

$$\mathbf{a}_1 = (0, \frac{a}{2}, \frac{a}{2}) \tag{2-33a}$$

$$\mathbf{a}_2 = (\frac{a}{2}, 0, \frac{a}{2}) \tag{2-33b}$$

$$\mathbf{a}_3 = (\frac{a}{2}, \frac{a}{2}, 0) \tag{2-33c}$$

It should be noted that a is the size of the side of the FCC lattice unit cell. For any direct lattice there is a reciprocal lattice which is defined, like the direct lattice, with three primitive reciprocal lattice vectors which are called $\mathbf{b}_1$, $\mathbf{b}_2$, and $\mathbf{b}_3$. These vectors are related to the direct lattice's primitive vectors as follows:

$$\mathbf{b}_1 = 2\pi \frac{\mathbf{a}_2 \times \mathbf{a}_3}{(\mathbf{a}_1 \times \mathbf{a}_2) \cdot \mathbf{a}_3} \tag{2-34a}$$

$$\mathbf{b}_2 = 2\pi \frac{\mathbf{a}_3 \times \mathbf{a}_1}{(\mathbf{a}_1 \times \mathbf{a}_2) \cdot \mathbf{a}_3} \tag{2-34b}$$

$$\mathbf{b}_3 = 2\pi \frac{\mathbf{a}_1 \times \mathbf{a}_2}{(\mathbf{a}_1 \times \mathbf{a}_2) \cdot \mathbf{a}_3} \tag{2-34c}$$

The reciprocal lattice is made by translating a point with the primitive reciprocal vectors and their linear combinations. By introducing the reciprocal lattice we will be able to represent k, the wave vector, as a point in the reciprocal lattice space. We can define the first Brillouin zone as the smallest polyhedron that is made by the planes that are perpendicularly bisecting the reciprocal lattice vectors. In figure 2-4 the reciprocal lattice that is found for an FCC lattice can be seen. It is seen that the reciprocal lattice for an FCC lattice is a body-centered cubic (BCC) lattice. The first Brillouin zone is also depicted in figure 2-4. The symmetry of the Brillouin zone is determined by the symmetry of the lattice, because the primitive lattice vectors of the reciprocal lattice are directly related to the primitive lattice vectors of the direct lattice.

Figure 2-4. The FCC lattice's reciprocal lattice with the first Brillouin zone shown in the figure [28].

$$\mathbf{b}_3 = 2\pi \frac{\mathbf{a}_1 \times \mathbf{a}_2}{(\mathbf{a}_1 \times \mathbf{a}_2) \cdot \mathbf{a}_3} \qquad (2\text{-}34c)$$

The reciprocal lattice is made by translating a point with the primitive reciprocal vectors and their linear combinations. By introducing the reciprocal lattice we will be able to represent k, the wave vector, as a point in the reciprocal lattice space. We can define the first Brillouin zone as the smallest polyhedron that is made by the planes that are perpendicularly bisecting the reciprocal lattice vectors. In figure 2-4 the reciprocal lattice that is found for an FCC lattice can be seen. It is seen that the reciprocal lattice for an FCC lattice is a body-centered cubic (BCC) lattice. The first Brillouin zone is also depicted in figure 2-4. The symmetry of the Brillouin zone is determined by the symmetry of the lattice, because the primitive lattice vectors of the reciprocal lattice are directly related to the primitive lattice vectors of the direct lattice.

Figure 2-4. The FCC lattice's reciprocal lattice with the first Brillouin zone shown in the figure [28].

The primitive lattice vectors of the reciprocal lattice of the direct FCC lattice can be derived from the formulae given in equation (2-34). They are as followed:

$$\mathbf{b}_1 = \frac{2\pi}{a}(-1,1,1) \qquad\qquad (2\text{-}35a)$$

$$\mathbf{b}_2 = \frac{2\pi}{a}(1,-1,1) \qquad\qquad (2\text{-}35b)$$

$$\mathbf{b}_3 = \frac{2\pi}{a}(1,1,-1) \qquad\qquad (2\text{-}35c)$$

The symmetry points of the Brillouin zone are shown in figure 2-4 with letters X, Γ, L, and K. It should be noted that the center of Brillouin zone is always denoted as Γ. There are three high-symmetry directions in the FCC lattice's Brillouin zone which are the [100], [110], and [111] directions. As it can be seen this Brillouin zone is a high-symmetry Brillouin zone that doesn't change by some rotation translations. It also doesn't change under reflection translations through some planes. We should always have in mind that these symmetry relations that exist for the Brillouin zone are directly related to the direct lattice symmetries.

It should be noted that the line Δ is the line in Brillouin zone from Γ to X and is in [100] direction. The line Λ is in direction [111] and is from Γ to L. And at last the line in direction of [110] is called Σ and passes from Γ and K. It should also be noted that if a line or point can be shown to be the translation of another line or point under certain symmetry operation the lines or points are said

to be equivalent. If two or more axis or points are equivalent, then it is only necessary to calculate the energy bands of the electron in only one of them.

2.2 Different Methods of Finding the Electronic Band Structure

In this part we will have a brief look at three other methods of finding the electronic band structure of a lattice. At first we will start with the empty lattice or the nearly free electron method. This method requires very deep insight into lattice symmetries and translational properties of lattice, so we will only have a very brief look and show some of the results of the method without any proof only for later comparisons and more understanding about the importance of the symmetries that exist in crystals.

As a second method we will introduce the k.p method which deals more about a small part of the energy band structure other than the complete energy band structure of a lattice and is most suitable for direct materials with optical uses. This method is accurate only for the k values that are near $k = 0$.

The third method being introduced in brief will be the Tight-binding Method, also known as LCAO or Linear Combination of Atomic Orbitals method. We will show that this method is good for metals and semimetals but not as good for semiconductors because of accuracy problems in the prediction of the conduction bands, which will be shown and discussed later.

2.2.1 Empty Lattice or Nearly Free Electron Method

The nearly free electron method is a method which concentrates more on the symmetry properties of the crystals than what the crystal is made up of. Because of this fact, we know that the outcome of this method is not an accurate representation of the energy band structure of a crystal, but a schematic of how the energy band structure will generally look like. For example, two diamond lattices with same lattice constants that are made of two different materials will give the same results.

In this method the electron is assumed to be in a crystal with negligibly small potentials, so the electron feels free but as it moves in the presence of a lattice potential the energy band structure will be changed according to the symmetry properties of the crystal that this electron is moving inside. It is known that the wave function and energy of a free electron are as shown in equation (2-11) and equation (2-32) respectively. In a three dimensions, the wave function will be different but the energy will stay the same. The wave function of an electron in three dimensions is:

$$\psi(x, y, z) = e^{i(k_x x + k_y y + k_z z)} \qquad (2\text{-}36)$$

or:

$$\psi(\vec{r}) = e^{i\vec{k}.\vec{r}} \qquad (2\text{-}37)$$

As we know, the energy of the free electron is a parabola if we plot it in the extended zone scheme. In the nearly free electron method, we plot this parabola in the reduced zone and we take advantage of all the translational symmetries

we know about the crystal that the electron is moving in. This reduced zone scheme plot will look so complicated because it is based on a variety of translational symmetries.

As the zinc-blende lattice and the diamond lattice have slightly different translational symmetries, their energy band structure using the nearly free electron method will be nearly the same with little differences because the potentials are assumed to be negligibly small so that the electron feels free. The two different lattices look the same with negligibly small potentials, because the only difference between them had been the potentials and they had made the two lattices to be different in translational symmetry terms. To have a feeling why the two potentials are seem to be the same but the results are slightly different, it should be noted that it is like that we first do the calculations for a real potential and then find the limit for the calculations when the potential is reaching zero. In this way we know that for zinc-blende lattice and diamond lattice there are two totally different energy band structures and it is not surprising that the limit of the energy band structures when the lattice potential is reaching zero should be different. So, the two different sets of translational symmetry properties that have been used will result in nearly the same energy band structure with little differences for zinc-blende and diamond lattice structures. The energy band structures of zinc-blende and diamond lattices are shown in figure 2-5. As we are not discussing this method in detail, we do not go into the details of figure 2-5 and we will just use it as a reference to show how important symmetries can be

for the energy band structure of a crystal and how much effect the translational symmetries have on the real energy band structure.
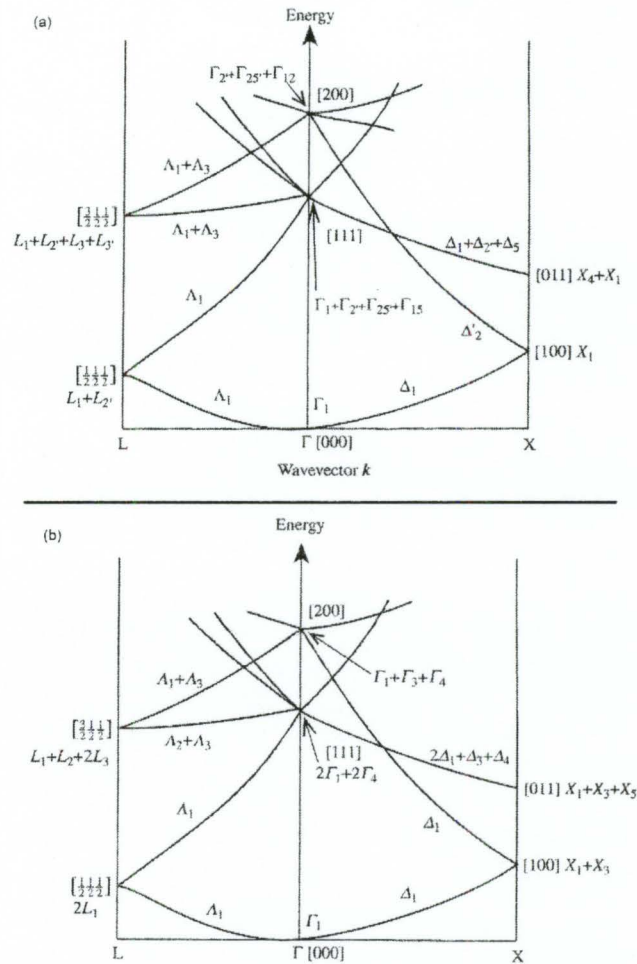
Figure 2-5. (a)The diamond lattice nearly free electron energy band structure. (b)The zinc-blende lattice nearly free electron energy band structure [28].

We will use the energy band structures seen in this part to show the effects of translational symmetries in more accurate energy band structures that will be seen in the next parts. As this method needs deep knowledge on group

theory and translational symmetries, we will not look into it in more details. we limit our discussion to what was discussed about how this method is being implemented only and move on to the next methods of finding the energy band structure of crystals.

2.2.2 The k.p Electronic Band Structure Calculation Method

The k.p method is suitable for situations in which we are only interested in the electronic band structure of the lattice we are working with, near the $k = 0$ point. As we get farther from $k = 0$, the accuracy of the method will becomes less and less. In this method we will first solve the Schrödinger equation at $k = 0$ and then use the perturbation theory to find the rest of the energy band structure of the material near $k = 0$. The reason for less accuracy when distancing from $k = 0$ is that the perturbation terms are proportional to k and it works best when the values are small and close enough to $k = 0$ [33].

The k.p method is a suitable method for calculating the optical spectra of the direct band-gap semiconductor materials. One can also extract the band dispersion and effective masses analytically using this method. As we know the Schrödinger equation is as follows:

$$[-\frac{\hbar^2}{2m}\nabla^2 + V(\vec{r})]\psi_{nk}(\vec{r}) = E_{nk}\psi_{nk}(\vec{r})$$

(2-38)

Because we are in the periodic potential of a crystalline lattice, we can use the Bloch theorem:

$$\psi_{nk}(\vec{r}) = e^{i\vec{k}\cdot\vec{r}} u_{nk}(\vec{r})$$ (2-39)

If we substitute equation (2-39) in equation (2-38) we will get the following equation, which is the basic for the k.p method. The details of the derivation of this equation are presented in Appendix B.

$$(\frac{p^2}{2m} + \frac{\hbar \vec{k}\cdot\vec{p}}{m} + \frac{\hbar^2 k^2}{2m} + V)u_{nk} = E_{nk}u_{nk}$$ (2-40)

If we just want to solve equation (2-40) for $\vec{k}_0 = (0,0,0)$, the equation will reduce to the simpler form of:

$$(\frac{p^2}{2m} + V)u_{n0} = E_{n0}u_{n0}$$ (2-41)

Equation (2-41) will be solved for $n = 1,2,3,\ldots$. This equation is solved knowing that the functions u_{n0} are periodic, so solving this equation will be rather easy. It will lead to an orthonormal and also complete set of basis functions. Now that the energies E_{n0} and the functions u_{n0} are known, we can use the perturbation theory to add the terms $\frac{\hbar \vec{k}\cdot\vec{p}}{m}$ and $\frac{\hbar^2 k^2}{2m}$ as a perturbation to equation (2-41) and solve it again. This action is equal to solving equation (2-40) for $\vec{k}$ near $\vec{k} = 0$. As a general idea we can also solve equation (2-40) for any k_0 and then solve for any $\vec{k}$ near $\vec{k}_0$ as a perturbation. In the process of k.p method the spin of the electrons are also have to be taken care of by changing the Hamiltonian. We will leave the discussion of the k.p method to this point as this method is especially good for only the materials with optical properties and not all

the materials with crystalline structure. For more details and information on the k.p method, one can refer to [34].

2.2.3 Tight-Binding or LCAO Method

In Tight-Binding method, we assume that the atoms are far from each other so that they do not have any force on each other. In this case each atom is an individual unit. So the electrons are tightly bound to their respective atom. As we know if the distance between the atoms becomes like the lattice constant, they should make the crystal that we are trying to calculate the energy band structure for. The first step in calculating the energy band structure of the lattice is to calculate the wave functions of the electrons in the single atoms that are far from each other. As we bring the atoms closer, the wave functions of the different atoms' electrons will overlap. As it can be suggested from the second name of the method which is Linear Combination of Atomic Orbitals, LCAO, we will approximate the wave functions of the lattice as the linear combination of the wave functions of the individual atoms that are being brought together to form the crystal.

As we know the electrons in the valence band of the semiconductor materials are very much concentrated to their place and can be approximated by the electrons that are bounded by the individual atoms. This means that the valence band electrons have got many of their properties from some orbitals called bonding orbitals in the atoms and molecules that have created the crystal.

From this explanation we should know that this method will give a good approximation of the valence band of the crystal that we are working on. But the approximation of the conduction band will not be the same as will be shown later in comparisons. The band structure of the lattice is found by combining a number of the orbitals of the adjacent atoms in the crystal using the overlap parameters.

The concept of this method is that we will have the energy band structure of the crystal by assuming that the orbitals of an atom in the lattice is overlapped by the other atoms surrounding the specific atom we are talking about. The usual method is to only take into account the nearest atoms that are surrounding our atom. What we will get from these calculations will be the energy band structure of the crystal. Two kinds of bonding and antibonding orbitals will result from the overlapping of the atoms' orbitals. These orbitals are schematically shown in figure 2-6 for s and p orbitals. It is assumed in this figure that the two atoms are getting close to each other in the x direction. As we know, p_y and p_z are identical for this situation, so only the p_y overlap is shown in figure 2-6 in the next page.

The interactions of the two atoms are calculated based on the interaction Hamiltonian of the system. The interaction will produce two new orbitals instead of the two existing orbitals. This interaction will change the energies in the orbitals. One of the orbitals' energies, typically the antibonding orbital, will be raised and the other one's energy, typically the bonding orbital, will be reduced. So the two orbitals that had the same energy in two separate atoms will now,

after interaction, be two orbitals, namely bonding and antibonding, with two different energies. In a lattice's energy band structure calculations with LCAO method, this is the foundation of the generation of different valence and conduction bands.
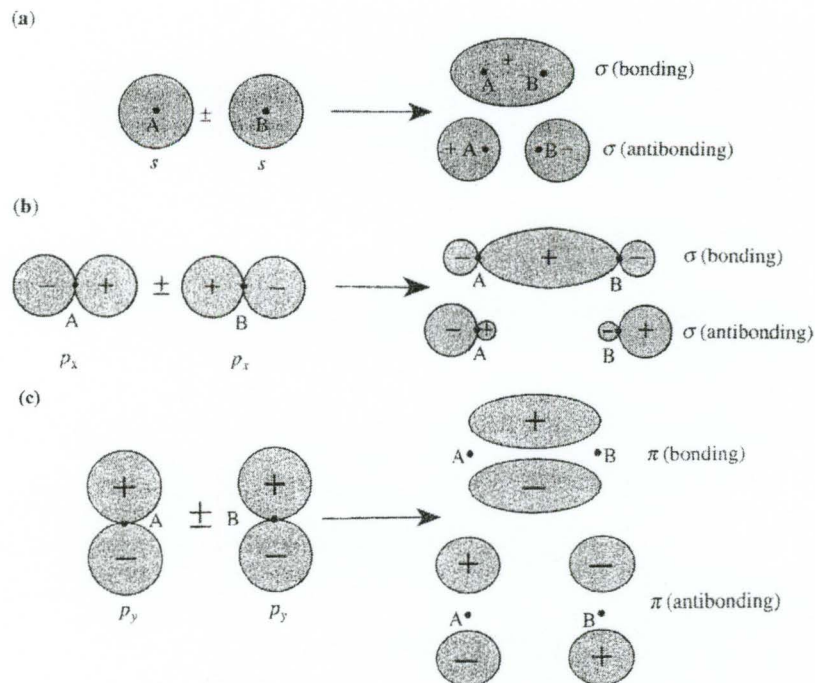
Figure 2-6. (a) Two s orbitals forming the bonding and antibonding σ orbitals. (b) Two p_x orbitals forming the bonding and antibonding σ orbitals. (c) Two p_y orbitals forming the bonding and antibonding π orbitals. Note that p_z is identical to p_y when the two atoms are getting close to each other in the x direction [28].

As it was mentioned previously, this method gives a good approximation of the valence bands but as it will be presented, it is not satisfactory in approximating the conduction bands of many semiconductors. As an example,

the valence band of Si is calculated with both EPM (Empirical Pseudopotential Method) and tight-binding in figure 2-7. As it is seen, these methods are resulting in pretty much the same bands for the valence bands of silicon.
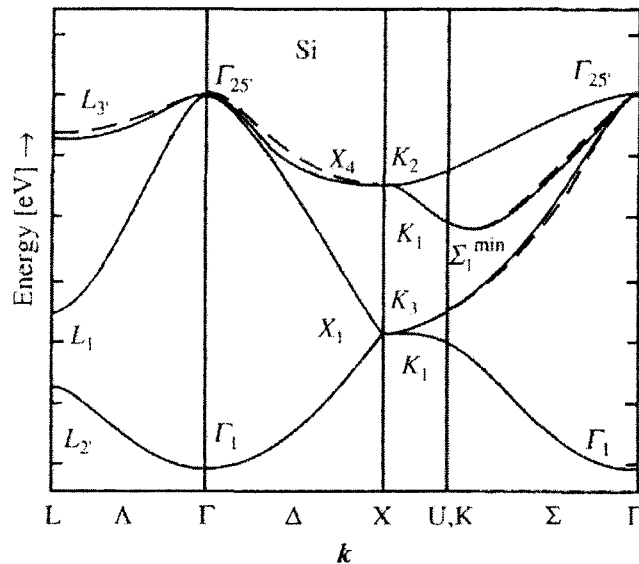
Figure 2-7. The valence bands of silicon calculated by EPM (the solid lines) and the tight-binding method (the broken lines) [28]

As a second example the energy band structure of germanium, calculated with LCAO method and EPM Method are compared side by side. As we know the EPM is very accurate as it uses many experimental data to fix the energy band structure that it is calculating on the true bands, so it sometimes is called the true bands. As we see in figure 2-8, the conduction band is totally different using the LCAO method. A side by side comparison of LCAO method with the nearly free electron method is also presented in figure 2-9. It can be seen that the nearly

free electron general shape of conduction band shows that the conduction band in the LCAO method is not accurate.

(a) LCAO Bands   (b) True bands
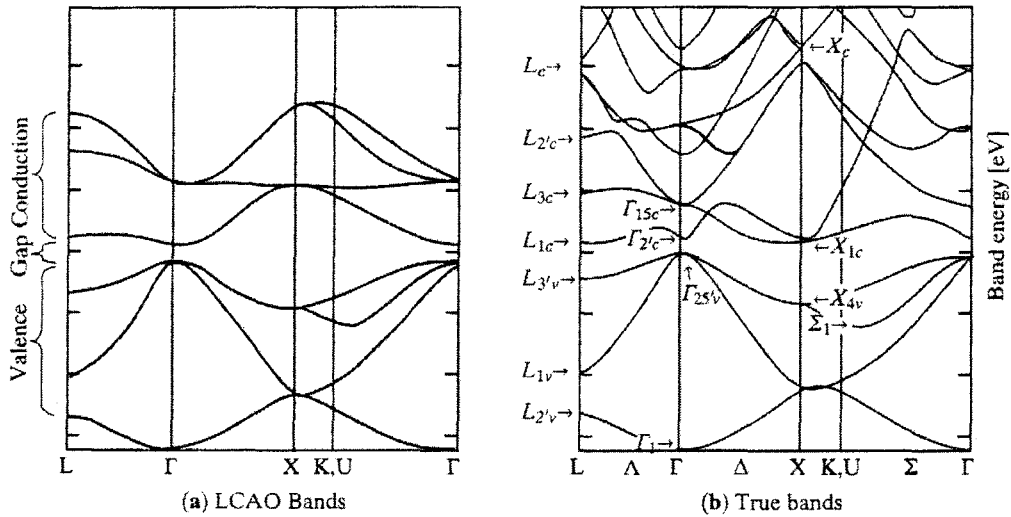
Figure 2-8. Side by side comparison of the band structure of germanium Using (a) LCAO Method, and (b) EPM Method [28].

The accuracy of the conduction band is low because the electrons in the conduction band are delocalized and do not fit into the localized electron categories that this LCAO method takes into account. It can of course be improved by taking into account additional overlap parameters and not limiting the calculations to the nearest neighboring atoms of the base atom. The other shortcoming of LCAO is that there is only four conduction bands that are calculated here because only s and p orbitals making four sp^3 orbitals in each atom, have been used in the calculations of the bands. To correct this problem, the d orbitals have to be added to the calculations and new overlap parameters

and interaction matrices will have to be calculated, which causes huge complexity. The simplicity of this method has to be compromised to calculate conduction bands accurately.

(a) LCAO Bands   (b) Free-electron bands
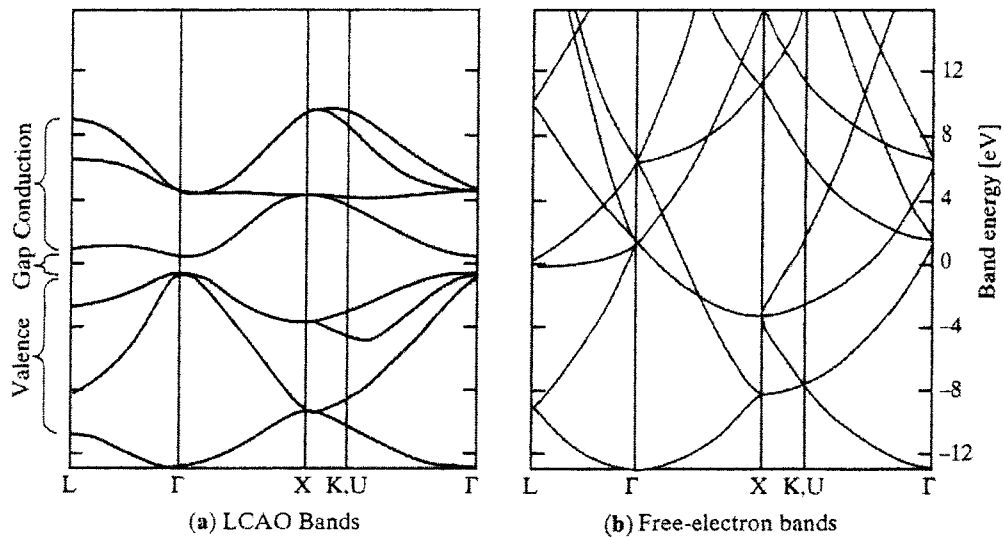
Figure 2-9. Side by side comparison of the band structure of germanium Using (a) LCAO Method, and (b) Nearly Free Electron Method [28].

Even looking at the nearly free electron method, it can be seen that the conduction band of the LCAO method used for calculation of the germanium energy band structure, is not like what it should be because of the symmetries that exist in the crystalline lattice of a diamond structure.

2.3 The Empirical Pseudopotential Method

In this section the reasons of the similarities between the nearly free electron approach and this approach will be discussed. The basics of the Empirical Pseudopotential Method, EPM, will then be introduced. Some of the formulation will then be discussed. At last the band structures of Si and GaAs calculated with this method will be shown.

2.3.1 Similarities with Nearly Free Electron Method

If we compare the pseudopotential calculated results with the nearly free electron method, we will see many similarities between them. One can compare the two methods in figure 2-10. As it is known, the nearly free electron method energy band structure is just consisted of the parabolas that are redrawn in the first Brillouin zone, but pseudopotential method is a set of complex numerical calculations that will result in the energy band structure of a material. The fact that these two have similarities can be somehow explained. The answer can be found in the basic concepts of the pseudopotential method.
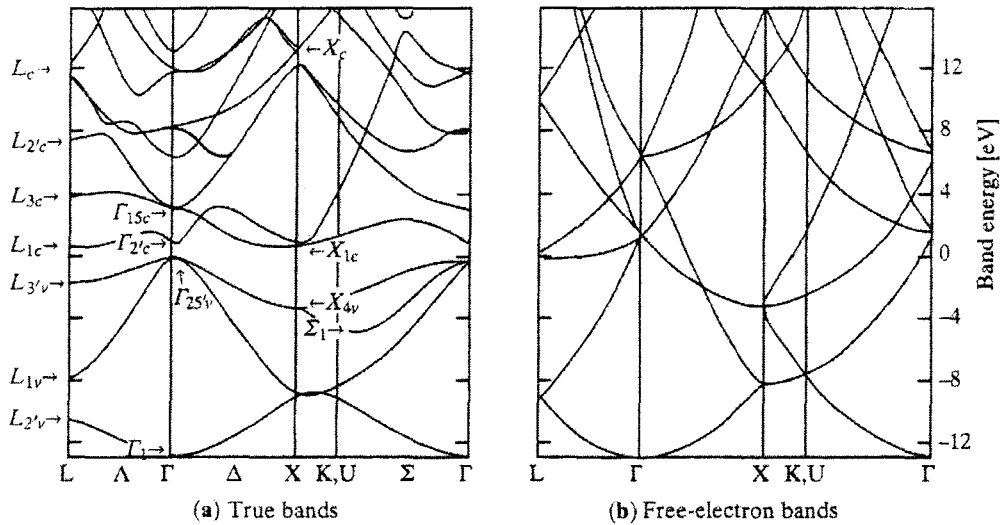
Figure 2-10. Side by side comparison of the band structure of germanium Using (a) EPM Method, and (b) Nearly Free Electron Method [28].

Let us consider Si as an example to build the case for the similarities. The electrons in Si atom are configured as $1s^2 2s^2 2p^6 3s^2 3p^2$. In the crystalline silicon we will have all the electrons except the ones in $3s^2$ and $3p^2$ as the core electrons. The core electrons are restricted to their own atoms and are not free to be in other places in lattice. As in the valence orbitals of $3s^2$ and $3p^2$, the $3p^2$ orbital is partially filled, the orbitals will form the hybridized sp^3 orbitals. The silicon atom will share its four valence electrons with the four neighboring atoms in a tetrahedral arrangement which is the basis of the diamond structure of the silicon lattice. These electrons are partially free and cannot be restricted to one atom only. These nearly free electrons in silicon diamond lattice have a great share in making the backbone of silicon's energy band structure. It is the

41

screening effect lets the valence electrons not be bond to their nucleus. The core electrons screen the effects of the nucleus charge so that the valence electrons cannot feel much of the force of the nucleus. Because the valence electrons are not in the core their wave function are normal to the core states. This can also be explained by the Pauli's exclusion law as there are no more states left for any more electrons in the core region because of this law, So the valence electrons will feel a strong repulsion energy if they enter that region. As a result, the wave functions of the valence electrons have very strong spatial oscillations near the core region. This is what makes the Schrödinger equation so hard to solve for the valence electrons. To overcome this difficulty, with the usage the pseudopotential method, the wave function will be divided into a smooth part and an oscillatory part. The smooth function will then be called the pseudo-wave function. And the oscillatory function is the part which resulted in strong repulsion due to the Pauli's exclusion law near the core region. In pseudopotential method, the true potential will be replaced with the weaker effective potential for the valence electrons. This new potential function is called the pseudopotential. The main job of this potential is to eliminate the oscillatory part of the valence electrons' wave functions near the core region. A schematic of such potential is depicted in figure 2-11.
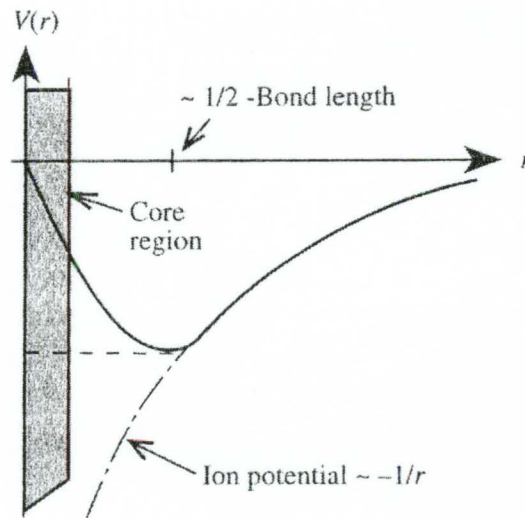
Figure 2-11. The Schematic of an Si atom's pseudopotential. The solid function is called the soft core pseudopotential and the dashed function for the core is called the hard core pseudopotential [35].

As it can be seen in figure 2-11, the tail part of the pseudopotential shown is like the coulomb potential of the Si^{4+} ion. The core region in the soft core pseudopotential is close to the free electron as the potential is approaching zero in the core region. In fact in almost all cases of pseudopotential calculations the soft core pseudopotential is used. And as it can be seen from figure 2-11 the near-the-core potential almost resembles the nearly free electron and that accounts for many of the similarities between the two methods of pseudopotential and nearly free electron method. In fact this similarity is used in the pseudopotential method as will be seen in the next parts.

2.3.2 Basics of Empirical Pseudopotential Method

Let us continue our discussion from the last part and see how the change from the true potential to a pseudopotential changes different things; The smooth part of the wave functions of the valence electrons will not be affected much because they have little weight in the core region of the atom and this fact makes the smooth parts of the valence electrons' wave functions of little sensitivity to the core region potential. It can be mathematically shown that the replacement of the true potential with a wisely chosen pseudopotential will result in the same valence and conduction band [35]. It means that the valence and conduction bands can be correctly calculated from a pseudopotential instead of the true potential. This replacement also eliminates some of the irrelevant core states that will result while using the true potential [35].

Let us now consider a one electron Schrödinger equation and replace the potential inside the equation with the pseudopotential. We will call this new equation the pseudo-wave equation.

$$[\frac{p^2}{2m}+V(r_i)]\psi_k(r_i) = E_k\psi_k(r_i) \qquad (2\text{-}42)$$

Because we are using the pseudopotential in the place of the true potential, we will call ψ the pseudo-wave-function. As it was discussed in the previous paragraphs, the smooth part of the wave function which is outside the core region changes negligibly by the change from true potential to the

44

pseudopotential. So the pseudo-wave-function is a good approximation of the true wave function outside the core region although it has been calculated from the pseudopotential. The pseudo-wave-function can be used for properties of the crystal which are only dependent on the valence and conduction electrons because the near-the-core-region part of the pseudo-wave-function is not like the real wave function in that region, so any property which needs information from the core of the atoms cannot be calculated using this method. As for our objective which is calculating the energy band structure of the crystalline lattices this method can be of great help.

As explained before the core region of the soft core pseudopotential, which we will use in this part, resembles the nearly free electrons. So we will write the pseudo-wave-function as a sum of plane waves to solve our pseudo-wave equation. It should be noted that the notation $|\ \rangle$ refers to a state or in other words, wave function for a specific situation.

$$\psi_k = \sum_g a_g |k+g\rangle \qquad (2\text{-}43)$$

The vectors, g, in equation (2-43) are the reciprocal lattice vectors. And $|k\rangle$ is a plane wave with wave vector k. If we substitute equation (2-43) in equation (2-42), we can solve for E_k and a_g through the secular equation obtained from the substitution shown as equation (2-44).

$$\det\left|[\frac{\hbar^2 k^2}{2m} - E_k]\delta_{k,k+g} + \langle k|V(r)|k+g\rangle\right| = 0 \qquad (2\text{-}44)$$

45

The second term in equation (2-44) shows the matrix elements of $V(r)$ which can be replaced as follows:

$$\left\langle \vec{k} \left| V(\vec{r}) \right| \vec{k} + \vec{g} \right\rangle = \left[\frac{1}{N} \sum_{R} e^{-i\vec{g}\cdot\vec{R}} \right] \frac{1}{\Omega} \int_{\Omega} V(\vec{r}) e^{-i\vec{g}\cdot\vec{r}} dr \qquad (2\text{-}45)$$

In equation (2-45), Ω is the volume of a primitive cell and the vectors named as $\vec{R}$ are the direct lattice vectors. The summation in equation (2-45) will ensure mathematically, the matrix elements of the pseudopotential will be zero unless $\vec{g}$ is a reciprocal lattice vector. The summation will be equal to one when $\vec{g}$ is a reciprocal lattice vector. This means that the matrix elements are the Fourier components of our pseudopotential, which we will call V_g, in the reciprocal lattice space or in other words, the inverse of the real space or the direct lattice space. So if $\vec{g}$ is a reciprocal lattice vector we will have:

$$V_g = \frac{1}{\Omega} \int_{\Omega} V(\vec{r}) e^{-i\vec{g}\cdot\vec{r}} dr \qquad (2\text{-}46)$$

These Fourier components of the pseudopotential are also called the pseudopotential form factors when there is only one atom in the primitive cell of the lattice. Now let us suppose that there are different atoms in the primitive cell. We can calculate V_g for each of them and define a new factor, namely the structure factor, to show the positions of each different kind of atom in the primitive cell. As an example, let us suppose we have a lattice with two different atoms of α and β making it. As a first step, we can calculate V_g for each of the

atom potentials and get $V_{g\alpha}$ and $V_{g\beta}$. It should be noted that these form factors should be calculated using the volume of the atoms. For example $V_{g\alpha}$ should be calculated over the corresponding volume of one α atom. As a next step we calculate a structure factor which is one in the atom positions and zero in all other places to be able to put the potentials at the desired places in the space. This should be done separately for both α and β atoms. Structure factors will be denoted as S_g. As an example the structure factor for the α atoms is:

$$\vec{S}_{g\alpha} = \frac{1}{N_\alpha} \sum_j e^{-i\vec{g}\cdot\vec{r}_{\alpha j}} \qquad (2\text{-}47)$$

N_α is the number of α atoms in the primitive cell and the positions of the α atoms in the primitive cell are denoted by $\vec{r}_{\alpha j}$. We can calculate the structure factor for the β atoms in the same way. Having the form factors for α and β atoms and the structure factor for them as well, we can now express our pseudopotential in terms of the calculated structure and form factors as follows:

$$V(r) = \sum_g (V_{g\alpha}\vec{S}_{g\alpha} + V_{g\beta}\vec{S}_{g\beta})e^{i\vec{g}\cdot\vec{r}} \qquad (2\text{-}48)$$

What we are essentially doing to get the matrix elements of the pseudopotential, is that the pseudopotential mixes the free electrons which have a wave vector difference equal to a reciprocal lattice vector. As an example, looking at equation (2-45), we see that it has been done for a lattice with one kind of atoms. And if we have two degenerate states and the form factor is not zero, the degeneracy will split and open up by the pseudopotential introduced in the

process of mixing the electron states. This fact can also be justified using the Bragg reflection law as the free electron plane waves will be reflected by the introduced pseudopotential. The crystalline structure formation of the pseudopotentials mixes the free electron plane wave functions and results in standing waves. Knowing the basics of the pseudopotential theory now, we will move on to find the pseudopotential form factors for diamond and zinc-blende crystals and pointing out their differences.

2.3.3 Diamond and Zinc-Blende Lattices Pseudopotential Form Factors

In Empirical pseudopotential method we do not always use all of the form factors and usually a small number of form factors are enough to have a good and almost exact approximation of the energy band structure of the lattices we are working on. This is what makes this method useful and easy to use. The number of form factors needed for energy band structure calculation of diamond structures with good accuracy is only three. For zinc-blende structures, six form factors are needed for accurate calculations.

The unit cell in diamond and zinc-blende crystals are made of two atoms. To be general we refer the to atoms pseudopotentials as V_a and V_b, and assume that they are positioned in the unit cell at $\vec{r}_a$ and $\vec{r}_b$. In this way we are able to have discussed both diamond and zinc-blende crystals at the same time. So in the space we have $V_a(\vec{r} - \vec{r}_a)$ and $V_b(\vec{r} - \vec{r}_b)$. To get the Fourier components, namely form factors, we will use equation (2-46).

$$V_g = \frac{1}{\Omega} \int [V_a(\vec{r} - \vec{r}_a) + V_b(\vec{r} - \vec{r}_b)] e^{i\vec{g}\cdot\vec{r}} d\vec{r} \tag{2-49}$$

Through the properties of the Fourier series we can rewrite equation (2-49) as below:

$$V_g = \frac{1}{\Omega} \int [V_a(\vec{r}) e^{-i\vec{g}\cdot\vec{r}_a} + V_b(\vec{r}) e^{-i\vec{g}\cdot\vec{r}_b}] e^{i\vec{g}\cdot\vec{r}} d\vec{r} \tag{2-50}$$

As we know, in diamond and zinc-blend lattices, if we assume that one atom in the unit cell is at the origin, the other atom will be at $\frac{a}{4}(1,1,1)$. But for the propose of simplifying the equation that we have, we will assume that one of the atoms is at $-\frac{a}{8}(1,1,1)$ and the other one is at $\frac{a}{8}(1,1,1)$. It should be reminded that this change will not change any of the physics of the system and is just a mathematical calculation and does not have any affects on the physics of the system. Let us define s as:

$$\vec{s} = \frac{a}{8}(1,1,1) \tag{2-51}$$

And let us assume that:

$$\vec{r}_a = \vec{s} \tag{2-52a}$$

$$\vec{r}_b = -\vec{s} \tag{2-52b}$$

With the new formalism, we can rewrite the argument in the integral of equation (2-50) as below:

$$V_a(\vec{r}) e^{-i\vec{g}\cdot\vec{r}_a} + V_b(\vec{r}) e^{-i\vec{g}\cdot\vec{r}_b} = V_a(\vec{r}) e^{-i\vec{g}\cdot\vec{s}} + V_b(\vec{r}) e^{i\vec{g}\cdot\vec{s}} \tag{2-53a}$$

$$V_a(\vec{r})e^{-i\vec{g}\cdot\vec{s}} + V_b(\vec{r})e^{i\vec{g}\cdot\vec{s}} = (V_a + V_b)\cos(\vec{g}\cdot\vec{s}) - i(V_a - V_b)\sin(\vec{g}\cdot\vec{s}) \tag{2-53b}$$

As the sine and cosine arguments are not dependent on $\vec{r}$ they can be taken out of the integral of equation (2-50). We can now divide V_g to two symmetric and asymmetric components and define them as follows:

$$V_g^s = \frac{1}{\Omega}\int(V_a + V_b)e^{-i\vec{g}\cdot\vec{r}}\,d\vec{r} \tag{2-54a}$$

$$V_g^a = \frac{1}{\Omega}\int(V_a - V_b)e^{-i\vec{g}\cdot\vec{r}}\,d\vec{r} \tag{2-54b}$$

Now we can have the integral of equation (2-50) written in terms of the symmetric and asymmetric form factors.

$$V_g = V_g^s\cos(\vec{g}\cdot\vec{s}) - iV_g^a\sin(\vec{g}\cdot\vec{s}) \tag{2-55}$$

By using the symmetric and asymmetric notation, we are able to eliminate the asymmetric part of the form factor for the diamond structure. This is because the potentials V_a and V_b are the same for the diamond structures. And now we can say that for the diamond structure, the term $\cos(\vec{g}\cdot\vec{s})$ is the structure factor just like what we had in equation (2-47). As for the zinc-blende structures, the asymmetric part of the form factor does not vanish. Only if the anion and cation potentials have very small difference then the asymmetric potential will be much smaller than the symmetric part. In most cases we have to take into account both symmetric and asymmetric potentials should be taken into account. Knowing what we have to take into account, we now take a look at the reciprocal lattice

vectors in diamond and zinc-blende structures. they are listed in the order of magnitude below:

$$g_0 = \frac{2\pi}{a}(0,0,0) \tag{2-56a}$$

$$\vec{g}_3 = \frac{2\pi}{a}(1,1,1), \frac{2\pi}{a}(1,1,-1),..., \frac{2\pi}{a}(-1,-1,-1) \tag{2-56b}$$

$$\vec{g}_4 = \frac{2\pi}{a}(2,0,0), \frac{2\pi}{a}(-2,0,0),..., \frac{2\pi}{a}(0,0,-2) \tag{2-56c}$$

$$\vec{g}_8 = \frac{2\pi}{a}(2,2,0), \frac{2\pi}{a}(2,-2,0),..., \frac{2\pi}{a}(0,-2,-2) \tag{2-56d}$$

$$\vec{g}_{11} = \frac{2\pi}{a}(3,1,1), \frac{2\pi}{a}(-3,1,1),..., \frac{2\pi}{a}(-3,-1,-1) \tag{2-56e}$$

The pseudopotential form factors when $g^2 > 11(\frac{2\pi}{a})^2$ can generally be neglected because V_g decreases like g^{-2} for large $\vec{g}$. A schematic of how V_g changes with respect to $\vec{g}$ is shown in figure 2-12.
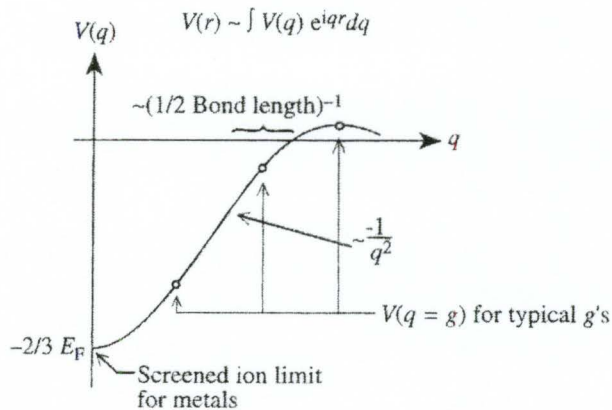
Figure 2-12. A schematic of the dependency of V_g, the pseudopotential form factor, on $\vec{g}$ in the reciprocal lattice [35].

As we can see from equation (2-49) or equations (2-54a) and (2-54b) the first form factor which corresponds to $\vec{g}_0$ will be a constant number, which in fact makes a shift in the entire energy scale of the calculations, therefore we can choose it to be any convenient value for us. It can be assumed to be zero or any other number to make the calculations easier. We will refer to any pseudopotential form factor corresponding to $\vec{g}_i$ as V_i. As we said the only terms that we will discuss will be $\vec{g}_0$, $\vec{g}_3$, $\vec{g}_4$, $\vec{g}_8$, $\vec{g}_{11}$ because the other terms will be small and negligible. The pseudopotential form factor for the equivalent reciprocal lattice vectors will be the same because of the symmetry that exists in the crystal, so, as an example, the for all the $\vec{g}_3 = \dfrac{2\pi}{a}(\pm1,\pm1,\pm1)$ the form factors are equal because of the symmetry and we denote all of them as stated earlier as V_3.

Now, it will be shown that considering only $\vec{g}_3$, $\vec{g}_4$, $\vec{g}_8$, $\vec{g}_{11}$ reciprocal lattice vectors, the number of form factors required to calculate the energy band structure of a diamond structure is only three factors and the number of form factors needed to calculate the energy band structure of a zinc-blende structure is six. Because the form factors for $\vec{g}_0$ are constant and can be chosen to be any value to shift the whole energy band structure up or down, they are not included in the calculations. It is clear from equation (2-54b) that all V_i^a are zero for the

diamond structures and thus they are not considered for the calculations. The symmetric form factors should all be considered, but if we take a closer look at the structure factor for the symmetric form factors in equation (2-55), it is clear that it will be zero for V_4^s. As we know in equation (2-55), $\vec{s} = \frac{a}{8}(1,1,1)$ and for V_4^s we have $\vec{g}_4 = \frac{2\pi}{a}(2,0,0), \frac{2\pi}{a}(-2,0,0),..., \frac{2\pi}{a}(0,0,-2)$ so the symmetric structure factor $\cos(\vec{g} \cdot \vec{s})$ can be calculated for g_4 as follows:

$$\cos(\vec{g} \cdot \vec{s}) = \cos(\pm \frac{\pi}{2}) = 0 \tag{2-57}$$

The point shown for V_4^s and its structure factor is correct for both diamond and zinc-blende structures. we can neglect V_4^s and do not take it into account because the structure factor for it is zero. So for the diamond structure we only need to take V_3^s, V_8^s, and V_{11}^s into account for the EPM calculations. So we only have to take three terms into account for the diamond structure that makes this method a favorable method despite its other complexities. For the zinc-blende structure we have to take the asymmetric terms into account too, but just like the symmetric structure factor, if we look at the structure factor for the asymmetric form factors too, we see that the structure factor for $\vec{g}_8 = \frac{2\pi}{a}(2,2,0),..., \frac{2\pi}{a}(0,-2,-2)$ will be zero. As we know $\vec{s} = \frac{a}{8}(1,1,1)$ and the asymmetric structure factor is $\sin(\vec{g} \cdot \vec{s})$, so the asymmetric structure factor for $\vec{g}_8$ is as follows:

$$\sin(\vec{g} \cdot \vec{s}) = \sin(0, \pm \pi) = 0 \qquad (2\text{-}58)$$

So there is no need to take V_8^a into account for the EPM calculations of any zinc-blende structure. As a result we will only need to take V_3^s, V_8^s, V_{11}^s, V_3^a, V_4^a, and V_{11}^a into account for the empirical pseudopotential method calculations of the zinc-blende structure. The need for only six terms for calculating the energy band structure of a zinc-blende structure is in fact a good point that makes this method a good way of calculating the full energy band structure of the zinc-blende structures. In many studies, which only the optical properties of the zinc-blend materials are important, k.p. method is used to calculate a partial energy band structure of these structures around $\vec{k} = 0$ point.

2.3.4 The Empirical Pseudopotential Method Algorithm

As we discussed in the last parts, this method is based on form factors and structure factors. The EPM uses the form and structure factors and solves the pseudo-wave equation. After solving the equation, the solutions are used to calculate some properties of the lattice being discussed and the results of the calculations will be compared to the experimental data. The form factors will be changed and the pseudo-wave equation will be solved again until an agreement between the calculated and experimental properties is made. There are many experimental properties that can be used as a refining tool for the pseudopotential and the form factors. Position of optical peaks in optical

54

reflectivity spectra, density of states, and features in the photoelectron spectra are some of the properties that can be used in the process of the empirical pseudopotential method to calculate the energy band structure of the lattices.

To summarize this method in a few lines, we can introduce the following general procedure for the empirical pseudopotential method:

a. Calculate V_g, the form factors.

b. Calculate $V(\vec{r})$ as a sum of the form factors:

$$V(\vec{r}) = \sum_g V_g e^{-i\vec{g}\cdot\vec{r}}$$
(2-59)

c. Calculate the Hamiltonian:

$$H = \frac{p^2}{2m} + V(\vec{r})$$
(2-60)

d. Solve the pseudo-wave equation:

$$H\psi_k(\vec{r}) = E_k\psi_k(\vec{r})$$
(2-61)

and obtain E_k and ψ_k.

e. Calculate physical, electrical, or optical properties of the lattice and compare with experimental data.

f. If there is no satisfactory agreement between the calculated and experimental data, change and/or refine V_g, the form factors, and repeat from start.

There are two major disadvantages in this method. The first one is that this method needs experimental data inputs in the process of finding the energy band structure. In fact, this way, we are not working only using a theory but using some experimental inputs that must be known before hand when starting calculations. So this method cannot be good to predict the properties of the materials that are not yet made and scientists do not have a way of making them yet, because to get results from this method we have to have some experimental data on hand to use in the process of refining and changing the pseudopotential to reach the correct energy band structure for the discussed material.

The second disadvantage is that there is no solid way to change the pseudopotential when it does not agree with the experimental data, because there are several different experimental data that can be considered for the pseudopotential refining process, one should make their own way of refining the pseudopotential according to the experimental data that is being used which leads to many different approaches and not one solid standard process. Of course, one would argue this is giving the method some kind of flexibility that other methods do not have, but this might result in excessive complexity which is not desired in any process. However this may be useful for some particular cases.

The first disadvantage can also be considered less important as in many cases a pseudopotential that is calculated for one particular atom in a lattice and results in the correct energy band structure, can be transferred and be used in

other structures containing that same atom. For example, the pseudopotential for Ga that is resulting in the right energy band structure in the zinc-blende structure of GaAs, can be used for the calculations of other structures such as GaSb and GaP. Sometimes there are cases that will need some calculations and changes on the pseudopotential before the pseudopotential is ready to be used for other structures.

2.4 The Self-Consistent Pseudopotential Method

Self-consistent pseudopotential method is also called ab-initio pseudopotential method, because this method solves the energy band structure problems from first principles only. The Latin word, ab-initio, means from first principles. In this method, the pseudopotential is changed based on the information that we get from the results of the Schrödinger equation with the pseudopotential introduced instead of the real potential, or in other words, the pseudo-wave equation. Using only the results of the method and some theoretical formulae, the self-consistent pseudopotential method relies only on the principles of physics rather than on experimental results. The experimental results can be of great use too, but the goal is to use minimal number of experimental results or none at all [36].

The Self-Consistent Pseudopotential Method, also called SCPM in this thesis, is like the empirical pseudopotential method in the sense that both will solve the pseudo-wave equation or in other words the Schrödinger equation with

the pseudopotential applied, and then change the pseudopotential based on the results of the pseudo-wave equation. The general algorithm of the self-consistent pseudopotential method is as follows: [28]

a. A pseudopotential for the ions in the crystalline lattice, $V_{ion}(\vec{r})$, is chosen.

$$V(\vec{r}) = V_{ion}(\vec{r}) \tag{2-62}$$

b. The Hamiltonian is calculated for a single electron in the lattice:

$$H = \frac{p^2}{2m} + V \tag{2-63}$$

c. The Schrödinger equation for the pseudopotential, pseudo-wave equation, is solved:

$$H\psi = E\psi \tag{2-64}$$

d. The charge density for the occupied states of the calculated pseudo-wave functions are found:

$$\rho = \sum_{occ} \psi^* \psi \tag{2-65}$$

e. The Hartree potential is calculated using the Poisson's equation:

$$\nabla^2 V_{Hartree} = \frac{\rho}{\varepsilon_0} \tag{2-66}$$

f. As the equations are solved for one electron in the lattice, the effect of other electrons in the lattice will be included with an exchange and correlation potential term which is a function of the charge distribution calculated from the pseudo-wave function. The functions used in this

part are a large variety, but one of the best approximations that is used

is the Local Density Approximation function or the LDA function:

$$\nabla^2 V_{Hartree} = \frac{\rho}{\varepsilon_0}$$
(2-67)

g. The self-consistent potential which will be added to the pseudopotential, or the $V_{ion}(r)$ in the first step of the algorithm, is calculated as a sum of the Hartree potential and the exchange and correlation potential:

$$V_{sc} = V_{Hartree} + V_{xc}$$
(2-68)

h. The pseudopotential will be modified to the following:

$$V(r) = V_{ion} + V_{sc}$$
(2-69)

i. The new pseudopotential is applied to "b" and the loop continues until the charge density, ρ, that is derived from the new pseudopotential and the old pseudopotential are equal or close to each other with the accuracy that is desired.

There are a number of ways of utilizing this algorithm to work for us. There are three major parts that differ in different algorithms. The first point of difference in different algorithms is the starting pseudopotential or the so-called ion pseudopotential. There are a great number of starting pseudopotentials and every research may or may not use one that has been used before. There are however some pseudopotentials that have been used more than others. The

second point of the division is solving the pseudo-wave equation. This part of the algorithm along with calculating the exchange and correlation potential, which may be called XC potential hereafter, are the most time-consuming parts of the algorithms. So choosing a good way to solve the Schrödinger equation efficiently and accurately is a critical point for a good algorithm. The third part that is different in algorithms is the approximation in finding the exchange and correlation potential, where LDA has proved to be a reliable method. There are both simpler approximations and more sophisticated approximations but the simpler approaches are not as accurate and the more sophisticated approximations, such as non-local density approximation, do not add as much to the accuracy as they take away the efficiency of the whole algorithm. So, to maintain a good level of both the accuracy and efficiency, most algorithms rely on the LDA or some modification of it rather than using any other approximation. However, if the goal is only the accuracy and not the cost and efficiency some algorithms may use sophisticated methods like the non-local density approximation. So this part will be a third point of difference between algorithms for this sake. The different choices of pseudopotentials will be discussed briefly with a few different pseudopotentials introduced. Different methods to solve the Schrödinger equation will not be discussed in detail as it is more a mathematical procedure than an important theoretical part of this method. For the exchange and correlation potential approximation part, LDA will be discussed in detail but

other methods will not be discussed as they are rarely used to approximate the exchange and correlation potential in self-consistent pseudopotential method.

2.4.1 Different Pseudopotential Choices for SCPM

Through the years many pseudopotentials have been introduced. Some have introduced pseudopotentials that are just good for one material [37], others have introduced methods of producing efficient pseudopotentials or a property to be added to an existing pseudopotential to make it more efficient that can be used for many materials [21, 22, 25]. All of the methods in introducing pseudopotentials replace the core potential with another function and leave the tail potential unchanged and that of the lattice ions. It should however be noted that the cut-off radius which sets the boundary for the core and tail region is different in different methods. Theoretically, the number of the pseudopotentials that can lead to the same electronic energy band structure are limitless. The goal is to have the most efficient pseudopotential that will need the least number of calculation loops until the electronic band structure is calculated. The choice of pseudopotentials can be different based on different methods of iteration.

Appelbaum and Hamann [37] introduced a pseudopotential for the silicon ions which could be used for the self-consistent pseudopotential method and the energy gaps in the electronic band structure derived from this pseudopotential agreed with the experimental results for silicon. They had replaced the core potential with an exponential function and they had left three parameters to be

set for the best efficiency. They have introduced a set of numbers for the parameters that they assumed are the best but have left it to other researchers to use that numbers or use their own numbers that they feel would make the pseudopotential more efficient. This gives their pseudopotential the possibility to even be reproduced for other materials if their theory is used for other materials. Although it is one of the early works of introducing pseudopotentials but it proves to be a good pseudopotential as it leads to the results that agree with experiment.

In 1979 Hamann, *et al.* [21] introduced the norm-conserving pseudopotentials. Other pseudopotentials which gave the results did calculate the wave functions but they differed from the real wave functions with a normalization factor. The norm-conserving pseudopotentials do not have this effect and result in the same wave function in the valence band region, or the tale region, without the need for a normalization factor. The general formula that they give for the pseudopotential is:

$$V_{ps} = (1 - f(\frac{|\vec{r}|}{r_c}))V(r) + cf(\frac{|\vec{r}|}{r_c}) \tag{2-70}$$

where $V(r)$ is the real potential and c is a parameter that can be chosen depending on r_c. $f(x)$ is a function that approaches zero as $x \to \infty$ and it has a cut-off of $x = 1$, so the pseudopotential will be like the real potential after the cut-off radius. One of the choices that have been introduced by them for this function is:

$$f(x) = e^{-x^4} \qquad\qquad\qquad\qquad (2\text{-}71)$$

This pseudopotential can be modified so that it will be a soft-core pseudopotential.

In 1982, Bachelet, *et al.* [22] introduced a general method for generating pseudopotentials for any material. Although this method can be very useful for materials that are not very much discussed and are relatively less known and used but it is not the best way of choosing a pseudopotential when discussing highly used materials like silicon, germanium, Gallium or Arsenide. It is best to use the methods that are considered standards like the norm-conserving pseudopotentials or a method of our own if we would like to use our own pseudopotentials.

One of the latest and most important improvements on the pseudopotentials was done in 1990 when Vanderbilt [25] introduced the soft pseudopotentials where the norm-conservation constraints were removed. These pseudopotentials were especially good for general eigen-value problems and for plane-wave basis calculations. This method has highly modified the works of Hamann, *et al.* [21]. After the works of Vanderbilt, many of the calculations in the self-consistent pseudopotential method are done using the soft and ultra-soft pseudopotentials although many researchers also use their own pseudopotentials which are best suitable for the materials they are trying to calculate their properties.

2.4.2 Solving the Schrödinger Equation

There are many methods for solving Schrödinger equation in different studies. For the self-consistent pseudopotential method for solving the electronic band structure for the crystalline lattices, the problem of solving the Schrödinger equation has to be solved for a more defined environment so the general ways of solving the Schrödinger equation in general cases will not prove the most efficient. Methods like Finite Difference method are used in many cases for solving the Schrödinger equation in general problems. But as the environment is being defined, methods that are designed and made for that environment will prove faster and more reliable. For crystalline lattices or in other words, the 3D periodic potentials in the space, in mathematical terms there are a number of methods that are being used to solve the Schrödinger equation with. The most widely used method is the Orthogonal Plane Wave method, OPW. This method will be discussed in detail in the next chapters. However there are other methods that are being used to solve the Schrödinger equation and will only be introduced here briefly. References are provided for these methods for follow up but as these are more mathematical methods and they are not part of the theory of the self-consistent pseudopotential method, they are only introduced very briefly. It should be noted that from the numerical calculations point of view it is one of the most efficient ways to be used. Other famous methods such as APW and KKR are allowing solutions for a wide class of materials but they require very complex and non-efficient numerical calculations that make it nearly impossible for being

used for truly self-consistent calculations [38] and they may need limited experimental data for best results.

The Augmented Plane Wave method or APW is introduced and discussed in details in references [39-40]. The KKR method was developed by Korringa [41], Kohn and Rostoker [42]. This method is also known as the Green's function method. The KKR method tries to solve the all electron method from the start instead of solving the one electron method and including the exchange and correlation potential later. More information on this method can also be found in [43]. Another method to be mentioned here for reference is Linear Muffin-Tin Orbital method also known as LMTO. This method can be used for a variety of materials but acts best for close-packed solids [24]. For more details on LMTO method the reader is referred to [38, 44]. There are some other methods for solving Schrödinger equation in crystals but as a matter of fact, OPW is one of the widely used methods so we will only discuss this method in the next chapters.

2.4.3 Exchange and Correlation Potential: The LDA Approach

The exchange and correlation potential does not have any simple expression for an arbitrary density function, [14] therefore there are different approximations for this potential. To be able to explain the LDA in detail, one needs to get familiar with the Density Functional Theory, DFT. In LDA method, one assumes that the exchange and correlation energy at a point is only a

function of the density functional at the same point. In other words the density of the electrons at other parts of space has no effect on the exchange and correlation energy at the specific point that is being discussed. In this part we will have an introduction to the density functional theory, and after that we will discuss the LDA and finally a sample platform of a set of self-consistent iterating equations for solving a system will be developed.

2.4.3.1 An Introduction to the Density Functional Theory

To solve the many body systems using the Schrödinger equation, one has to deal with a wave function that is dependant on the position of all the particles. If there are N particles in the system, then the wave function will be a function of $3N$ variables. To avoid the complexity, the density functional theory assumes that the density functional of the system is the central variable rather than the wave function. This assumption reduces the number of variables from $3N$ to only 3 and reduces the complexity of the problems. The density functional theory was first developed by Thomas [45] and Fermi [46] in the late 1920's. They had treated the kinetic energy of a system of electrons as a function of the density of electrons, but like the Hartree-Fock method, they had not included anything about the electrons exchange and correlation energies. In early 1930's, Dirac [47] couldn't improve the method significantly by adding the exchange and correlation through a set of formulae. This method was being refined and improved over the time, but got the most attention only after the refinements that

are known as Hohenberg-Kohn-Sham formulation of DFT [13, 14]. This formulation is one of the state-of-the-art formulations that is applied in the electronic band structure theory in many of the cases. Hereafter, we will discuss the

Hohenberg-Kohn-Sham DFT. This theory is based upon a remarkable and not so complex theorem. It should be noted that instead of dealing with the lattice we assume that we have an electron gas in a large box and the electrons are moving under the influence of an external potential of $v(\vec{r})$, which we consider it to be v_{ion}. Under this assumption the theorem is as follows:

- Theorem: the external potential is a unique function of the density of electrons only.

When the external potential is a function of the density of the electrons, so will the Hamiltonian and the ground state properties be a function of the density of electrons.

It is known that the Hamiltonian of the many-body system will determine the ground state of the system. So this theorem concludes that this Hamiltonian itself is a function of the density of electrons. Based on this, the kinetic and electron-electron interaction energies themselves, which include the exchange and correlation energies, will also be functions of the density of electrons, $\rho(\vec{r})$. The function is then defined as:

$$F[\rho(\vec{r})] = \langle \Psi | (T + U) | \Psi \rangle \tag{2-72}$$

T is the operator for the kinetic energy and U is the operator for the electron-electron interaction energy. This function is a general function which is right for any system with any external potential because it has the same dependence on electron density in any system.

For a given external potential, $v(\vec{r})$, the energy functional of the system can be described as:

$$E[\rho(\vec{r})] = \int v(\vec{r})\rho(\vec{r})d\vec{r} + F[\rho(\vec{r})] \qquad (2\text{-}73)$$

As mentioned, $F[\rho(\vec{r})]$ is a general function of electron density for any system but it is an unknown function yet. The energy functional in terms of the Hamiltonian of the many body system and its wave function, Ψ, can be written as:

$$E[\rho(\vec{r})] = \langle \Psi | H | \Psi \rangle \qquad (2\text{-}74)$$

where the Hamiltonian of the system is:

$$H = f + V \qquad (2\text{-}75a)$$

and:

$$f = T + U \qquad (2\text{-}75b)$$

The discussions above can help us in proving the first theorem which is an important part of the DFT. This theorem is proven by *reductio ad absurdum*. Assume that there are two different external potentials, $v_1(\vec{r})$ and $v_2(\vec{r})$, which do not differ by only a constant, i.e. $v_1(\vec{r}) - v_2(\vec{r}) \neq const$. These potentials will in turn

lead to two different ground state energies, E_1 and E_2, and two different wave functions, Ψ_1 and Ψ_2, but they will lead to the same electron density of $\rho(\vec{r})$.

As it is assumed that E_1 is the ground state energy of the first system, any other energy related to this system is more than E_1. This fact results in the following inequality:

$$E_1 < \langle \Psi_2 | H_1 | \Psi_2 \rangle = \langle \Psi_2 | H_2 | \Psi_2 \rangle + \langle \Psi_2 | H_1 - H_2 | \Psi_2 \rangle \tag{2-76a}$$

$$\Rightarrow E_1 < E_2 + \int \rho(\vec{r})[v_1(\vec{r}) - v_2(\vec{r})]d\vec{r} \tag{2-76b}$$

The same argument can be made for the second system and the following inequality can be reached in the exact same way:

$$E_2 < E_1 + \int \rho(\vec{r})[v_2(\vec{r}) - v_1(\vec{r})]d\vec{r} \tag{2-77}$$

By adding the inequalities in equations (2-76b) and (2-77) we will have an inconsistency:

$$E_1 + E_2 < E_1 + E_2 \tag{2-78}$$

Thus we proven the theorem that $v(\vec{r})$ is a unique functional of $\rho(\vec{r})$. And because the many-body system's Hamiltonian is a function of $v(\vec{r})$, it can be concluded that the many-body system's ground state is a unique functional of $\rho(\vec{r})$ too.

As said before we are assuming that we are dealing with an electron gas in a large box and the electrons are moving under the influence of an external

potential of $v(\vec{r})$. Let us now introduce the Hamiltonian in more details. As it is known:

$$H = V + T + U \tag{2-79}$$

The following describes each part of the Hamiltonian in atomic units: [13]

$$T \equiv \frac{1}{2}\int \nabla \psi^*(\vec{r})\nabla \psi(\vec{r})d\vec{r} \tag{2-80}$$

$$V \equiv \int v(\vec{r})\psi^*(\vec{r})\psi(\vec{r})d\vec{r} \tag{2-81}$$

$$U = \frac{1}{2}\iint \frac{1}{|\vec{r}-\vec{r}'|}\psi^*(\vec{r})\psi^*(\vec{r}')\psi(\vec{r}')\psi(\vec{r})d\vec{r}d\vec{r}' \tag{2-82}$$

And most importantly: [13]

$$\rho(\vec{r}) \equiv \langle \Psi | \psi^*(\vec{r})\psi(\vec{r}) | \Psi \rangle \tag{2-83}$$

For any external potential the energy functional of the system is:

$$E[\rho(\vec{r})] = \int v(\vec{r})\rho(\vec{r})d\vec{r} + F[\rho(\vec{r})] \tag{2-84}$$

If we choose the density of the electrons, $\rho(\vec{r})$, correctly, this energy functional will be the ground state energy of the many-body system. If it is shown that this energy functional will have its minimum value for the correct electron density, with all the applied electron densities having the following property in equation (2-85), we are able to find the electron density functional through minimizing the energy functional. It means an electron density functional which minimizes the energy functional in equation (2-88) is the correct electron density functional of the system.

$$N[\rho] = \int \rho(\vec{r})d\vec{r} = N \tag{2-85}$$

where N is the number of particles in the many-body system.

It is known that for a system with the correct ground state of Ψ, the energy functional for any state of Ψ' in which the number of electrons remains the same, is:

$$E[\Psi'] = \langle \Psi'|V|\Psi' \rangle + \langle \Psi'|(T+U)|\Psi' \rangle \tag{2-86}$$

And it is known that this function has its minimum at the correct ground state of Ψ. Now if we let Ψ' be the ground state of another system with the external potential of $v'(\vec{r})$, by using (2-86) and (2-72) it can be said that:

$$E[\Psi'] = \int v(\vec{r})\rho'(\vec{r})d\vec{r} + F[\rho'(\vec{r})] > E[\Psi] = \int v(\vec{r})\rho(\vec{r})dr + F[\rho(\vec{r})] \tag{2-87}$$

So the fact that the energy functional is minimal with the electron density functional corresponding to the ground state energy is proved relative to all other density functions that are associated with another external potential. This makes finding the correct electron density function and the ground state energy functional a minimization problem, but the major complexity of this problem is to find the Universal function of $F[\rho]$. More details on finding this function in different systems can be found in [13]. It is only noted that for finding this function it also is spitted to two functions, one of which is the coulomb energy and the other which is described as $G[\rho]$, is a universal function which is unknown at this time and will be revealed after some calculations for a given system.

$$F[\rho] = \frac{1}{2} \iint \frac{\rho(\vec{r})\rho(\vec{r}')}{|\vec{r} - \vec{r}'|} d\vec{r}d\vec{r}' + G[\rho] \qquad (2\text{-}88)$$

An approximation to $G[\rho]$ is calculated for two systems in [13]. One of which is an electron gas of almost constant density and the other is an electron gas with slowly varying density. To follow more on DFT, one can also read [48].

2.4.3.2 Local Density Approximation: The Kohn-Sham equations

As it was shown in the last section the ground energy functional of an electron gas system is equal to:

$$E = \int v(\vec{r})\rho(\vec{r})d\vec{r} + \frac{1}{2} \iint \frac{\rho(\vec{r})\rho(\vec{r}')}{|\vec{r} - \vec{r}'|} d\vec{r}d\vec{r}' + G[\rho(\vec{r})] \qquad (2\text{-}89)$$

To include the exchange and correlation energy, $G[\rho]$ is written as:

$$G[\rho] \equiv T_s[\rho] + E_{xc}[\rho] \qquad (2\text{-}90)$$

It is reminded that this expression is a minimum for the correct electron density function of $\rho(\vec{r})$. The approximation expression for $T_s[\rho]$ in a system of slowly-varying electron density is [14]:

$$T_s[\rho] \cong \int \frac{3}{10}(3\pi^2 \rho(\vec{r}))^{\frac{2}{3}} \rho(\vec{r})dr \qquad (2\text{-}91)$$

One can also use more complicated approximations or even use exact formula for $T_s[\rho]$, but for band structure calculations in ordinary materials which are generally in the category of slowly-varying electron density systems, this is a

good approximation which also prevents extreme complexities in the calculations of the electronic band structure. Now that a good approximation of $T_s[\rho]$ is specified, the only part that remains be specified is the exchange and correlation energy.

The exchange and correlation energy in the Kohn-Sham approximation is defined as:

$$E_{xc}[\rho(\vec{r})] = \int \rho(\vec{r})\varepsilon_{xc}(\rho(\vec{r}))d\vec{r} \qquad (2\text{-}92)$$

In equation (2-92), $\varepsilon_{xc}(\rho(\vec{r}))$ is the exchange and correlation energy of a single electron in a uniformly distributed electron gas with the density of $\rho(\vec{r})$. There are several good approximations that can be used to describe $\varepsilon_{xc}(\rho(\vec{r}))$. The most commonly used parameterization for the homogenous electron gas's ε_{xc} is developed by Perdew and Zunger [49], however, in the original Kohn-Sham approximations that of [50] was originally used. The Perdew-Zunger Method is based on the Monte Carlo calculations done by Ceperly and Alder [51]. There are other methods developed for calculation of an approximation to ε_{xc} such as Cole-Perdew method [52], Lee-Yang-Parr Method [53], and Perdew-Wang Method [54]. It should be noted that none of these methods give a single formula for ε_{xc}, but they rather give an algorithm of finding ε_{xc} at any point or in a more general manner some would show how to find the exchange energy and the correlation energy separately. After finding these two energies separately, they will be added for the total which is the Exchange and Correlation Energy.

As these methods contain a lot of mathematics and will not help the understanding of the whole idea, we will not discuss them here and continue the discussion with the assumption that $E_{xc}[\rho(\vec{r})]$ is now available. After finding the exchange and correlation energy, the next step is to find the new effective potential to solve the Schrödinger equation again with it. As a matter of fact, having the total energy functional of the system, finding the new effective potential is not a complex job. The new effective potential can be calculated using the following formula:

$$v_{eff}(\vec{r}) = v(\vec{r}) + v_{Hartree}(\vec{r}) + v_{xc}(\vec{r}) \tag{2-93}$$

where $v_{Hartree}(\vec{r})$ and $v_{xc}(\vec{r})$ can be calculated using the following equations:

$$v_{Hartree}(\vec{r}) = \int \frac{\rho(\vec{r}')}{|\vec{r} - \vec{r}'|} d\vec{r}' \tag{2-94}$$

$$v_{xc}(\vec{r}) = \frac{\delta E_{xc}[\rho(\vec{r})]}{\delta \rho(\vec{r})} = \frac{\partial[\rho(\vec{r})\varepsilon_{xc}(\rho(\vec{r}))]}{\partial \rho(\vec{r})} \tag{2-95}$$

Knowing the new effective potential, the iteration scheme for finding the effective potential which ultimately leads to the density function that minimizes the energy functional of the system is completed. The iteration should be continued until the desired accuracy is reached. It should be noted that this effective potential is also called the Kohn-Sham effective potential.

2.5 Applications of the Pseudopotential Method

The pseudopotential method has contributed a lot to science and engineering. This method has lots of applications and it is difficult to count them all. In this part, we will divide the applications into two groups. The first group of applications are the empirical pseudopotential method, EPM, applications and the second group are the self-consistent pseudopotential method, SCPM, applications. A small number of applications will be introduced in each part.

2.5.1 EPM Applications

The EPM has been used to solve the electronic band structures of molecules as well as semiconductor lattices, semiconductor superlattices, nanostructures and metals. Although there are lots of work that has been done in molecular level but because most of it is in chemistry field, we will only mention one example in this part which is being worked on now in nanotechnology. Among the works done in molecular level, the work done by Jiang and Gan [55] on the C_{60} molecule is a great example. In this work an empirical pseudopotential has been developed to calculate the energy levels of the C_{60} molecule for further use.

From the works done on metals using the EPM, we can mention the calculation of the energy band structure of Copper [56] as a good example. Finding the electronic band structure of the metals that have electrons in their d orbitals has always been a hard task. But in [56], the band structure of Copper

has been calculated successfully and it is stated that other noble metals, noble metal compounds and even the transition metals can be subject to the pseudopotential like the one that has been developed for solving the band structure of Copper empirically. Another example of applications of the empirical pseudopotential method in metals is [57] which has calculated the properties of the transition metal compound niobium nitride, including its electronic band structure and density of states.

We will mention a few of the works from the works done on semiconductors using the empirical pseudopotential method. D. Brust has done the calculations of the electronic band structure of silicon and germanium with empirical pseudopotential with very good accuracy in [58]. Others like [59] have derived other properties of silicon (or other semiconductors) after calculating the electronic band structure with the use of empirical pseudopotential calculations. In [59] a frequency dependent dielectric function as well as a wave-vector dependent dielectric function for silicon has been found after calculating the electronic band structure of silicon with EPM. Among works done on superlattices we can mention the work done on SiGe superlattices in [60]. The electronic band structure of the SiGe superlattices have been found by finding the best suiting pseudopotentials for silicon and germanium which can reproduce the correct electronic band structure of the $Si_{1-x}Ge_x$ Superlattice in a wide range. The works done on binary semiconductors like GaAs, GaP, etc. should also be mentioned. As an example the reader can be referred to [61] which has

calculated the electronic band structure of GaAs, GaP, ZnSe, and ZnS as well as their reflectivity and modulated reflectivity. Although there is a lot of research that has been done in empirical pseudopotential method, we have shown different works in different areas of this method which gives a whole picture of the research that has been done in this field.

2.5.2 SCPM Applications

There are a significant number of works that have been done in the field of self-consistent pseudopotential method. There are a number of research works that have been referenced in this thesis in the background of research part. However, we will introduce some other researches as well as introducing some of the works already referenced here for completeness of this part.

Self consistent pseudopotential has been used to find the electronic band structure of many metals [16], Semiconductors [37, 62], and even insulators like NaCl [63], NaBr [18], and KCl [19]. In [16] a new form of pseudopotential that is suitable for being used for metals has been introduced and the electronic band structure of Lithium has been calculated. Although the use of the LCAO method for finding the electronic band structure of the metals is common, but because of the inaccuracy of that method in the core bands which might be useful to find some of the properties of the materials, some researchers prefer to use the EPM or SCPM to find the electronic band structure metals. There are many applications for SCPM in semiconductors, the most important of them is finding some of the basic and even advanced properties of the semiconductors like the

electronic band structure, dielectric constant, optical band gap, charge density, etc.

There are many researches that have been done on finding the electronic band structure of silicon alone. Among these researches the reader is referred to [37]. Although there are a lot of research works done on binary, ternary, and more complicated semiconductors, we refer to [62] as the first research done on a II-VI compound semiconductor, MgO, to calculate its energy band structure using the SCPM, through the Hartree-Fock scheme. In [64], the reader can find the application of SCPM in finding the ground state properties of GaAs and AlAs which is an example of the works that have been done on III-V semiconductor materials. As for germanium, there are a number of researches done for finding the electronic band structure. The reader is referred to [65] for the application of SCPM for finding the electronic band structure of germanium.

As mentioned, there are a number of works that have calculated the electronic band structure of the insulators. Other than the ones mentioned before, the reader is referred to the study done on boron to find its electron affinity in [66]. Studies on boron are important for some researchers as this material is used as doping for silicon.

There are also research works being done on molecules and atoms using the SCPM. From these researches, one can point to [67] as it develops a method and uses it for the Si_2 molecule. Most of the usage of SCPM on the molecules is

related to the field of chemistry so we will not introduce anymore applications for molecules.

There are other applications to the SCPM that are not related to this thesis and they are not discussed here, but it should be noted that the usage of the SCPM is not limited to finding the band structure of the molecules or bulk materials only. It can also be used to find the surface states of a material, to study the properties of a junction, and many other properties of the materials.

2.6 Summary

In this chapter an introduction to quantum mechanics were reviewed. The idea of the translational symmetry in the crystals was carefully investigated and the Brillouin zones were introduced.

Different methods of finding the electronic band structure of the crystalline materials were reviewed. Table (2-1) summarizes the Advantages and Limitations of these methods.

Calculation Method	Advantages	Limitations
NFEM	1.Gives a general picture based on symmetrical properties 2.Very fast	1.Only relative values obtained 2.No energy quantities
k.p	1.Direct band gap semiconductors band structures 2.Useful when the full band structure is not needed	1.Calculates band structure only in small k intervals (no use for full band structure) 2.Error increased when far from extreme points.
LCAO	1.Good for the calculation of band structure of metals 2.Good accuracy for conduction band calculations	1.Lower accuracy for valence band calculations 2.Not good for large band gap materials
EPM	1.Accurate results 2.Less complex than SCPM	1.Trial and error 2.Uses experimental data
SCPM	1.No need for experimental data 2.Iteration based on physical data (no trial and error) 3.Accurate results	1.Complexity (extensive data handling) 2.Generally less efficient than other methods.

Table 2-1. A summary of the advantages and limitations of different energy band structure calculation methods.

Nearly free electron method which gives a general picture of the electronic band structure through studying the translational symmetries that exist in the crystalline materials was reviewed. It was noted that this method will only represent a whole picture of the electronic band structure and is not accurate for being used in studies of the properties of the materials based on their electronic band structure. The k.p method was introduced as a method to find the electronic band structure of a crystalline material near a maximum in the valence band of a crystalline lattice. This method was only capable of calculating a partial part of the band structure of a material near a k-point and was only suitable when

dealing with optical properties of the direct band gap materials which only needs the electronic band structure near the band gap around $k = 0$. The tight-binding, LCAO, method was introduced briefly. The inaccuracies associated with the calculations of the valence band of the semiconductors in LCAO method were discussed.

Empirical pseudopotential method, EPM, was discussed. The similarities in the basics of the method with the nearly free electron method were reviewed. And the basics of EPM were explained and the form factors for the zinc-blende and diamond lattices were found. An algorithm for using this method was introduced.

After the discussion of EPM, explaining the self-consistent pseudopotential method, SCPM, is much easier as the two methods share many similarities. Different ways of choosing a pseudopotential was discussed. Different methods of solving the Schrödinger equation, also called the pseudo-wave equation in SCPM, were introduced. The local density approximation, LDA, for finding the exchange and correlation potential was discussed. In the discussion of the LDA, the density functional theory, DFT, was introduced and the LDA was explained using the Kohn-Sham equations.

The applications of both EPM and SCPM in finding different properties of materials including their electronic band structure were reviewed. These applications were not limited only to semiconductors. It was shown that these methods can be used for molecules, metals, semiconductors and even

insulators. It was also noted that these methods can be used to calculate the surface states, junction properties and many other properties of the materials studied.

Chapter 3: The 1D Crystal Electronic Band Structure Solver

3.1 Introduction

In this chapter, the 1D Crystal Electronic Band Structure Solver will be discussed. This solver is very important because the algorithm can be used for a 3D solver with some minor changes in calculation methods and data handling. The major parts of this algorithm are not subject to change. In fact the means of handling the algorithm will be subject to most of the changes that will take place to reach a 3D solver. This solver can be considered as a showcase of the 3D solver as it is not different in the basics and the equations that have to be solved. When moving from 1D solver to the 3D solver there will be a very significant change in the amount of data that has to be handled which is the main difference between the solvers. The amount of data in the 3D solver can be anywhere from about 1300 times to more than 20000 times of what should be handled by the 1D solver based on the matrix sizes being processed.

In this chapter, the algorithm developed for the 1D solver will be reviewed and explained in detail. The calculation methods of each step of the algorithm will be discussed and the results of the solver will be assessed. They will be compared with benchmark results obtained from the literature and it will be shown that the solver is accurate by comparing the results with the benchmark results. The efficiency of the algorithm will also be discussed. Reviewing the 1D

solver will prove useful for introducing the 3D solver in the next chapter of this thesis.

3.2 The Algorithm

The first step in this solver is to have a starting pseudopotential. The ion potential is chosen based on the next steps in the algorithm. By choosing a good pseudopotential, the next steps can be performed faster and easier. The pseudopotential should replace the real potential of the chosen atom without its outermost electrons which we call the ion potential.

After having the ion potential, the Hamiltonian for the Schrödinger equation is calculated. It is only in the first Hamiltonian calculation that only the ion potential is taking part. After calculating the Hamiltonian, the solver is ready for the next major step which is solving the Schrödinger equation.

The next step to take is to solve the Schrödinger equation which is a second order differential equation in which the wave function and the eigen values which are to be the electronic band structure are the unknowns. The complexity of solving this equation is that the potentials are a function of position and are multiplied by the wave function. The way to solve this equation will be discussed in the calculation methods part. By solving the Schrödinger equation, the wave functions and the eigen values are now known.

Knowing the wave functions, the density function can be formed. The density function of the system is the parameter which has to be compared each

step of the way with the one that has been calculated before. In the first step we only have to calculate and store the density function for later comparison.

Using the density function we can calculate the Hartree potential energy which will be added to the ion potential energy. The equation to be solved is the Poisson equation:

$$\nabla^2 V_{Hartree} = \frac{\rho}{\varepsilon_0}$$ (3-1)

After calculating the Hartree potential energy, the solver will calculate the exchange and correlation potential. By calculating all the necessary potentials the solver is then ready to solve all the equations again using the new potential. Having the ion potential energy and the Hartree potential energy, we only have to transform the exchange and correlation potential into its potential energy to be ready to plug it in the Schrödinger equation without any further calculations. The potential energy is shown in capital cases and the potentials are shown in lower cases. The potential is as follows in equation (3-2):

$$v(r) = v_{ion} + v_{Hartree} + v_{xc}$$ (3-2)

It should be noted that the solver do not directly involve itself with the position dependant function and rather uses a plane wave expansion of the functions that are dependant on the wave vector, k, to speed up the process. More on this side will be discussed in the calculation methods part of this chapter.

Having calculated the new pseudopotential, the Schrödinger equation will be solved again using the pseudopotential and the new wave functions and eigen values are found. The density function will be calculated and the new energy functional of the system will be calculated after that. Based on the Kohn-Sham algorithm the energy functional should be smaller than that of the last step. The density function obtained in the last step will be compared with the one calculated using the new wave functions. If the results are not satisfactory and there is an obvious difference between the two density functions, a new pseudopotential will be formed after calculating the Hartree potential energy and the exchange and correlation potential energy. The new pseudopotential will be calculated using equation (3-2) and the old Hartree potential and exchange and correlation potential will not take part in the formation of the new potential and are neglected. v_{ion} is being used in all the steps and is not subject to change at any step. It can be changed if it is decided that another ion potential can perform better in the algorithm but it should be done in the first part of the algorithm. Changing the ion potential in the middle of the algorithm can result in divergence of the results. The solver diverges also in the occasion that the ion potential does not resemble the real potential outside the core region or the ion potential has a large positive amount in the core region.

If the new density function which is derived from the newly calculated wave functions has a negligibly small difference with the results from the last iteration, the new energy functional is checked and compared with the last one to

make sure that it is smaller than the last step. This is always the case if the ion potential is chosen correctly and is not much different from the real lattice potential. If both arguments are correct the eigen values of the new Schrödinger equation which is solved are chosen as the electronic band structure of the lattice under calculation. The eigen values derived in our method are calculated as a function of the wave vector, k. A flowchart of the 1D energy band structure solver is shown in figure 3-1.
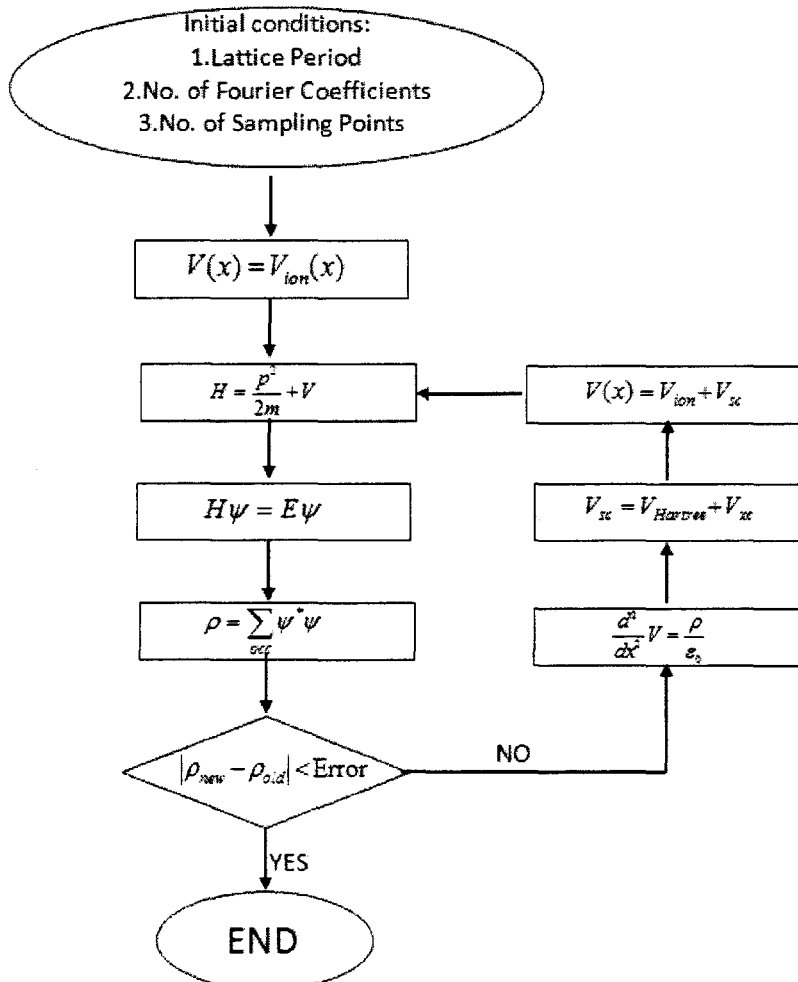
Figure 3-1. The 1D energy band structure solver's algorithm.

3.3 Calculation Methods

In this section the methods that are used in this solver for the calculations and the solving equations will be discussed. The main idea that we will emphasize is using the orthogonal plane wave expansion of the pseudopotentials and adapting all equations to be compatible with the Orthogonal Plane Wave, OPW, method. By converting the known data into the sum of a set of plane waves, many mathematical operations such as derivatives or integrals will be easier to perform. But to perform the plane wave expansion, many integrals have to be calculated in advance. It is an overall beneficial procedure to do the OPW expansion in this solver. Performing the parameterization integrals more efficient will prove very useful as they have to be done many times for the OPW parameters to be found.

The efficiency of each calculation method or in other words, its calculation speed, is of special importance in this thesis. Each of the methods chosen to be used in the 1D solver are chosen to be a very good optimization of efficiency and accuracy. The methods that are chosen must be accurate but accuracy is not the only goal of the solver. So maintaining a good accuracy, each calculation method is an efficient method too.

It will be shown that the Schrödinger equation can be converted into an eigen value problem for the crystalline lattices when using the plane wave expansion method. A justification of using the OPW Method will follow this introduction which shows how this expansion will help converting the Schrödinger equation into an eigen value problem. Changing the Schrödinger equation to an

eigen value problem will ensure efficiency of the solver and will ease the usage of the results for usage in the next steps of the algorithm.

In the next parts the solution of the Hartree potential and the exchange and correlation potential will be discussed shortly as they will just contain simple calculations and no unordinary calculation will be performed that will need further explanation like the explanation needed for the Schrödinger equation. The comparison procedure of the density functions will then be discussed at the end of this section.

3.3.1 Justification of the OPW Expansion

In this part it will be shown that for a crystalline bulk lattice the Schrödinger equation which is the most complex part of this algorithm to be solved can be converted into an eigen value problem. Through the proof of this statement, the Bloch theorem will be used which is only true for a crystalline lattice.

As we know in a lattice, the lattice potential energy is a periodic function with the same period as the lattice's unit cell size. As the 1D lattice is being discussed in this chapter, the potential energy will also be in one dimension and will be periodic with the period of the lattice as follows:

$$V(x + na) = V(x) \text{ where } n \in Z \tag{3-3}$$

In this equation a is the period of the lattice being discussed. Because of the periodicity of the potential function it can be written in the form of Fourier series:

$$V(x) = \sum_{l=-\infty}^{\infty} c_l e^{i\frac{2\pi l}{a}x} \tag{3-4}$$

In equation (3-4) the terms c_l are the Fourier coefficients of the periodic lattice potential energy. The Fourier coefficients are found using the following integral:

$$c_l = \int_{-\frac{a}{2}}^{\frac{a}{2}} V(x) e^{-i\frac{2\pi l}{a}x} dx \tag{3-5}$$

From the Bloch theorem we know that the wave function which is the solution of our Schrödinger equation should be in the form of a periodic function with the same period as our potential times a plane wave function. So we will parameterize the wave function as below:

$$\psi(x) = \left(\sum_{l=-\infty}^{\infty} b_l e^{i\frac{2\pi l}{a}x}\right) e^{ikx} \tag{3-6}$$

The Schrödinger equation is repeated below as a starting point to reach the eigen value problem from it:

$$(V_{pp} - \frac{\hbar^2}{2m_0}\frac{d^2}{dx^2})\psi = E\psi \tag{3-7}$$

From the equation it is apparent that other than the potential and the wave function, the second derivative of the wave function, $\frac{d^2\psi}{dx^2}$, is also needed to be replaced in this equation. In this step an expression for $\frac{d^2\psi}{dx^2}$ will be calculated

from the wave function itself. We rewrite the wave function in the form below before differentiating:

$$\psi(x) = (\sum_{l=-\infty}^{\infty} b_l e^{i\frac{2\pi l}{a}x})e^{ikx} = \sum_{l=-\infty}^{\infty} b_l e^{i(\frac{2\pi l}{a}+k)x}$$

(3-8)

After the calculations the second derivative of the wave function is formulated as:

$$\frac{d^2\psi}{dx^2} = -[\sum_{l=-\infty}^{\infty} b_l (\frac{2\pi l}{a}+k)^2 e^{i\frac{2\pi l}{a}x}] \cdot e^{ikx}$$

(3-9)

After parameterizing the second derivative of the wave function, it is time to expand the Schrödinger equation and write down the parameterized values instead of the functions:

$$(V_{pp} - \frac{\hbar^2}{2m_0}\frac{d^2}{dx^2})\psi = E\psi \quad \Rightarrow \quad V_{pp}\psi - \frac{\hbar^2}{2m_0}\frac{d^2\psi}{dx^2} = E\psi$$

(3-10a)

$$\Rightarrow \sum_{j=-\infty}^{\infty} c_j e^{i\frac{2\pi j}{a}x} \cdot (\sum_{n=-\infty}^{\infty} b_n e^{i\frac{2\pi n}{a}x})e^{ikx} + \frac{\hbar^2}{2m_0}[\sum_{l=-\infty}^{\infty} b_l (\frac{2\pi l}{a}+k)^2 e^{i\frac{2\pi l}{a}x}] \cdot e^{ikx} = E(\sum_{-\infty}^{\infty} b_l e^{i\frac{2\pi l}{a}x})e^{ikx}$$

(3-10b)

As it can be seen, the terms e^{ikx} can be cancelled throughout the equation and the equation (3-10b) can be rewritten as:

$$\sum_{j=-\infty}^{\infty}\sum_{n=-\infty}^{\infty} c_j b_n e^{i\frac{2\pi(j+n)}{a}x} = \sum_{l=-\infty}^{\infty} b_l[E - \frac{\hbar^2}{2m_0}(\frac{2\pi l}{a}+k)^2]e^{i\frac{2\pi l}{a}x}$$

(3-11)

If this equation is solved for all b_M values as well as E, the wave functions is found and therefore the Schrödinger equation is solved. To solve for

a specific b_M we have to multiply both sides by $e^{-i\frac{2\pi M}{a}x}$ and integrate over

$(-\frac{a}{2},\frac{a}{2})$. After integration we will have:

$$b_M[E - \frac{\hbar^2}{2m_0}(\frac{2\pi M}{a}+k)^2] = \sum_{j=-\infty}^{\infty} b_j c_{M-j} \qquad (3\text{-}12)$$

In equation (3-12) all of the parameters are known except E and the

Fourier coefficients of the wave function which are b_j for all j. If this equation is

written for all the different M values or in other words for all b_M, we will have

infinite equations and infinite unknowns to be found. As it is known, it is

impossible to solve infinite equations and infinite unknowns. To make the

equations practical for numerical solving we will select M so that we will get an

acceptable accuracy without losing efficiency. It will be shown in the assessment

section of this chapter that in fact we can choose a relatively small M without

losing the accuracy of the calculations which helps the efficiency of the program

very much.

These equations can be written in the form of a matrix equation. For the

sake of simplicity, let us assume that the number of Fourier coefficients of the

wave function needed in an example is from b_{-20} to b_{20}. After converting all the

equations into a matrix equation we will have:

$$
\begin{bmatrix}
E - \dfrac{\hbar^2}{2m_0}\left(\dfrac{2\pi(-20)}{a}+k\right)^2 & 0 & 0 & & \\
0 & E - \dfrac{\hbar^2}{2m_0}\left(\dfrac{2\pi(-19)}{a}+k\right)^2 & & & \\
0 & & \ddots & & 0 \\
& & & E - \dfrac{\hbar^2}{2m_0}\left(\dfrac{2\pi(19)}{a}+k\right)^2 & 0 \\
& 0 & 0 & & E - \dfrac{\hbar^2}{2m_0}\left(\dfrac{2\pi(20)}{a}+k\right)^2
\end{bmatrix}
\cdot
\begin{bmatrix}
b_{-20} \\ b_{-19} \\ \vdots \\ b_{19} \\ b_{20}
\end{bmatrix}
$$

$$
=
\begin{bmatrix}
c_0 & c_{-1} & \cdots & c_{-39} & c_{-40} \\
c_{+1} & c_0 & \cdots & c_{-38} & c_{-39} \\
\vdots & & \ddots & & \vdots \\
c_{+39} & c_{+38} & \cdots & c_0 & c_{-1} \\
c_{+40} & c_{+39} & \cdots & c_{+1} & c_0
\end{bmatrix}
\cdot
\begin{bmatrix}
b_{-20} \\ b_{-19} \\ \vdots \\ b_{19} \\ b_{20}
\end{bmatrix}
\tag{3-13}
$$

If all the E values are kept in the left-hand-side and all other terms in the left-hand-side matrix are transferred to the right-hand-side matrix, it can be easily seen that equation (3-13) is an eigen value problem. The simplified equation after the transfers is as follows:

$$
E\bar{b} =
\begin{bmatrix}
c_0 + \dfrac{\hbar^2}{2m_0}\left(\dfrac{2\pi(-20)}{a}+k\right)^2 & c_{-1} & \cdots & c_{-39} & c_{-40} \\
c_{+1} & c_0 + \dfrac{\hbar^2}{2m_0}\left(\dfrac{2\pi(-19)}{a}+k\right)^2 & \cdots & c_{-38} & c_{-39} \\
\vdots & & \ddots & & \vdots \\
c_{+39} & c_{+38} & \cdots & c_0 + \dfrac{\hbar^2}{2m_0}\left(\dfrac{2\pi(19)}{a}+k\right)^2 & c_{-1} \\
c_{+40} & c_{+39} & \cdots & c_{+1} & c_0 + \dfrac{\hbar^2}{2m_0}\left(\dfrac{2\pi(20)}{a}+k\right)^2
\end{bmatrix}
\cdot \bar{b}
\tag{3-14}
$$

After solving the eigen value problem we will have the eigen values and eigen vectors we should carefully look for the eigen vector which satisfies the normalization property of the wave function which is:

$$\sum_{j=-\infty}^{\infty} b_j b_j^* = 1 \qquad (3\text{-}15)$$

In the case of example that was demonstrated, the normalizing equation should change to:

$$\sum_{j=-20}^{+20} b_j b_j^* = 1 \qquad (3\text{-}16)$$

It should be noted that this eigen value problem has to be solved for each needed value of k in order to find the eigen values and the wave functions at different k values. In this numerical solution we will show that the eigen value problem needs to be solved for only a minimal number of k values. The efficiency of the program in solving this eigen value problem has a linear dependence on the number of k values for which the equation has to be solved.

With this calculations, it has been shown that the plane wave expansion of the potentials that are used in the Schrödinger equation and the use of the Bloch theorem to parameterize the wave function of a crystalline lattice will simplify the Schrödinger equation and transform it into an eigen value problem which is much more suitable to be solved numerically than a complex differential equation.

In the next parts we will briefly discuss the method of performing the integrals to calculate the Fourier series of the pseudopotentials, or in other words to calculate the parameters of the plane wave expansion of the pseudopotentials.

3.3.2 Integral Calculations for the OPW Expansion

To have more accuracy in doing the integral and also keep the program efficient, the solver uses the trapezoidal Riemann sum, also called the trapezoidal approximation [68].

Although this method is simple and only uses only sums and multiplication, it is one of the time consuming parts of the program if the number of Fourier coefficients needed for the pseudopotential is relatively small. It should be noted that if the efficiency and time are very important, the number of points used for this integration could be as low as fifty to a hundred without losing a lot of accuracy and damaging the outcome results. But as a general rule the more sampling points used for calculating the integral, the more accurate the results will be. It should be noted that the accuracy will not double if we double the number of sampling points if the function being sampled is not changing very fast over the space.

As this method is very simple it will only be discussed briefly here. Let us assume that $f(x)$ is the function that it's integral is needed to be calculated over the period of $[a,b]$. In general this period can be divided to n non-equal intervals, but in the solver's case the interval will be divided to n equal intervals. The general trapezoidal method is demonstrated in figure 3-2.
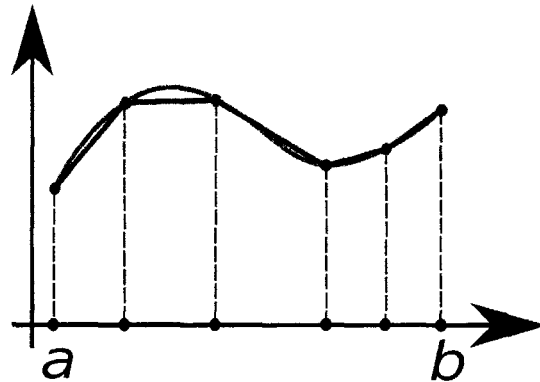
Figure 3-2. A demonstration of how the trapezoidal method divides the functions into intervals. These intervals can be equal or not equal depending on the situation [69].

As it was mentioned, in the solvers case the intervals are equal. Let us assume that there are n equal intervals. There will be $n+1$ points at which the value of the function is important to the calculations. These points are named as $x_0, x_1, ..., x_n$ where $x_0 = a$ and $x_n = b$.

Instead of calculating the area under $f(x)$ in period $[a,b]$, the area of the trapezoids that are formed in each integral will be calculated. So the integral is approximated to be the area of the trapezoids. As it can be seen in figure 3-2, if the rate of change of the function is not very high in relation to the interval lengths, this method can result in very accurate approximations of the integral. The integral in terms of the trapezoid area sums can be written as below:

$$\int_a^b f(x)dx \approx \frac{b-a}{n} \cdot \frac{1}{2}(f(x_0) + f(x_1)) + \frac{b-a}{n} \cdot \frac{1}{2}(f(x_1) + f(x_2)) + ... + \frac{b-a}{n} \cdot \frac{1}{2}(f(x_{n-1}) + f(x_n))$$

(3-17)

These terms can be simplified into the following equation:

$$\int_a^b f(x)dx \approx \frac{b-a}{2n}(f(x_0) + 2f(x_1) + \ldots + 2f(x_{n-1}) + f(x_n)) \qquad \text{(3-18)}$$

This equation will be used to find the Fourier series coefficients of the pseudopotentials in the solver program. The trapezoidal method is an effective method which helps the 1D solver to calculate the plane wave parameterization of the pseudopotentials. In the next section the method for solving the eigen value problem which is solved instead of the Schrödinger equation will be discussed.

3.3.3 The Solution Method of the Eigen Value Problem

In this part it is shown that because the 1D potential is a real function, the matrix of the eigen value problem will be a Hermitian matrix. Because of this property of the matrix, the Cholesky method will be the fastest method which can be used to solve the eigen value problem. To prove that the matrix of the eigen value problem is a Hermitian matrix, it is shown here one more time and it is investigated that because the potential is a real function, this matrix will be a Hermitian matrix. The matrix is as follows:

$$
M = \begin{bmatrix}
c_0 + \dfrac{\hbar^2}{2m_0}(\dfrac{2\pi(-20)}{a}+k)^2 & c_{-1} & \cdots & c_{-39} & c_{-40} \\
c_{+1} & c_0 + \dfrac{\hbar^2}{2m_0}(\dfrac{2\pi(-19)}{a}+k)^2 & \cdots & c_{-38} & c_{-39} \\
\vdots & & \ddots & & \vdots \\
c_{+39} & c_{+38} & \cdots & c_0 + \dfrac{\hbar^2}{2m_0}(\dfrac{2\pi(19)}{a}+k)^2 & c_{-1} \\
c_{+40} & c_{+39} & \cdots & c_{+1} & c_0 + \dfrac{\hbar^2}{2m_0}(\dfrac{2\pi(20)}{a}+k)^2
\end{bmatrix}
$$

$$(3\text{-}19)$$

If M is Hermitian, the following equations should hold true:

$$
\begin{aligned}
c_{+1} &= c_{-1}^* \\
c_{+2} &= c_{-2}^* \\
&\vdots \\
c_{+39} &= c_{-39}^* \\
c_{+40} &= c_{-40}^*
\end{aligned}
$$

$$(3\text{-}20)$$

To show this fact is true, it is proved that equation (3-20) is true for any real function. It is known that for any real function, the Fourier terms of sine and cosine will have real coefficients as sine and cosine are real functions themselves. The pseudopotential is written as below:

$$
V(x) = \sum_{l=-\infty}^{\infty} c_l e^{i\frac{2\pi l}{a}x}
$$

$$(3\text{-}21)$$

We can write down the potential in terms of sine and cosine functions to see the coefficients of sines and cosines in terms of the c_l's. The transformation is shown in two stages as follows:

$$
V(x) = c_0 + \sum_{l=1}^{\infty} c_l [\cos(\frac{2\pi l}{a}x) + i\sin(\frac{2\pi l}{a}x)] + c_{-l}[\cos(\frac{2\pi l}{a}x) - i\sin(\frac{2\pi l}{a}x)] \quad (3\text{-}22)
$$

So the potential in terms of sine and cosine will be:

$$V(x) = c_0 + \sum_{l=1}^{\infty} (c_l + c_{-l}) \cos(\frac{2\pi l}{a} x) + i(c_l - c_{-l}) \sin(\frac{2\pi l}{a} x) \qquad (3\text{-}23)$$

Because the potential is real and the sine and cosine functions are real, the coefficients of sine and cosine should also be real. It should be noted that based on equation (3-23), c_0 has to be real as well. As a result, the following should hold:

$$(c_l + c_{-l}) \in \Re \quad \Rightarrow \quad imag(c_l) = -imag(c_{-l}) \qquad (3\text{-}24a)$$

$$i(c_l - c_{-l}) \in \Re \quad \Rightarrow \quad real(c_l) = real(c_{-l}) \qquad (3\text{-}24b)$$

Based on equations (3-24a) and (3-24b) and the fact that c_0 is real, it is proven that:

$$c_l = c_{-l}^* ; \text{ for all } l \qquad (3\text{-}25)$$

Based on equation (3-25) it is shown that the eigen value problem matrix is a Hermitian matrix which can be solved most efficiently by Cholesky decomposition method. For more on Cholesky decomposition method the reader is referred to [70-72].

3.3.4 The Calculation of Hartree and XC Potential Energies

To calculate the Hartree and the exchange and correlation potential energies, one should first have calculated the density function of the system being discussed and for that matter the wave functions of the system that is being solved need to be calculated. Let us consider the example that we started

in the last sections for a limited number of coefficients. As the size of the matrix formed for the eigen value problem is forty one by forty one, there will be forty one eigen values and eigen vectors. Each eigen vector is representing a wave function. Each value in the eigen vector is a Fourier coefficient of a plane wave that will make up the wave function. The eigen value problems are solved for one k value at a time. By knowing the density function at all the different k values, we can calculate the density function of the system. As a first step the method of calculations of the partial density functions at each k value is demonstrated. Suppose that we have the eigen vectors of the system at k_1. There are forty one different eigen vectors found at this wave vector value. Each of these eigen vectors that represent a wave function has the following form:

$$v_j = \begin{bmatrix} b_{-20}^j & b_{-19}^j & \cdots & b_{19}^j & b_{20}^j \end{bmatrix} \tag{3-26}$$

The wave function represented by such wave vector has the following form:

$$\psi_j(x)\big|_{k_1} = [b_{-20}^j e^{i\frac{2\pi(-20)}{a}x} + b_{-19}^j e^{i\frac{2\pi(-19)}{a}x} + \cdots + b_{19}^j e^{i\frac{2\pi(19)}{a}x} + b_{20}^j e^{i\frac{2\pi(20)}{a}x}]e^{ik_1 x} \tag{3-27}$$

The density function at each specific wave function at k_1 can be calculated from the following formula:

$$\rho_j^{k_1}(x) = \psi_j(x)\big|_{k_1} \psi_j^*(x)\big|_{k_1} \tag{3-28}$$

The conjugate of the wave function has the following form:

$$\psi_j^*(x)\big|_{k_1} = [b_{-20}^{*j} e^{-i\frac{2\pi(-20)}{a}x} + b_{-19}^{*j} e^{-i\frac{2\pi(-19)}{a}x} + \cdots + b_{19}^{*j} e^{-i\frac{2\pi(19)}{a}x} + b_{20}^{*j} e^{-i\frac{2\pi(20)}{a}x}]e^{-ik_1 x} \tag{3-29}$$

The multiplication in equation (3-28) will result in the sum of eighty one plane wave functions. The density function has the following form:

$$\rho_j^{k_1}(x) = u_{-40}^j e^{i\frac{2\pi(-40)}{a}x} + u_{-39}^j e^{i\frac{2\pi(-39)}{a}x} + \cdots + u_{39}^j e^{i\frac{2\pi(39)}{a}x} + u_{40}^j e^{i\frac{2\pi(40)}{a}x} \qquad (3\text{-}30)$$

The coefficients of the plane waves in the density function of this specific wave function at k_1 are as follows:

$$u_l^j = \sum_{\substack{m=-20 \\ m-n=l}}^{20} \sum_{n=-20}^{20} b_m^j b_n^{*j}; \text{ where } m-n=l \qquad (3\text{-}31)$$

The total density function at the wave vector k_1 is the sum of all density functions at different states associated with different wave functions.

$$\rho^{k_1}(x) = \sum_{j=-20}^{20} \rho_j^{k_1}(x) \qquad (3\text{-}32)$$

To have the total density function which is not associated with a single wave vector value an integral over all values of k should be calculated. To calculate this integral the solver needs to sample the density function at a number of sample wave vector values. Let us suppose that we have sampled h different k values in a Brillouin zone. The wave vector values in the Brillouin zone of a 1D system vary from $-\frac{\pi}{a}$ to $\frac{\pi}{a}$ where 'a' is the lattice constant. Using the trapezoidal rule for the integration the total density function of the system can be calculated using the following formula:

$$\rho(x) = \frac{\pi}{ah}[\rho^{k_1}(x) + 2\rho^{k_2}(x) + 2\rho^{k_3}(x) + \cdots + 2\rho^{k_{h-2}}(x) + 2\rho^{k_{h-1}}(x) + \rho^{k_h}(x)]$$

$$(3\text{-}33)$$

This summation is in fact being translated into the summation of the coefficients of each partial density function. After the calculations of the coefficients, the density function is written in the following form:

$$\rho(x) = \sum_{l=-40}^{40} U_l e^{i\frac{2\pi l}{a}x}$$

$$(3\text{-}34)$$

Now that the density function of the system is known, calculating the Hartree potential and the exchange and correlation potential are very easy. In fact both of these potentials are integrals. Calculation of both potentials will be discussed here after. First the calculation of the Hartree potential is demonstrated. As it is known the Hartree potential is found by solving the Poisson equation below:

$$\nabla^2 V_{Hartree} = \frac{\rho}{\varepsilon_0}$$

$$(3\text{-}35)$$

The Hartree potential will be:

$$V_{Hartree} = \iint \frac{\rho}{\varepsilon_0} dxdx$$

$$(3\text{-}36)$$

which is equivalent to the following:

$$V_{Hartree} = \iint \sum_{l=-40}^{40} \frac{U_l}{\varepsilon_0} e^{i\frac{2\pi l}{a}x} dxdx \Rightarrow V_{Hartree} = \sum_{l=-40}^{40} \iint \frac{U_l}{\varepsilon_0} e^{i\frac{2\pi l}{a}x} dxdx$$

$$(3\text{-}37)$$

So the Hartree potential is calculated as:

$$V_{Hartree} = \sum_{l=-40}^{40} \frac{-U_l}{\varepsilon_0 (\frac{2\pi l}{a})^2} e^{i\frac{2\pi l}{a}x} \qquad (3\text{-}38)$$

By knowing the form of the Hartree potential from the calculations here, the solver only needs to plug in the plane wave coefficients of the Hartree potential which are calculated using only basic mathematical operations like summation and multiplication. The exchange and correlation potential energy is different in calculations. The exchange and correlation energy has been defined in equation (2-95) and is called E_{xc}. This equation is repeated here and this energy will be called V_{xc} for having the same notations of this chapter because in this chapter the potential energies are in capital letters and the potentials are in lower cases.

$$V_{xc}[\rho(x)] = \int \rho(x)\varepsilon_{xc}(\rho(x))dr \qquad (3\text{-}39)$$

Unfortunately, equation (3-39) cannot be solved without performing the integral and for this reason the exchange and correlation energy cannot be calculated as fast as the Hartree potential. Again for this integral the trapezoidal method will be used.

The new potential energy which is plugged in the Schrödinger equation needs the ion potential energy, the Hartree potential energy and the exchange and correlation potential energy. As a remainder it should be noted that at each stage the ion potential energy is calculated using the following formula:

$$V_{ion}(x) = \int v_{ion}(x)\rho(x)dx \qquad (3\text{-}40)$$

Having calculated all the energies, the new total potential energy of the system is as follows:

$$V_{eff} = V_{ion} + V_{Hartree} + V_{xc}$$ (3-41)

3.3.5 The Comparison of Density Functions

To compare the new and old density functions as a measure of the convergence of the solver, one has to use a method which gives a sense of how much difference two functions have. The method used for comparing the old and new density functions in this solver is the Root Mean Square Error, RMSE, which is also called Root Mean Square Deviation, RMSD. As this method is used for discrete functions, to use this method the density functions have to be sampled at several points. The number of points that the density functions are sampled at is dependent on the lattice constant. The larger the lattice constant, the more points of the density functions have to be sampled for comparison. In this solver the distance between two sampled points should be set somehow that the solver can have enough sampled points of the density functions. To be able to use the outcome of this method as a measure for the convergence of the solver, the out come shall be divided by the value of the Root Mean Square, RMS, of the old density function so that we have a relative value of the difference between the old and the new density function. For more information on RMSE the reader is referred to [73]. For more information on RMS the reader is referred to [74]. The

104

RMSE and the calculations used for implementation of this method are discussed hereafter.

The RMSE for two sets of n numbers named X and Y is calculated through the following equation:

$$RMSE(X,Y) = \sqrt{\frac{\sum_{i=1}^{n}(x_i - y_i)^2}{n}}$$

(3-42)

Let us suppose that the sampled old density function is called $\rho_{s,old}$ and is a vector consisted of n numbers. Performing the same for the sampled new density function, it is called $\rho_{s,new}$ and it is a vector of n values.

$$\rho_{s,old} = \begin{bmatrix} \rho_{old,1} \\ \rho_{old,2} \\ \vdots \\ \rho_{old,n-1} \\ \rho_{old,n} \end{bmatrix}$$

(3-43a)

$$\rho_{s,new} = \begin{bmatrix} \rho_{new,1} \\ \rho_{new,2} \\ \vdots \\ \rho_{new,n-1} \\ \rho_{new,n} \end{bmatrix}$$

(3-43b)

The difference vector is calculated by subtracting the vectors in equations (3-43a) and (3-43b).

$$\Delta\rho_s = \begin{bmatrix} \Delta\rho_1 \\ \Delta\rho_2 \\ \vdots \\ \Delta\rho_{n-1} \\ \Delta\rho_n \end{bmatrix} \tag{3-44}$$

Instead of doing all the calculations to find the summation in equation (3-42), the following is calculated in the solver which results in the same value of summation but will be performed faster by the CPU as all the multiplications will be done together and not just one by one.

$$\sum_{i=1}^{n}(x_i - y_i)^2 = \Delta\rho_s \cdot \Delta\rho_s^{T} \tag{3-45}$$

As a result the RMSE can be written as:

$$RMSE(\rho_{s,old}, \rho_{s,new}) = \sqrt{\frac{\Delta\rho_s \cdot \Delta\rho_s^{T}}{n}} \tag{3-46}$$

The RMS value of the old density function can be calculated using the same idea:

$$RMS(\rho_{s,old}) = \sqrt{\frac{\rho_{s,old} \cdot \rho_{s,old}^{T}}{n}} \tag{3-47}$$

The relative change of the density function is called $\Delta\rho_{rel}$ and can be formulated as:

$$\Delta\rho_{rel} = \frac{RMSE(\rho_{s,old}, \rho_{s,new})}{RMS(\rho_{s,old})} = \sqrt{\frac{\Delta\rho_s \cdot \Delta\rho_s^{T}}{\rho_{s,old} \cdot \rho_{s,old}^{T}}} \tag{3-48}$$

The solver will only calculate equation (3-48) as a relative change of the density function. Although the value of n is not reflected in the relative change, it

is important for the accuracy of the results. A small number of sampling points could result in unacceptable error because a small number of sampling points will not transfer enough information from the continuous density function to the vector made up of the sampled points.

The value of the relative change of the density functions that is needed to deem convergence depends on the level of accuracy and efficiency that is needed. If a very small relative change is needed the number of iterations will be very high as the number of iterations will grow at a very fast rate when the relative change is decreased. By setting the goal relative change in density functions to a value between $\Delta\rho_{rel} = 0.01$ to $\Delta\rho_{rel} = 0.005$, the solver will have excellent accuracy without satisfying the overall efficiency. For best results, it is better to set the relative change to the smallest value possible as long as it doesn't cost the program to lose its efficiency.

3.4 Assessment

The energy band structure of a benchmark lattice [75] will be compared to the results calculated by the 1D Solver. The first value to be set is the relative change in the density function which is set to the least value that doesn't affect the efficiency dramatically. The effects of other parameters on the accuracy of the solver will be studied. To assess the 1D Solver two different Kronig-Penney Lattices studied and solved analytically in [75] are used as benchmarks. The results of the 1D Solver are compared to the analytical results and the lower

limits for the amount of data that is needed for an accurate calculation will be found. The Kronig-Penney lattices that are being studied are parameterized using the coefficients figure 3-3.
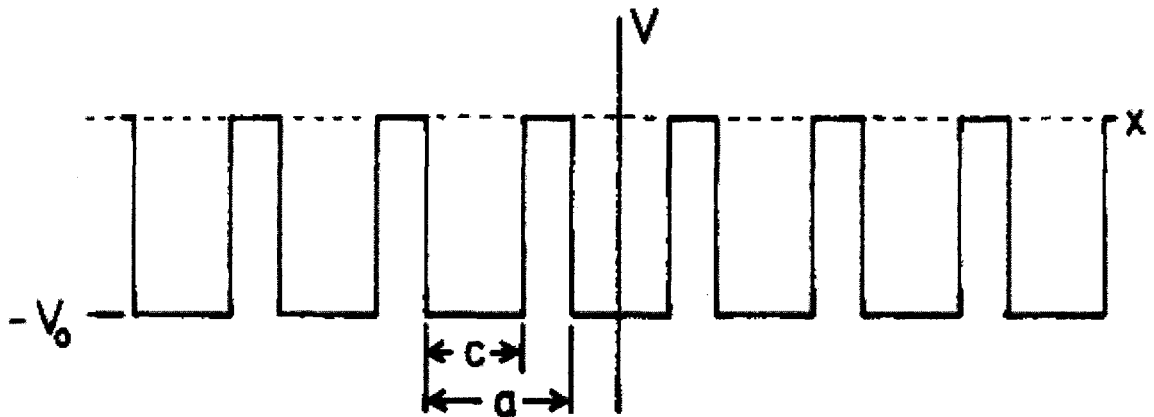
Figure 3-3. Visual description of the parameters of the Kronig-Penney lattice being studied [75].

The mathematical description for such lattice is as follows:

$$V(x) = \begin{cases} -V_0 & -\dfrac{c}{2} < x < \dfrac{c}{2} \\ 0 & \dfrac{c}{2} \le |x| \le \dfrac{a}{2} \end{cases} \quad \text{and} \quad V(x+a) = V(x) \qquad (3\text{-}49)$$

In the first Kronig-Penney lattice studied, which will be called Lattice No. 1, the parameters are as follows: $V_0 = 30eV$, $c = 2\text{Å}$, and $\dfrac{a}{c} = 1.1$. The second Kronig-Penney lattice, called lattice No. 2 hereafter, that has been studied here, is identical in sizes but its minimum potential is different which is $V_0 = 100eV$. To calculate the energy band structure of these structures the relative change in

density function is set to $\Delta\rho_{rel} = 0.005$. In the first step the results of the solver using a large number of Fourier coefficients and wave vector sampling points are calculated to ensure maximum accuracy possible. These results are compared to the analytical results that are available. The extreme points of the bands of lattice No. 1 and first band of Lattice No. 2 are as follows in Table (3-1): [75]

Lattice No. 1	Band No. 1	$-27.822\,eV$
	Band No. 2	$1.217\,eV$
Lattice No. 2	Band No. 1	$-95.225\,eV$

Table 3-1. Exact band extreme values of Lattice No1 and 2 which are calculated analytically in [75]. It should be noted that the only band extreme provided for lattice No. 2 if for its first band.

More information on Band No. 1 of each Lattice is provided in Table (3-2), [75] can be used to confirm the accuracy of the whole band for more reliable confirmation than only checking the accuracy of the extreme points. However it should be noted that matching extreme points with the analytical results is a good way of showing the accuracy of the solver.

The 1D solver takes the physical information about the lattice including the period (a), information on the shape of the structure ($\frac{a}{c}$) and the energy quantities (V_0) as inputs. The accuracy needed in the density function is another

input of the solver. It also receives the number of Fourier coefficients and wave vector sampling points to be used in the calculations as inputs.

Band No. 1 of $\dfrac{k.a}{\pi}$	Lattice No. 1 (eV)	Lattice No. 2 (eV)
0	-27.822	-95.225
0.2	-27.527	-95.006
0.4	-26.651	-94.382
0.6	-25.229	-93.466
0.8	-23.418	-92.541
1.0	-22.195	-92.119

Table 3-2. Analytical information [75] available for comparison with the calculated numerical results of the solver.

To calculate the results numerically using the solver, it will use one hundred Fourier coefficients and one hundred wave vector sampling points in order to ensure accuracy in the results that are obtained. The relative error in the results is calculated using the root mean square error over the RMS of the exact bands. It should be noted that although the numerical and analytical results can be compared on a point by point basis, the $\dfrac{RMSE}{RMS}$ value simplifies the whole process with having only one error value to deal with. In figure 3-4 the analytical energy band structure of lattice No. 1 is compared to the calculated results of the

solver side by side. The physical input information of lattice No. 1 are mentioned right after equation (3-49).
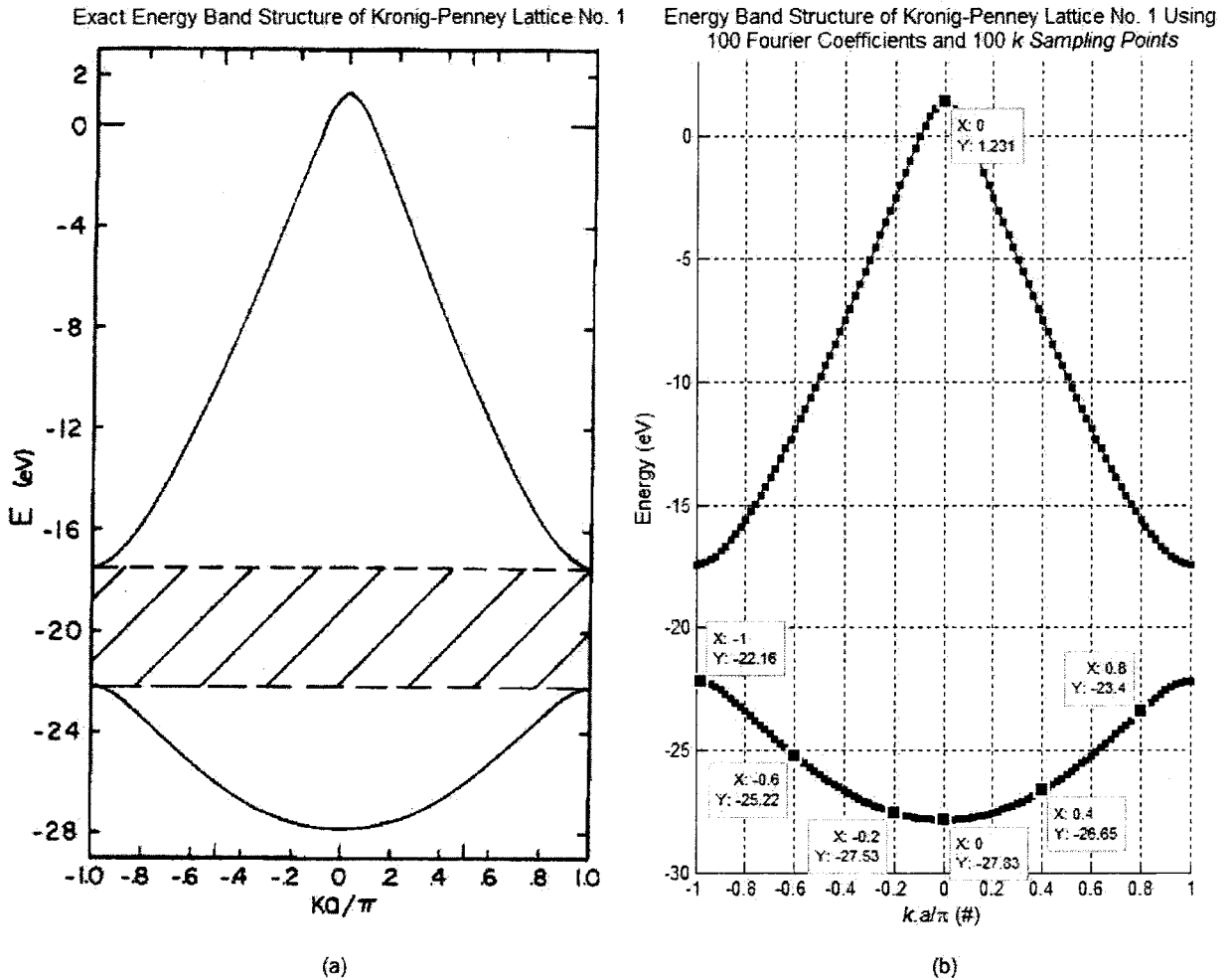
Figure 3-4. (a) Energy band structure of Kronig-Penney lattice No. 1 plotted with the exact results. (b) The same energy band structure plotted using the results of the 1D Solver. To calculate the results, one hundred Fourier coefficients and one hundred wave vector sampling points have been used. Calculation Time: 41.687s.

The results will be compared numerically but the match can be visually seen in figure 3-4 as well. Numerical error calculation is done in the later parts.

The same is done for Kronig-Penney lattice No. 2 in figure 3-5. The physical inputs for this case are shown after equation (3-49). The number of Fourier coefficients and sampling points used are mentioned above each figure.
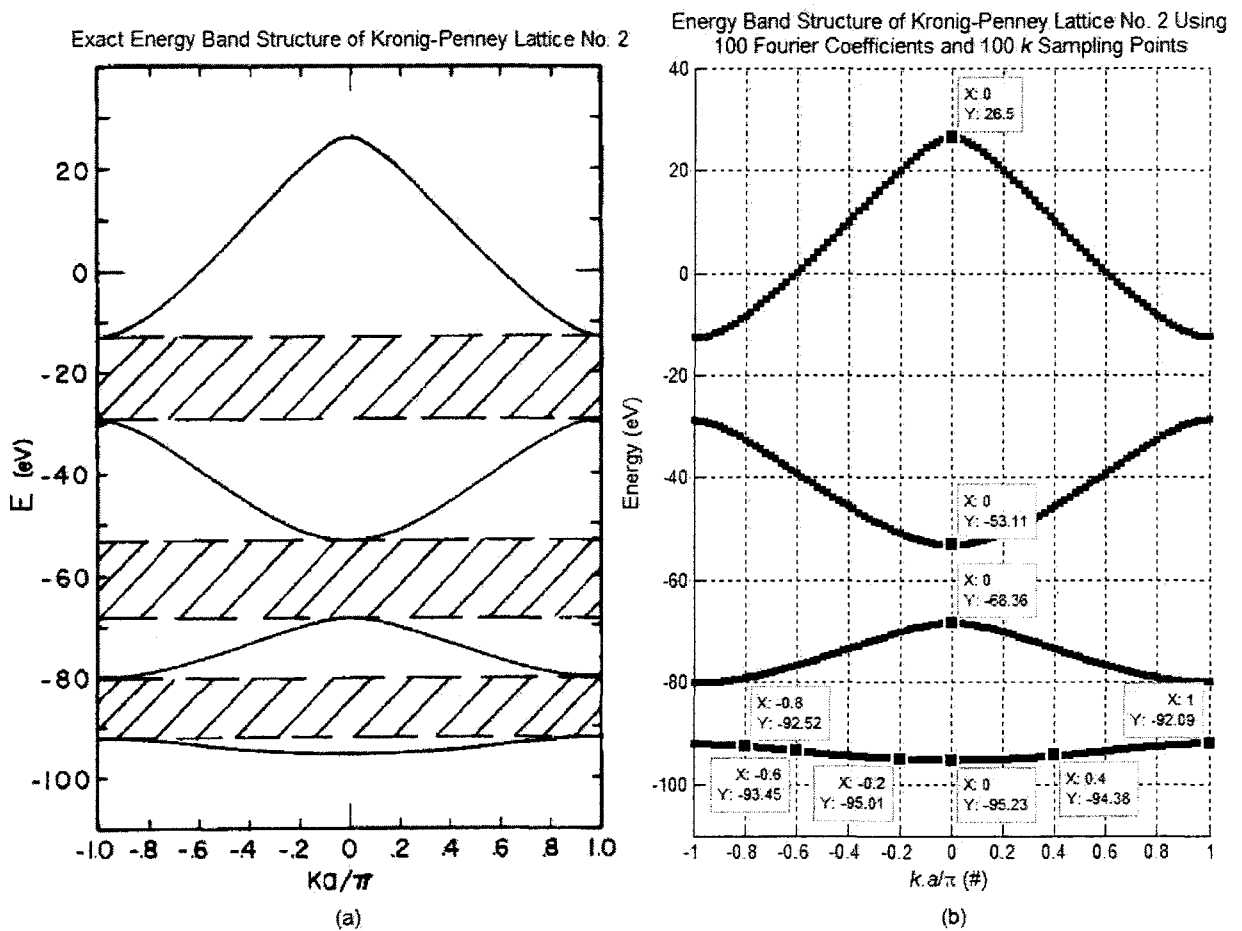
Figure 3-5. (a) Energy band structure of Kronig-Penney lattice No. 2 plotted with the exact results. (b) The same energy band structure plotted using the results of the 1D Solver. To calculate the results, one hundred Fourier coefficients and one hundred wave vector sampling points have been used. Calculation Time: 41.837s.

The relative error in the results of lattice No. 1 is calculated below:

$$\mathrm{Re}l.Error = \sqrt{\frac{(-27.822+27.83)^2+(-27.527+27.53)^2+...+(-22.195+22.16)^2}{(-27.822)^2+(-27.527)^2+(-26.651)^2+(-25.229)^2+(-23.418)^2+(-22.195)^2}}$$

(3-50a)

$$\mathrm{Re}l.Error = 0.000659 \quad \text{or} \quad \mathrm{Re}l.Error = 0.0659\%$$

(3-50b)

The relative error in the results of lattice No. 2 is calculated below:

$$\mathrm{Re}l.Error = \sqrt{\frac{(-95.225+95.23)^2+(-95.006+95.01)^2+...+(-92.119+92.09)^2}{(-95.225)^2+(-95.006)^2+(-94.382)^2+(-93.466)^2+(-92.541)^2+(-92.119)^2}}$$

(3-51a)

$$\mathrm{Re}l.Error = 0.000173 \quad \text{or} \quad \mathrm{Re}l.Error = 0.0173\%$$

(3-51b)

As it can be seen, the results are almost exact and there is negligible error in the results. However, the error is different from point to point. It is predictable that the relative error increases a little for upper bands but it will be in the order of the error that is obtained here. Now that the results of the solver are compared to the actual results and they are shown to be correct with excellent accuracy, the amount of information that the solver works with and the number of wave vector sampling points will be reduced to find the minimum number of Fourier coefficients and wave vector sampling points that are enough to get accurate and acceptable results. This is especially helpful for upgrading to the 3D solver because the amount of data is very high in that case and the solver should work with minimal amount of data that is enough for delivering accurate results. This will be studied on Kronig-Penney lattice No. 2 and each of the Fourier

coefficients and sampling points are studied separately and after that together to make sure one doesn't have any affect on the other.

First the effects of lowering the number of Fourier coefficients used to solve the energy band structure are studied. The Fourier coefficients are the elements that parameterize most of the functions in the solver, including the potentials, the wave functions and more. So a lower number of coefficients mean a less accurate representation of the functions in the solver which will in turn lead to inaccuracies in the results which are also dependant on the Fourier coefficient numbers used. It should be noted that because no function in this study changes very quickly a much lower number than the one hundred coefficients used in the last part is required but if the number of coefficients passes a limit, the error starts to increase and that is the point which is optimum for doing the calculations at.

To obtain the least number of coefficients that leads to accurate results, the number of wave vector sampling points is kept at one hundred. The results of the solver with forty and twenty Fourier coefficients are shown in figures 3-6 and 3-7. The relative error of the results is calculated under each figure.

The inputs to the figures hereafter are the physical data about lattice No. 2 and the information about the number of Fourier coefficients and wave vector sampling points. The latter two are mentioned in each figure's information.

Figure 3-6. Energy Band Structure of Kronig-Penney Lattice No. 2 numerically

calculated using forty Fourier coefficients and one hundred wave vector sampling

points. Calculation Time: 16.456s.

$$\mathrm{Re}\,l.Error = \sqrt{\frac{(-95.225+95.23)^2+(-95.006+95.01)^2+\dots+(-92.119+92.09)^2}{(-95.225)^2+(-95.006)^2+(-94.382)^2+(-93.466)^2+(-92.541)^2+(-92.119)^2}}$$

(3-52a)

$$\mathrm{Re}\,l.Error = 0.000173 \quad \text{or} \quad \mathrm{Re}\,l.Error = 0.0173\%$$ (3-52b)

As it is shown, the results are the same as the case with one hundred

Fourier coefficients.

115

Figure 3-7. Energy Band Structure of Kronig-Penney Lattice No. 2 numerically calculated using twenty Fourier coefficients and one hundred wave vector sampling points. Calculation Time: 8.446s.

$$\mathrm{Re}\,l.Error = \sqrt{\frac{(-95.225+95.23)^2+(-95.006+95.01)^2+\dots+(-92.119+92.09)^2}{(-95.225)^2+(-95.006)^2+(-94.382)^2+(-93.466)^2+(-92.541)^2+(-92.119)^2}}$$

(3-53a)

$$\mathrm{Re}\,l.Error = 0.000173 \quad \text{or} \quad \mathrm{Re}\,l.Error = 0.0173\%$$

(3-53b)

Even by reducing the number of Fourier coefficients used by the solver to twenty the results are still accurate and not different from the case with one hundred coefficients. Knowing that the number of Fourier coefficients can be

116

reduced significantly, the solver will calculate the results using even less data on Fourier coefficients. The results of the solver using fourteen and eight Fourier coefficients can be found in figures 3-8 and 3-9.

Figure 3-8. Energy Band Structure of Kronig-Penney Lattice No. 2 numerically calculated using fourteen Fourier coefficients and one hundred wave vector sampling points. Calculation Time: 6.298s.

As it is seen in figure 3-8, the results of the solver start to change, but it should be noted that the error for fourteen Fourier coefficients doesn't change much from the case of one hundred Fourier coefficients.

$$\text{Re}l.Error = \sqrt{\frac{(-95.225+95.22)^2 + (-95.006+95.00)^2 + \ldots + (-92.119+92.09)^2}{(-95.225)^2 + (-95.006)^2 + (-94.382)^2 + (-93.466)^2 + (-92.541)^2 + (-92.119)^2}}$$

(3-54a)

$$\text{Re}l.Error = 0.000182 \quad \text{or} \quad \text{Re}l.Error = 0.0182\%$$

(3-54b)

Although there is no significant change in accuracy, it is a sign that the solver does not have as much information as it had before.

Figure 3-9. Energy Band Structure of Kronig-Penney Lattice No. 2 numerically calculated using eight Fourier coefficients and one hundred wave vector sampling points. Calculation Time: 3.557s.

118

Although the results start to have more errors but it can be seen that the program is very robust against the changes in Fourier coefficient numbers and converges to the results with little error even with limited information. The relative error in the case of eight Fourier series coefficients is calculated below:

$$\text{Re}l.Error = \sqrt{\frac{(-95.225+95.18)^2+(-95.006+94.96)^2+...+(-92.119+92.08)^2}{(-95.225)^2+(-95.006)^2+(-94.382)^2+(-93.466)^2+(-92.541)^2+(-92.119)^2}}$$

(3-55a)

$$\text{Re}l.Error = 0.000446 \quad \text{or} \quad \text{Re}l.Error = 0.0446\%$$

(3-55b)

The error is still completely acceptable. The least information that can calculate four bands with the solver is only four Fourier coefficients. If it is shown that the solver can even solve the energy band structure with the minimum number of Fourier coefficients possible, this is a great step toward reducing the amount of data that has to be used in the 3D Solver in the next chapter. As a last step in studying the effect of the Fourier series coefficients the case of four coefficients is studied. Figure 3-10 shows the energy band structure calculated with four coefficients.

The relative error in this case is calculated below:

$$\text{Re}l.Error = \sqrt{\frac{(-95.225+94.99)^2+(-95.006+94.78)^2+...+(-92.119+92.08)^2}{(-95.225)^2+(-95.006)^2+(-94.382)^2+(-93.466)^2+(-92.541)^2+(-92.119)^2}}$$

(3-56a)

$$\text{Re}l.Error = 0.001800 \quad \text{or} \quad \text{Re}l.Error = 0.1800\%$$

(3-56b)

It is not only the error that has increased dramatically from the last calculations but there is also band deformation that can be seen if we look at data closely.
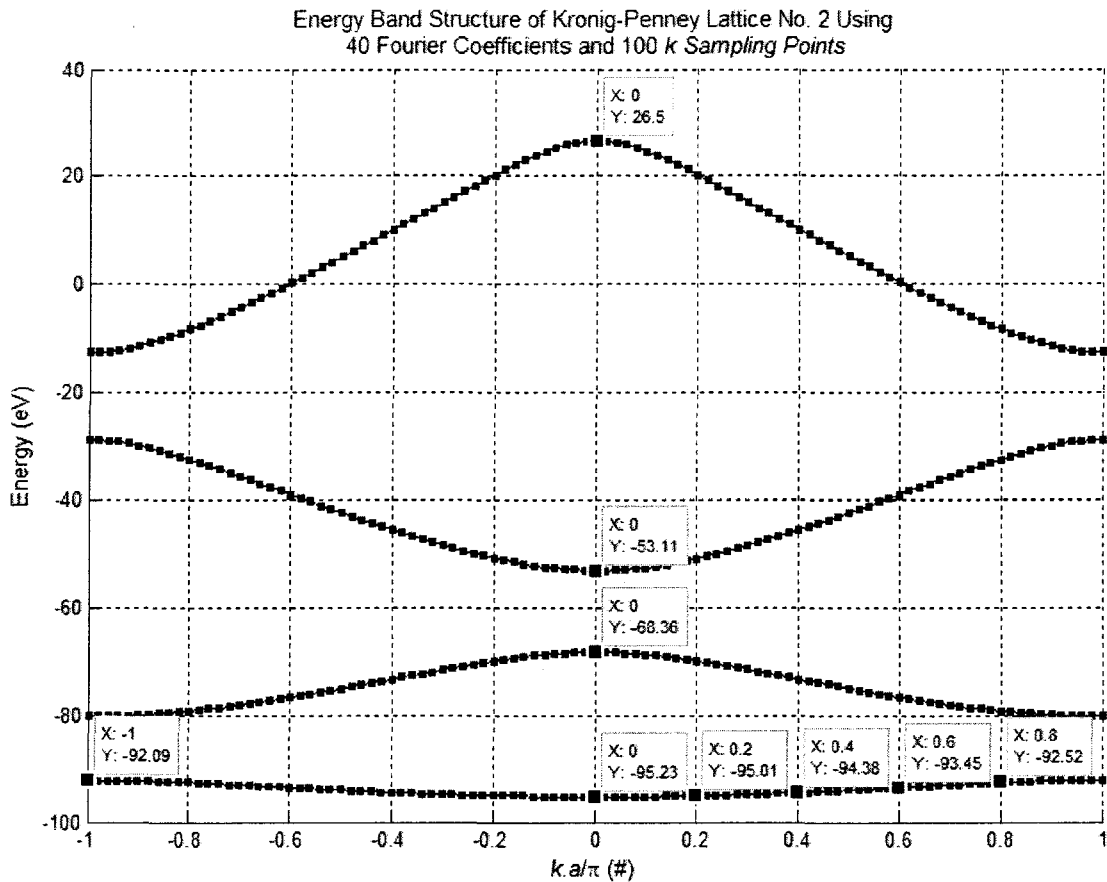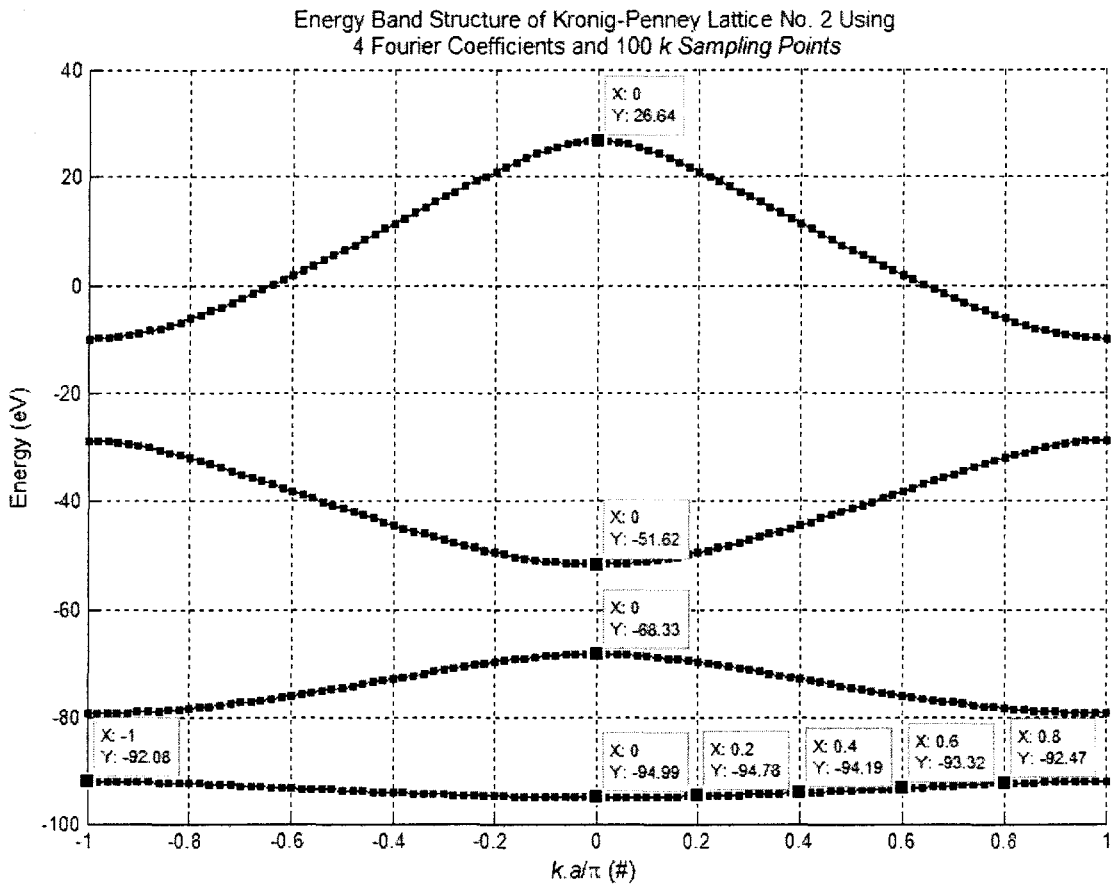
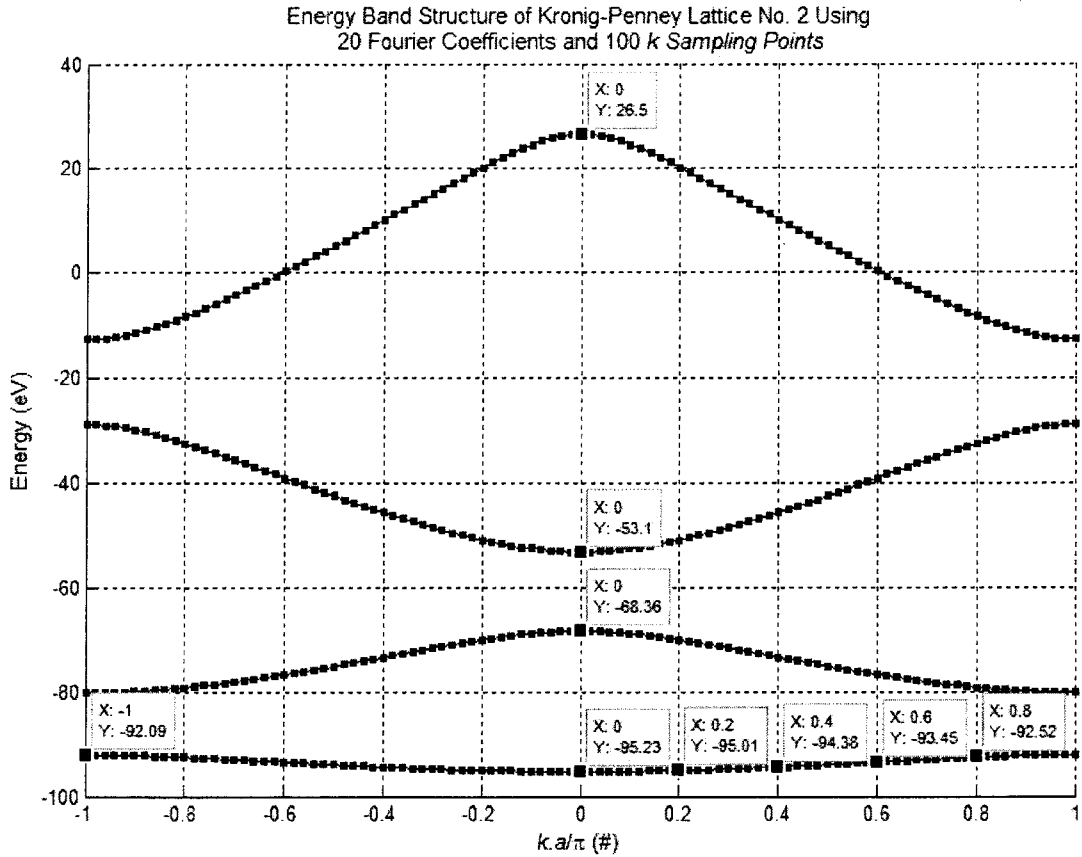

Figure 3-10. Energy Band Structure of Kronig-Penney Lattice No. 2 numerically calculated using four Fourier coefficients and one hundred wave vector sampling points. Calculation Time: 2.020s.

The closer to $\dfrac{k.a}{\pi} = 0$, the more the band has moved. Although this error is still small and the deformation is negligible, but it is wiser to use six or eight

Fourier terms as the minimum number of Fourier series coefficients used to find the results. It should be noted that the error for six coefficients is in the order of error for eight or more coefficients. Table (3-3) compares the calculation times and error levels for different numbers of Fourier coefficients as inputs to the solver.

No. of k sampling points (#)	No. of Fourier coefficients (#)	Calculation Time (sec)	Relative Error % (#)
100	100	41.837	0.0173
100	80	33.088	0.0173
100	60	24.776	0.0173
100	40	16.456	0.0173
100	20	8.446	0.0173
100	14	6.298	0.0182
100	8	3.557	0.0446
100	4	2.020	0.1800

Table 3-3. A comparison of the calculation time and relative error of the 1D solver based on different number of Fourier coefficient inputs.(Intel core 2 duo, 2.13Ghz, 2Gb Ram. All the Calculations are performed with the same system in this thesis)

To start studying the minimum number of wave vector sampling points that can be used for the solver, it should be noted as these sampling points are used for finding the total density functional. Because of that matter the number of sampling points should not decrease as much as the number Fourier coefficients

could decrease. The integral that calculates the density functional is directly dependant on the number of k points. And also, plotting the energy band structure smoothly and accurately needs a sufficient number of points in which we know the values of energies in all bands. Holding the number of Fourier coefficients at one hundred, we only study the cases of forty, twenty and sixteen k sampling points and will not decrease the number of k sampling points any less than sixteen. The energy band structures in each case are shown in figures 3-11 to 3-13.
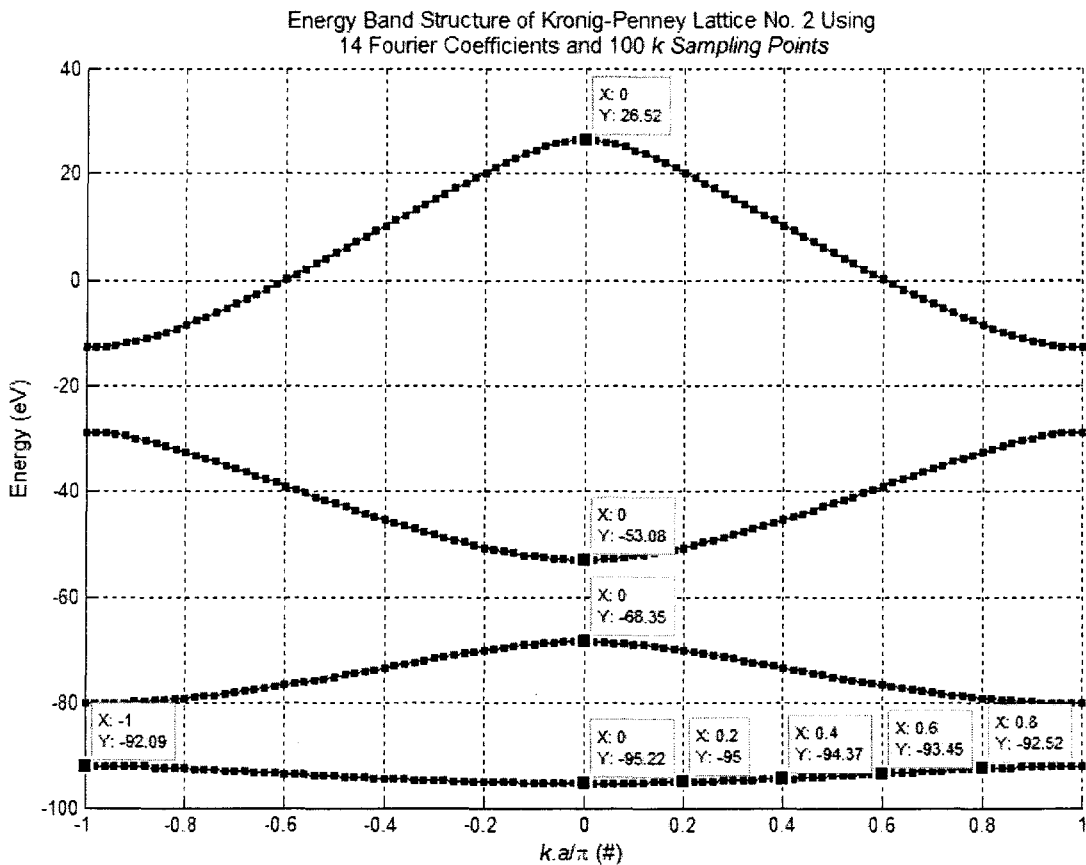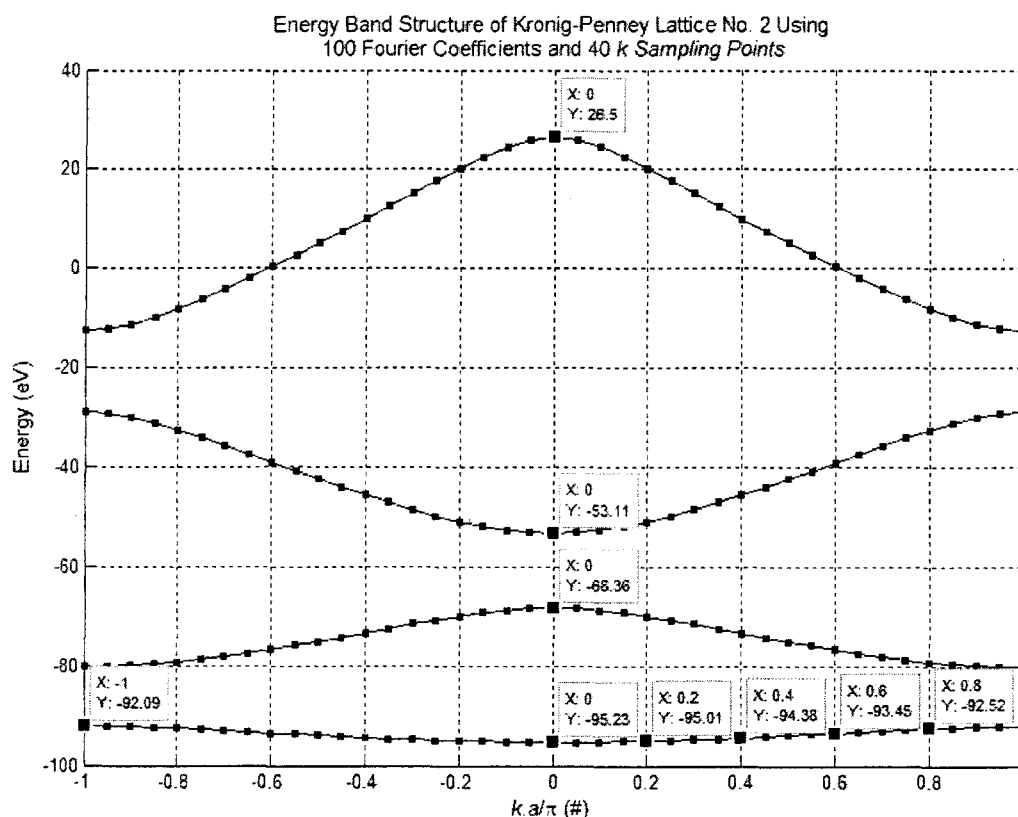

Figure 3-11. Energy Band Structure of Kronig-Penney Lattice No. 2 numerically calculated using one hundred Fourier series coefficients and forty wave vector sampling points. Calculation Time: 41.162s.

As it is seen in the figure the error levels do not change. It was expected as one of the most important parts that the number of wave vector sampling points has impact on is the calculation of density function, but because density function is slowly varying in case of semiconductors, it can be calculated using a small number of sampling points.
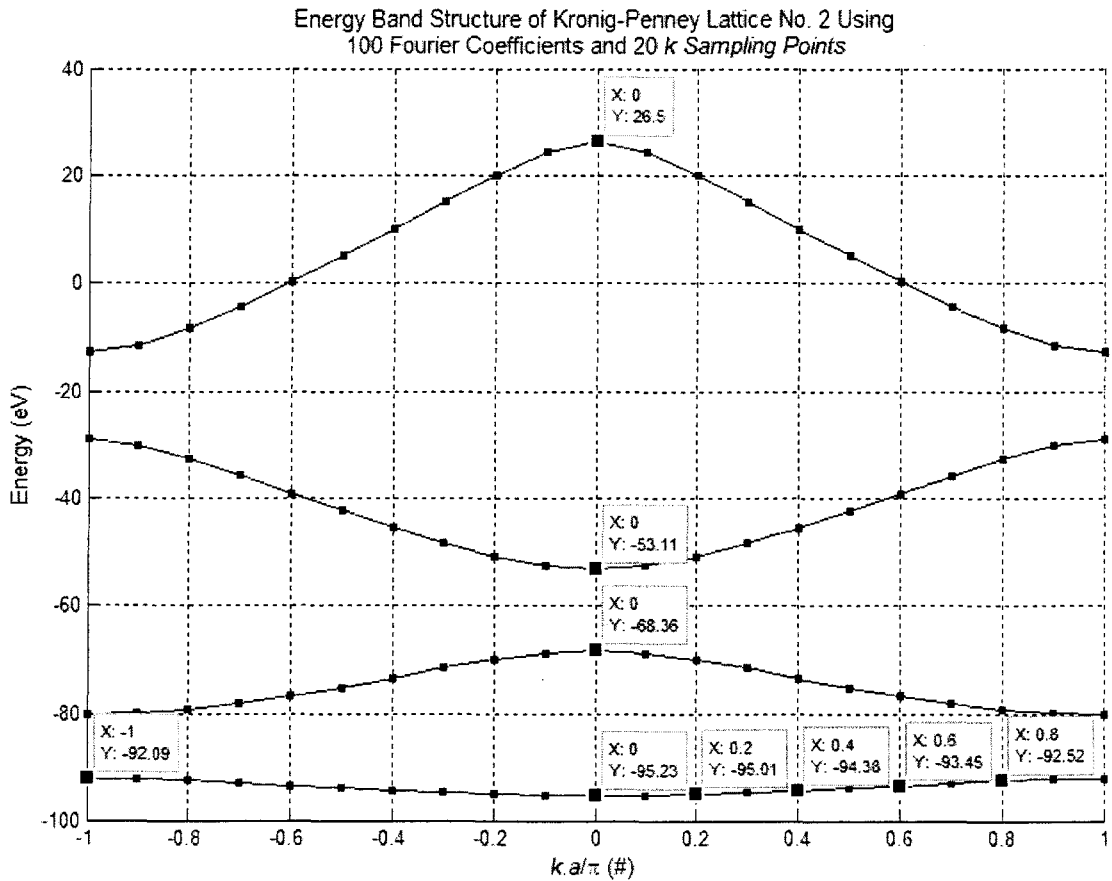
Figure 3-12. Energy Band Structure of Kronig-Penney Lattice No. 2 numerically calculated using one hundred Fourier series coefficients and twenty wave vector sampling points. Calculation Time: 40.574s.

Using twenty wave vector sampling points is satisfactory as well and there is no change in the final results using this number of sampling points.
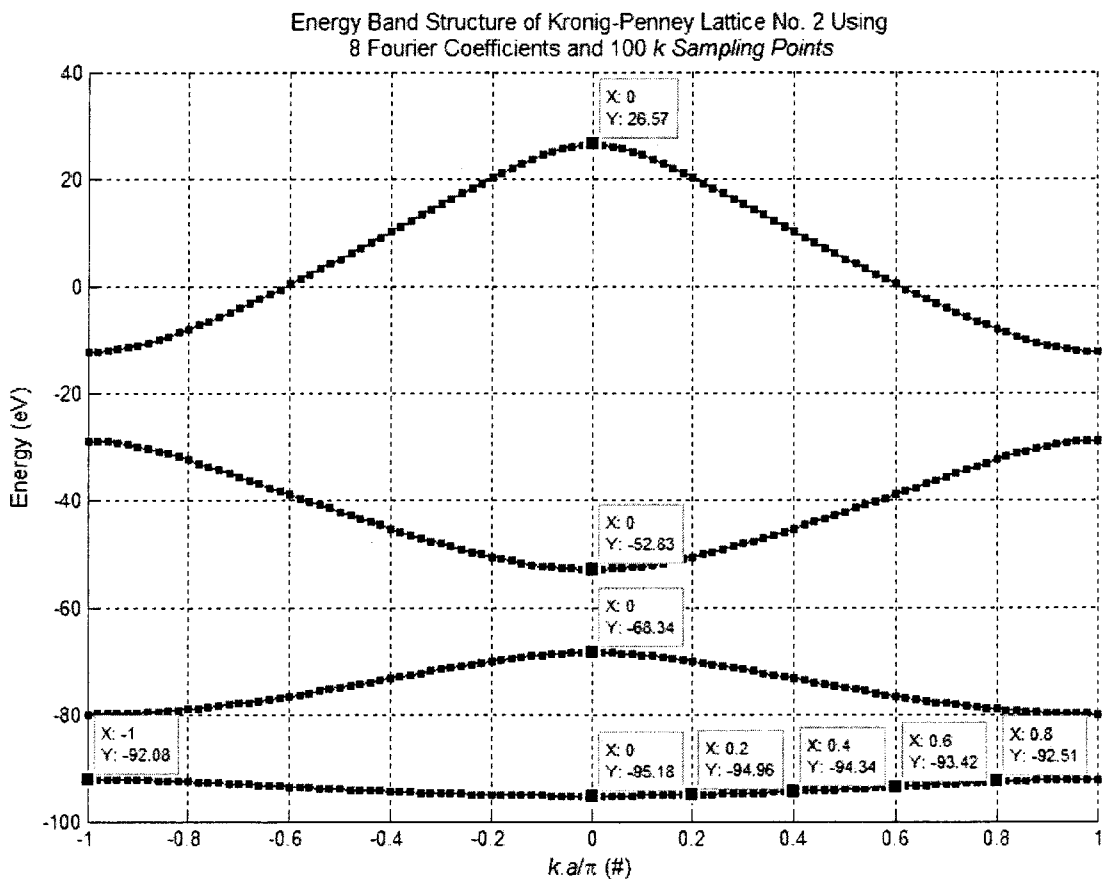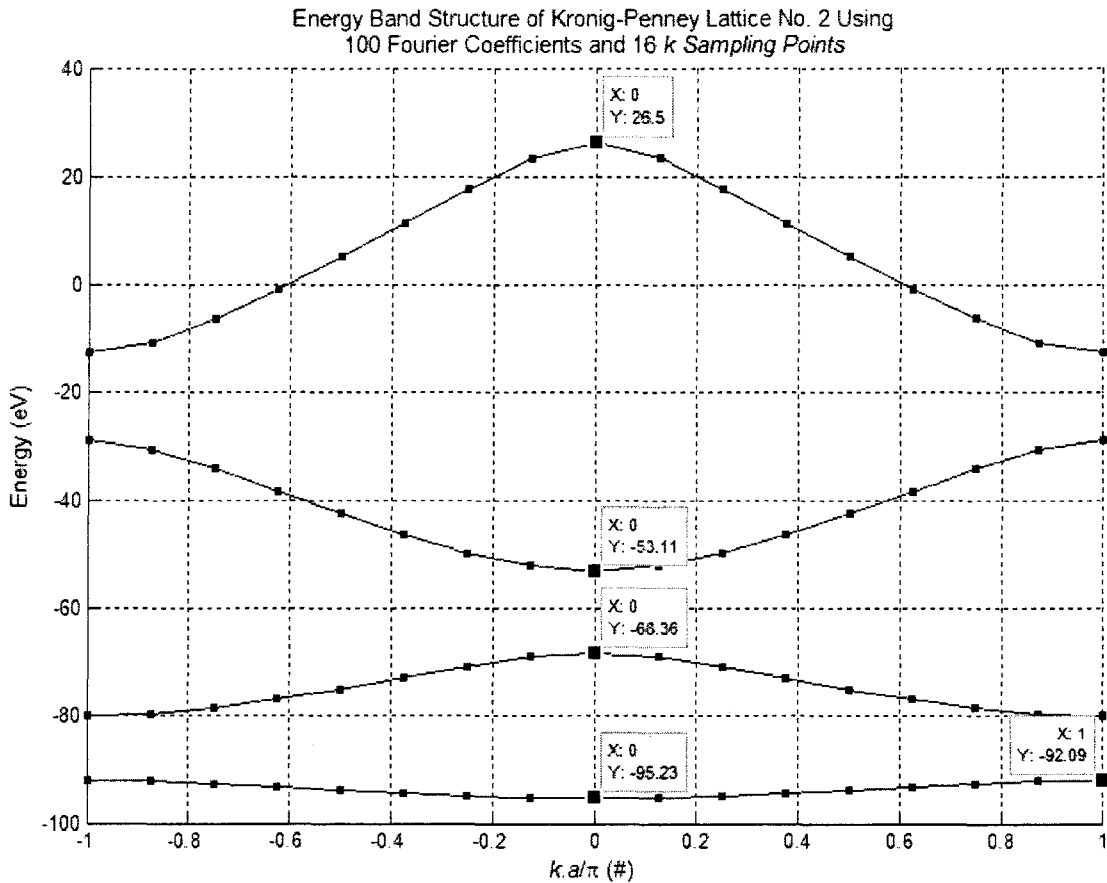

Figure 3-13. Energy Band Structure of Kronig-Penney Lattice No. 2 numerically calculated using one hundred Fourier series coefficients and sixteen wave vector sampling points. Calculation Time: 40.481s.

Unfortunately, using sixteen sampling points, the solver would not calculate data on the points that the exact results are available. But by finding the

values at this points that are available analytically, by averaging the values using the two nearest calculated points, it is seen that the error has increased slightly. This number of sampling points is chosen as the minimum used because the effects of a bad calculation of density function has to be avoided. Table (3-4) compares the calculation times and error levels for different numbers of k sampling points as inputs to the solver.

No. of Fourier coefficients (#)	No. of k sampling points (#)	Calculation Time (sec)	Relative Error % (#)
100	100	41.837	0.0173
100	80	41.553	0.0173
100	60	41.331	0.0173
100	40	41.162	0.0173
100	20	40.574	0.0173
100	16	40.481	> 0.0173

Table 3-4. A comparison of the calculation time and relative error of the 1D solver based on different number of k sampling point inputs.

As a last part of this section the energy band structure and the final potential energy of the Kronig-Penney lattice No. 2 is calculated using twenty Fourier coefficient terms and twenty wave vector sampling points to show that the two reductions in the amount of information can be combined and would not

result in more errors. The final potential energy is shown in figure 3-14 and the energy band structure using this information is shown in figure 3-15.
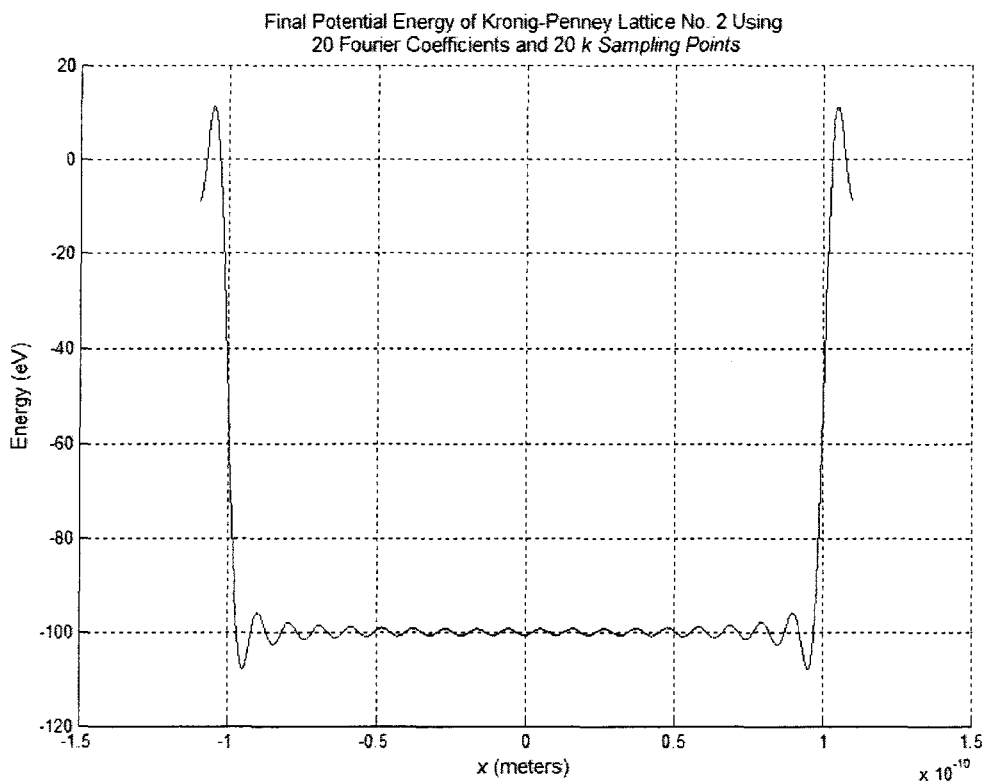
Figure 3-14. Final Potential Energy of Kronig-Penney lattice No. 2 using twenty Fourier coefficients and twenty wave vector sampling points as input information.
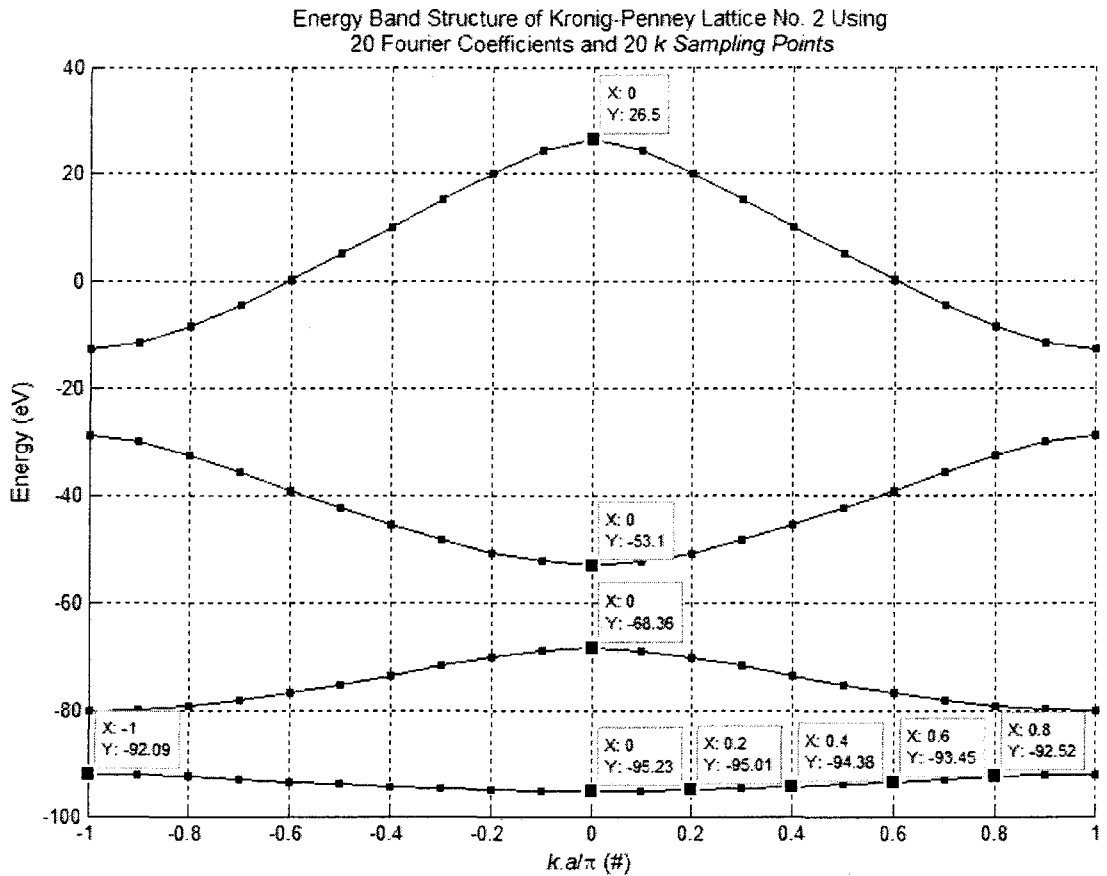
Figure 3-15. Energy Band Structure of Kronig-Penney Lattice No. 2 calculated using twenty Fourier series coefficients and twenty wave vector sampling points. Calculation Time: 8.412s.

By showing that the 1D Solver can deliver results using a minimal number of Fourier coefficients and wave vector sampling points, it is known that when this solver is modified to solve the 3D structures it can use small numbers of inputs. This helps the 3D solver not to have memory problems and have a reasonable amount of data to deal with.

3.5 Summary

In this chapter the 1D Electronic Band Structure Solver was discussed. The algorithm of the solver was discussed in details. The calculation methods in different parts of the algorithm are explained. The methods explained included the OPW expansion, the integral calculation method that used in the solver, solving the eigen value problem, calculation of Hartree and XC potential energies, and the method of comparing the old and new density functions.

The Solver was assessed using the benchmark results that were analytically calculated in [75]. The relative errors were calculated when the solver had a large amount of data available to it. For lattice No. 1, the relative error was measured to be 0.0659% and for lattice No. 2 it was measured at 0.0173%. The effect of changing the number of Fourier coefficients which is the data that the solver receives, and the number of wave vector sampling points which is used to handle and use the data were studied. It was shown that the solver can work with small numbers of Fourier coefficients and wave vector sampling points. It was also shown that having a small number of both Fourier coefficients and wave vector sampling points does not affect the results that were studied. As a result, it was concluded that when modifying the solver for solving the 3D structures to avoid handling a very large amount of data, small numbers of Fourier coefficients and wave vector sampling points can be used from the start of work.

Chapter 4: The 3D Crystal Electronic Band Structure Solver

4.1 Introduction

In this chapter the 3D Crystal Electronic Band Structure Solver will be discussed and studied. This solver is a changed version of the 1D solver that was discussed in the last chapter. This chapter will have the same major parts of the last chapter. Many of the parts require less explanation as there is little or no changes from the 1D solver in some parts. All of the changes of the solver will be discussed in details. Handling the data and fitting the information from a 3D structure into a single matrix by managing them properly will be explained in details.

An assessment of the 3D solver will be conducted using the Si lattice energy band structure. It should be noted that the program of the solver will be designed for Si lattice, but with modifications other lattices can be studied with the solver. The algorithm of the solver is good for all types of periodic crystalline lattices but each different lattice needs refinements on choosing the efficient number of wave vector sampling points for good convergence of the results and a good pseudopotential which may not be like the one used for Si in this solver.

4.2 The Algorithm

The algorithm of the 3D solver is the same as the algorithm of the 1D solver. The only difference is that all the equations to be solved are now 3D

equations that have to be solved numerically which will be dealt with in the calculation methods part. However, the algorithm of this solver will be discussed briefly here for convenience.

The first step is to choose a good pseudopotential to start with. This step was left to be discussed in details here from the last chapter because in the 1D solver the Kronig-Penney lattice was being discussed that didn't need to be changed and only needed to have smooth edges for the program. This part will be discussed in calculation methods part.

After choosing the pseudo potential which is also called the ion potential here, the Hamiltonian for the Schrödinger equation is calculated. After this step the Schrödinger equation is solved for the first time using the Hamiltonian calculated.

The results of the Schrödinger equation are used to calculate the density function of the system. These results will then be used to calculate the Hartree potential and the XC Potential. The potential that will be used for calculating the potential energy for solving the Schrödinger equation in the iteration that starts is always like the following:

$$v(r) = v_{ion} + v_{Hartree} + v_{xc} \qquad (4\text{-}1)$$

It should be noted again that v_{ion} will remain the same in this algorithm and is not changed in the process.

After solving the Schrödinger equation with the new potential, the new density function will be determined from the results of the Schrödinger equation.

This new density function is then compared with the old density function from the last step of iteration. The iteration ends if the difference between the density functions is less than a preset amount unless the new potential will be calculated using equation (4-1).

After the iteration ends the results of the last Schrödinger equation which is solved is the final solution to the problem. The results of this Schrödinger equation will be used to determine the energy band structure of the material being studied.

As it can be seen, the algorithm is like the one mentioned for the 1D Solver, however there are differences in calculation methods which originate from the additional dimensions being involved in the new solver. The differences in the calculation methods will be discussed in details in the next part. Any method that is the same as the 1D solver's calculation methods will only be reminded as not being different with the 1D solver.

A flowchart of the 3D energy band structure solver is shown in figure 4-1 in the next page.
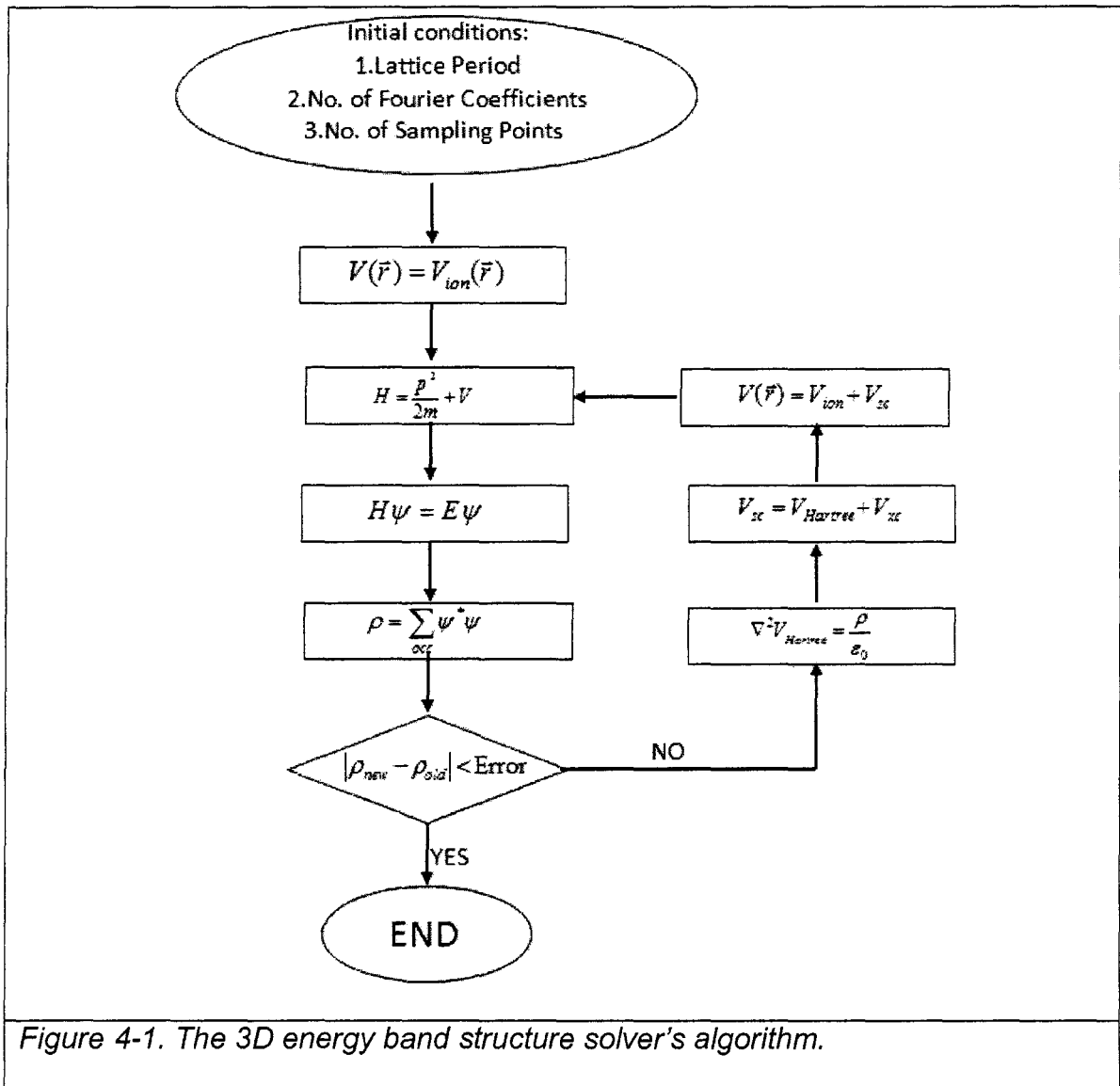
Figure 4-1. The 3D energy band structure solver's algorithm.

4.3 Calculation Methods

The calculation methods of the 3D solver in most cases are basically an expansion of the calculation methods that were used for the 1D solver. First of all an ion potential will be chosen for the program. The OPW expansion of the potentials is one of the methods that will be discussed in which the differences

with the 1D solver will be shown. The conversion of the Schrödinger equation into an eigen value problem will not be demonstrated for the 3D case and only a brief explanation of how it is done will be highlighted. To show how the data is converted to the sum of a plane wave basis set, the efficient integral methods that are used for the 3D solver will be discussed. The integrals will be done using the processors' capability to perform many multiplications or summations at the same time. The efficiency of each calculation method or in other words, its calculation speed, is of special importance in the 3D solver. The methods that are chosen must be accurate but because accuracy is not the only goal of the solver, each calculation method should be efficient enough as well.

The numerical method used for solving the eigen value problem, which replaces the Schrödinger equation, will be introduced and references about the method will be mentioned. The new solution to the Hartree potential problem which is basically another example of an expansion of a 1D calculation method will be discussed as the last part of this section which is different from the 1D solver.

4.3.1 Selection of the Ion Potential

As it is known, the potential of an ion in a point with the distance of r from it can be written in the form of a constant number (which can be found for any ion) over the distance from the ion. For simplicity, it is assumed that all the charges are located in the center of the ion. This assumption does not lead to

any mistake as the potential at ranges that are closer than a set value to the ion are being modified in the pseudopotential method and do not play a part in the calculations. The distance, r, can be described in Cartesian coordinates as below:

$$r = \sqrt{x^2 + y^2 + z^2} \tag{4-2}$$

So the ion potential is in the following form:

$$v_{ion}^{phys.} = \frac{const.}{r} = \frac{const.}{\sqrt{x^2 + y^2 + z^2}} \tag{4-3}$$

The ion potential that is used in this solver is a soft pseudopotential which means that it should be zero at the point that the ion is physically located. In the case that is being discussed it means that the pseudopotential should be zero at zero. As the potential of an ion has spherical symmetry, for more convenience, a case of 1D potential can be discussed first and then the results of the 1D case can be applied to the ion potential case to confirm that it is compatible with the 3D case.

A 1D ion potential, where the ion is placed at $x = 0$, is as follows:

$$v_{ion}^{1D} = \frac{const.}{|x|} \tag{4-4}$$

The pseudopotential should have the following form:

$$v_{pp}^{1D}(x) = \begin{cases} v_{ion}^{1D}(x) & |x| \geq d \\ f_{pp}^{1D}(x) & |x| < d \end{cases} \tag{4-5}$$

The pseudopotential should be smoothly continuous and should be zero at the point zero. And like the 1D potential, the pseudopotential must be an even function as only the distance from the charge is important for the potential function. These conditions are shown as below:

$$f_{pp}^{1D}(0) = 0 \qquad (4\text{-}6)$$

$$f_{pp}^{1D}(d) = v_{ion}^{1D}(d) \text{ and } f_{pp}^{1D}(-d) = v_{ion}^{1D}(-d) \qquad (4\text{-}7)$$

$$\frac{df_{pp}^{1D}(d)}{dx} = \frac{dv_{ion}^{1D}(d)}{dx} \text{ and } \frac{df_{pp}^{1D}(-d)}{dx} = \frac{dv_{ion}^{1D}(-d)}{dx} \qquad (4\text{-}8)$$

Both of the equations regarded as equation (4-8) are the same because the pseudopotential function should be an even function. The same applies to equations regarded as equation (4-9).

A fourth degree polynomial is chosen here to represent the new part of the ion pseudopotential. The function is shown as below:

$$f_{pp}^{1D}(x) = ax^4 + bx^3 + cx^2 + gx + p \qquad (4\text{-}9)$$

As the pseudopotential function is an even function with regard to x, before solving the equations it is known that b and g are zero to ensure that the function is even. So it is known that:

$$b = 0 \qquad (4\text{-}10)$$

$$g = 0 \qquad (4\text{-}11)$$

From equation (4-6) it is clear that:

$$p = 0 \qquad (4\text{-}12)$$

Equations (4-7) and (4-8) lead to the following:

$$ad^4 + cd^2 = \frac{const.}{d} \tag{4-13}$$

$$4ad^3 + 2cd = \frac{-const.}{d^2} \tag{4-14}$$

It should be noted that d is a value that is chosen and is considered as known in equations (4-13) and (4-14). Based on this fact, the values of a and c are calculated using the last two equations as follows:

$$a = -\frac{3}{2} \cdot \frac{const.}{d^5} \tag{4-15}$$

$$c = \frac{5}{2} \cdot \frac{const.}{d^3} \tag{4-16}$$

The function which replaces the near core part of the physical ion potential is:

$$f_{pp}^{1D}(x) = -\frac{3}{2} \cdot \frac{const.}{d^5} x^4 + \frac{5}{2} \cdot \frac{const.}{d^3} x^2 \tag{4-17}$$

Now that a pseudopotential that can replace the physical ion potential is found in the 1D case, the results of these calculations can be tested for a 3D case to verify that they are correct if x is replaced with the distance from the ion centre in the 3D case, assuming the ion is at $x = y = z = 0$. Having equation (4-2) in mind, the 3D ion pseudopotential is as follows:

$$v_{ion}(r) = \begin{cases} v_{ion}^{phys.}(x,y,z) & r \geq d \\ f_{pp}(r) & r < d \end{cases} \quad \text{where} \quad r = \sqrt{x^2 + y^2 + z^2} \tag{4-18}$$

The following conditions should be met:

$$f_{pp}(0) = 0 \tag{4-19}$$

$$v_{ion}^{phys.}(d) = f_{pp}(d) \tag{4-20}$$

$$\nabla v_{ion}^{phys.}(d) = \nabla f_{pp}(d) \tag{4-21}$$

It is noted that the function replacing the physical ion potential near the core is:

$$f_{pp}(r) = -\frac{3}{2} \cdot \frac{const.}{d^5} r^4 + \frac{5}{2} \cdot \frac{const.}{d^3} r^2 \quad \text{where} \quad r = \sqrt{x^2 + y^2 + z^2} \tag{4-22}$$

From equation (4-22) it is obvious that equation (4-19) holds. To check equation (4-20), $f_{pp}(d)$ is calculated as follows:

$$f_{pp}(d) = -\frac{3}{2} \cdot \frac{const.}{d} + \frac{5}{2} \cdot \frac{const.}{d} = \frac{const.}{d} = v_{ion}^{phys.}(d) \tag{4-23}$$

To ensure that equation (4-21) holds in the 3D case, the gradients of both $f_{pp}(r)$ and $v_{ion}^{phys.}(r)$ are calculated in the following equations:

$$\nabla f_{pp}(r) = [-\frac{6 \cdot const. \cdot x}{d^5}(x^2 + y^2 + z^2) + \frac{5 \cdot const. \cdot x}{d^3}]\hat{x} +$$
$$[-\frac{6 \cdot const. \cdot y}{d^5}(x^2 + y^2 + z^2) + \frac{5 \cdot const. \cdot y}{d^3}]\hat{y} + \tag{4-24}$$
$$[-\frac{6 \cdot const. \cdot z}{d^5}(x^2 + y^2 + z^2) + \frac{5 \cdot const. \cdot z}{d^3}]\hat{z}$$

$$\nabla v_{ion}^{phys.}(r) = \frac{-const. \cdot x}{(x^2 + y^2 + z^2)^{\frac{3}{2}}}\hat{x} + \frac{-const. \cdot y}{(x^2 + y^2 + z^2)^{\frac{3}{2}}}\hat{y} + \frac{-const. \cdot z}{(x^2 + y^2 + z^2)^{\frac{3}{2}}}\hat{z} \tag{4-25}$$

Equations (4-24) and (4-25) can be shown to be equal to each other at $r = d$ where $r = \sqrt{x^2 + y^2 + z^2}$. The value of each equation at $r = d$ will be:

$$\nabla v_{ion}^{phys.}(d) = \nabla f_{pp}(d) = -const. \cdot [\frac{x}{d^3}\hat{x} + \frac{y}{d^3}\hat{y} + \frac{z}{d^3}\hat{z}] \qquad (4\text{-}26)$$

As equation (4-26) shows, the last condition is met like the first two did. So it is shown that the ion pseudopotential, also called ion potential hereafter, has all the conditions for a good pseudo potential. So the ion potential in equation (4-18) will be used in the 3D solver.

4.3.2 Differences in the OPW Expansion in 3D Solver

As this matter has been discussed in the last chapter for the 1D case, this part will be dealing with the 3D case in a more brief way. The potential energy in a Lattice is periodical. To keep the generality of the case, it is assumed that the potential is periodic in x direction with period a, in y direction with period b, and in z direction with period c. It is shown mathematically as follows:

$$V(x,y,z) = V(x+a,y,z) = V(x,y+b,z) = V(x,y,z+c) \qquad (4\text{-}27)$$

The potential will be parameterized by the Fourier coefficients in the following way:

$$V(x,y,z) = \sum_l \sum_m \sum_n \alpha_{l,m,n} e^{i(\frac{2\pi l}{a}\hat{x} + \frac{2\pi m}{b}\hat{y} + \frac{2\pi n}{c}\hat{z})\cdot \vec{r}} \quad \text{where} \quad \vec{r} = x\cdot\hat{x} + y\cdot\hat{y} + z\cdot\hat{z}$$

$$(4\text{-}28)$$

$$\alpha_{l,m,n} = \int_{-\frac{a}{2}-\frac{b}{2}-\frac{c}{2}}^{\frac{a}{2}\frac{b}{2}\frac{c}{2}} \int \int V(x,y,z) e^{-i(\frac{2\pi l}{a}\hat{x} + \frac{2\pi m}{b}\hat{y} + \frac{2\pi n}{c}\hat{z})\cdot \vec{r}} dxdydz \qquad (4\text{-}29)$$

Based on Bloch theorem the wave function of the lattice can be parameterized as:

$$\psi(x,y,z) = [\sum_l \sum_m \sum_n \beta_{l,m,n} e^{i(\frac{2\pi l}{a}\hat{x}+\frac{2\pi m}{b}\hat{y}+\frac{2\pi n}{c}\hat{z})\cdot\vec{r}}]e^{i\vec{k}\cdot\vec{r}} \text{ where } \vec{k} = k_x\hat{x}+k_y\hat{y}+k_z\hat{z}$$

(4-30)

Equation (4-30) can be rewritten in the following way:

$$\psi(x,y,z) = \sum_l \sum_m \sum_n \beta_{l,m,n} e^{i[(\frac{2\pi l}{a}+k_x)\hat{x}+(\frac{2\pi m}{b}+k_y)\hat{y}+(\frac{2\pi n}{c}+k_z)\hat{z}]\cdot\vec{r}}$$

(4-31)

To rewrite the Schrödinger equation by replacing the wave function and the potential in it, $\nabla^2\psi(x,y,z)$ should be first parameterized in the same way. This value can be calculated using equation (4-31). After calculations this value is parameterized as follows:

$$\nabla^2\psi(x,y,z) = -[(\frac{2\pi l}{a}+k_x)^2 + (\frac{2\pi m}{b}+k_y)^2 + (\frac{2\pi n}{c}+k_z)^2]\psi(x,y,z)$$
$$= -D(\vec{k})\cdot\psi(x,y,z)$$

(4-32)

The Schrödinger equation is repeated here for substitution of the parameterized values:

$$(V - \frac{\hbar^2}{2m_0}\nabla^2)\psi = E\psi \Rightarrow V\psi - \frac{\hbar^2}{2m_0}\nabla^2\psi = E\psi$$

(4-33)

After the substitution, the Schrödinger equation will be as follows:

$$\sum_l \sum_m \sum_n \sum_p \sum_q \sum_t \alpha_{l,m,n} \beta_{p,q,t} e^{i(\frac{2\pi(l+p)}{a}\hat{x}+\frac{2\pi(m+q)}{b}\hat{y}+\frac{2\pi(n+t)}{c}\hat{z})\cdot\vec{r}} =$$

$$\sum_{l'} \sum_{m'} \sum_{n'} \beta_{l',m',n'} [E - \frac{\hbar^2}{2m_0} D(\vec{k})] e^{i(\frac{2\pi l'}{a}\hat{x}+\frac{2\pi m'}{b}\hat{y}+\frac{2\pi n'}{c}\hat{z})\cdot\vec{r}}$$

(4-34)

To solve for a specific $\beta_{L,M,N}$, both sides should be multiplied by

$e^{-i(\frac{2\pi l}{a}\hat{x}+\frac{2\pi m}{b}\hat{y}+\frac{2\pi n}{c}\hat{z})\cdot\vec{r}}$ and both sides of the equation should be integrated over one

cell, which is $\int_{-\frac{a}{2}}^{\frac{a}{2}} \int_{-\frac{b}{2}}^{\frac{b}{2}} \int_{-\frac{c}{2}}^{\frac{c}{2}} dxdydz$. After the integrations and calculations, the results are

as follows:

$$\beta_{L,M,N} [E - \frac{\hbar^2}{2m_0} D(\vec{k})] = \sum_l \sum_m \sum_n \beta_{l,m,n} \alpha_{L-l,M-m,N-n}$$

(4-35)

where:

$$D(\vec{k}) = [(\frac{2\pi l}{a} + k_x)^2 + (\frac{2\pi m}{b} + k_y)^2 + (\frac{2\pi n}{c} + k_z)^2]$$

(4-36)

As it can be seen, equation (4-35) is an expanded version of equation

(3-12). The two equations are mostly identical and the only difference is the

number of dimensions which causes the visual difference although equation

(3-12) is only a specific form of (4-35) in 1D.

To transform all the equations like equation (4-35) which are written for all

L, M, and N, they should be put in a matrix like the one made for the 1D case.

As there are three variables of L, M, and N other than just one in the 1D case,

the place of each of the unknowns in the wave vector that is to be found, should

be decided based on the variables L, M, and N. This can be done by having an index in which the place of each unknown is decided in the unknowns' wave vector.

There are no other differences in using the OPW expansion between the 1D case and the 3D case other than the mentioned data positioning and handling that can be done by any simple indexing method.

4.3.3 Integral Calculations for the OPW Expansion in 3D

Each integral in the 3D solver is calculated using a summation. The volume to be integrated over, the unit cell, is divided into a large number of smaller cubes, which in most cases is between 8000 and 64000. The solver calculates the value of the function to be integrated at the center point of each of the small cubes. The integral is calculated as the summation of the values of the function at each center point times the volume of a small cube. This is demonstrated in a simple form as bellow:

$$\int_{-\frac{a}{2}}^{\frac{a}{2}} \int_{-\frac{b}{2}}^{\frac{b}{2}} \int_{-\frac{c}{2}}^{\frac{c}{2}} f(x,y,z)dxdydz = \frac{abc}{n^3} \sum_p \sum_q \sum_t f(\frac{pa}{n},\frac{qb}{n},\frac{tc}{n}) \qquad (4\text{-}37)$$

where n is the number of divisions in each direction and n^3 is the number of small cubes used in the calculations. It should also be noted that $\frac{abc}{n^3}$ is the volume of a small cubes in the calculations.

The reason for the efficiency of the integral is not in the simplicity of what is being seen here in the mathematics. A summation of 64000 values and generating the values that include multiplying, which has to be done several hundred times in each iteration of the solver is not a small number that can be dealt with easily. This would take a lot of time if the summations are going to be done one at a time. This means 64000 times of adding two numbers. Instead, the solver uses the powers of the new processors and adds up to several hundred numbers at a time based on the processor capabilities. The solver generates the function values which should be integrated over the volume at all the points needed using a 3D array. A summation of all the values in the array is done based on the capabilities of the processor. The final summation is multiplied by the volume of the small cube. This process can reduce the time needed for the completion of the integrals by twenty to one hundred times based on the hardware being used.

4.3.4 The Solution Method of the Eigen Value Problem

Because of the method that the data is handled the matrix that is resulted from positioning the data into it is a full matrix that has no specific conditions or properties that can help finding the eigen values and eigen vectors based on the specific conditions or properties of the matrix. Based on this, a good general method of finding the eigen values should be utilized. One of the best methods that is used in the cases in which a matrix does not have any condition or

property that makes it suitable for a faster method designed for that specific condition or property is the QZ method which is also referred to as QR method.

The basic principal of this method is to decompose the input matrix into the product of an orthogonal matrix and a triangular matrix. This method needs iterations but it is a stable process and will converge. But the rate of conversion is dependant on the separation between the eigen values [76].

This method was developed by John G.F. Francis [77, 78] and Vera N. Kublanovskaya [79] independently at about the same time. More on the specifics of this method can be found in numerical calculations books. For more information on QR method the reader is referred to the "Numerical Recipes" book [72].

4.3.5 The Calculation of Hartree and XC Potential Energies

Although the calculations of the density function are very similar to the 1D calculations which were discussed in the last chapter, it will be reviewed briefly in this part because of minor differences. The calculation of the Hartree potential is a generalization of the 1D case which will be briefly reviewed as well. The XC potential is the same as the 1D case with the only difference of the integral calculation method and will not be discussed in this part.

The first step to find the density function of the system is to find the eigen vector of the eigen value problem. This eigen vector contains the Fourier coefficients of the wave function. Using the indexing method, each coefficient will

be multiplied by the correct plane wave basis function. For each $\bar{k}$ sampling point there are $(N+1)^3$ wave functions calculated where N is the number of Fourier coefficients used for each direction. The jth wave function at any $\bar{k}_{p,t,q}$ sampling point is formed as follows:

$$\psi_j(\vec{r})\Big|_{\bar{k}_{p,q,t}} = [\sum_l \sum_m \sum_n b^j_{l,m,n} e^{i(\frac{2\pi l}{a}\hat{x}+\frac{2\pi m}{b}\hat{y}+\frac{2\pi n}{c}\hat{z})\cdot\vec{r}}]e^{i\bar{k}_{p,q,t}\cdot\vec{r}} \qquad (4\text{-}38)$$

The density function at each wave function at any $\bar{k}_{p,t,q}$ can be calculated using the following equation:

$$\rho_j^{\bar{k}_{p,q,t}}(\vec{r}) = \psi_j(\vec{r})\Big|_{\bar{k}_{p,q,t}} \psi_j^*(\vec{r})\Big|_{\bar{k}_{p,q,t}} \qquad (4\text{-}39)$$

The conjugate of the wave function can be written in the following way:

$$\psi_j^*(\vec{r})\Big|_{\bar{k}_{p,q,t}} = [\sum_l \sum_m \sum_n b^{*j}_{l,m,n} e^{-i(\frac{2\pi l}{a}\hat{x}+\frac{2\pi m}{b}\hat{y}+\frac{2\pi n}{c}\hat{z})\cdot\vec{r}}]e^{-i\bar{k}_{p,q,t}\cdot\vec{r}} \qquad (4\text{-}40)$$

The density function described in equation (4-39) can be written as a sum of plane waves:

$$\rho_j^{\bar{k}_{p,q,t}}(\vec{r}) = \sum_l \sum_m \sum_n u^j_{l,m,n} e^{i(\frac{2\pi l}{a}\hat{x}+\frac{2\pi m}{b}\hat{y}+\frac{2\pi n}{c}\hat{z})\cdot\vec{r}} \qquad (4\text{-}41)$$

The coefficients of the plane waves in the density function described above are calculated using the following:

$$u^j_{l,m,n} = \sum_{l_1}\sum_{m_1}\sum_{n_1}\sum_{\substack{l_2\\l_1-l_2=l}}\sum_{\substack{m_2\\m_1-m_2=m}}\sum_{\substack{n_2\\n_1-n_2=n}} b^j_{l_1,m_1,n_1} b^{*j}_{l_2,m_2,n_2} \quad \text{where} \quad \begin{array}{l} l_1-l_2=l \\ m_1-m_2=m \\ n_1-n_2=n \end{array} \qquad (4\text{-}42)$$

144

The total density function at a $\vec{k}_{p,t,q}$ will be:

$$\rho^{\vec{k}_{p,q,t}}(\vec{r}) = \sum_{j=1}^{(N+1)^3} \rho_j^{\vec{k}_{p,q,t}}(r) \tag{4-43}$$

The total density function of the system is determined by an integral of the density function in equation (4-43) over all wave vector values in a Brillouin zone. To do this numerically, the density function should be calculated at a number of wave vector sampling points and the integral should be performed using the method explained in section 4.3.3. After the calculations the total density function can be written as the sum of plane wave functions as the integral is actually a summation of all of the density functions at sampling wave vector points times the volume of the small cubes that are assumed to have the same density function as their centers.

$$\rho(\vec{r}) = \sum_l \sum_m \sum_n U_{l,m,n} e^{i(\frac{2\pi l}{a}\hat{x} + \frac{2\pi m}{b}\hat{y} + \frac{2\pi n}{c}\hat{z}) \cdot \vec{r}} \tag{4-44}$$

Now that the density function of the system is known, the Hartree potential and the XC potential can be calculated. Calculations of the XC potential are exactly like the 1D case, which involves a direct integration and will not be discussed again here. The only difference in the two cases is the method that is used for integration. The Hartree potential, on the other hand, is a generalized case of the 1D case. The solution of the 3D case is a similar solution but is more complicated based on the more complex nature of the problem. The Poisson equation to be solved is:

$$\nabla^2 V_{Hartree} = \frac{\rho}{\varepsilon_0}$$ (4-45)

The equation can be rewritten as below:

$$(\frac{d^2}{dx^2} + \frac{d^2}{dy^2} + \frac{d^2}{dz^2})V_{Hartree} = \sum_l \sum_m \sum_n \frac{U_{l,m,n}}{\varepsilon_0} e^{i(\frac{2\pi l}{a}\hat{x} + \frac{2\pi m}{b}\hat{y} + \frac{2\pi n}{c}\hat{z})\cdot\vec{r}}$$ (4-46)

As this is a linear equation, it can be solved for each plane wave term in the summations separately and then the results can be added together to represent the result of the main equation. The solution to one term of the summation is:

$$V_{Hartree}^{l,m,n} = \frac{-U_{l,m,n}}{\varepsilon_0(\frac{2\pi}{a})^2} e^{i(\frac{2\pi l}{a}\hat{x} + \frac{2\pi m}{b}\hat{y} + \frac{2\pi n}{c}\hat{z})\cdot\vec{r}} + \frac{-U_{l,m,n}}{\varepsilon_0(\frac{2\pi}{b})^2} e^{i(\frac{2\pi l}{a}\hat{x} + \frac{2\pi m}{b}\hat{y} + \frac{2\pi n}{c}\hat{z})\cdot\vec{r}} + \frac{-U_{l,m,n}}{\varepsilon_0(\frac{2\pi}{c})^2} e^{i(\frac{2\pi l}{a}\hat{x} + \frac{2\pi m}{b}\hat{y} + \frac{2\pi n}{c}\hat{z})\cdot\vec{r}}$$

$$= \frac{-U_{l,m,n}}{\varepsilon_0[(\frac{2\pi}{a})^2 + (\frac{2\pi}{b})^2 + (\frac{2\pi}{c})^2]} e^{i(\frac{2\pi l}{a}\hat{x} + \frac{2\pi m}{b}\hat{y} + \frac{2\pi n}{c}\hat{z})\cdot\vec{r}}$$

(4-47)

So the solution to equation (4-46) is as follows:

$$V_{Hartree} = \sum_l \sum_m \sum_n \frac{-U_{l,m,n}}{\varepsilon_0[(\frac{2\pi}{a})^2 + (\frac{2\pi}{b})^2 + (\frac{2\pi}{c})^2]} e^{i(\frac{2\pi l}{a}\hat{x} + \frac{2\pi m}{b}\hat{y} + \frac{2\pi n}{c}\hat{z})\cdot\vec{r}}$$ (4-48)

By calculating the Hartree potential directly in the form of the summation of plane wave functions, it can be easily added to the new potential that is prepared for the next step of iteration. To add the Hartree potential, the respective terms of the ion potential and the Hartree Potential will be added without any further calculations. For the XC potential, the Fourier coefficient

146

terms have to be calculated first. The total effective potential for the next round of iteration is calculated as follows:

$$V_{eff} = V_{ion} + V_{Hartree} + V_{xc} \qquad (3\text{-}42)$$

It should be noted that the calculation method of the comparison of the old and new density functions is the same as the method that was introduced in the 1D case and no further discussion will be done concerning the comparison method calculations. Now that all the calculation methods are introduced for the 3D method, an assessment on the solver is conducted in the next part of this chapter.

4.4 Assessment

In this part the 3D solver will be assessed using two different benchmarks, one of which will be used for the Nearly Free Electron results and the other for the Self-Consistent Pseudopotential results. As a first step, the 3D solver will be used to calculate the Nearly Free Electron energy band structure of a diamond structure and it will be shown that this solver can successfully calculate the results for this method. As it was discussed before in chapter two of this thesis the Nearly Free Electron Method and the Pseudopotential Method are essentially using the same basic principles and that is why this 3D solver is capable of calculating the Nearly Free Electron Method results as well. To use the 3D solver for this method the inputs have to be changed to make the solver calculate the energy band structure using Nearly Free Electron Method. The benchmark used

for the first part is [28] and [80]. The Nearly Free Electron Method Solution that is expected can be found in Figure 2-5a. These calculations can be done with a very tiny amount of data as the Free Electron Method is not an accurate method.

As the second step in the assessment of the 3D Solver, the silicon band structure will be calculated using the Self-Consistent Pseudopotential Method with LDA. The benchmarks used in this part are [58], [81] and [82]. As the process of finding the minimum number of Fourier coefficients and wave vector sampling points has been once demonstrated in the last chapter for the 1D solver, it will not be done in this chapter and only the best case which uses the least number of Fourier coefficients and wave vector sampling points while keeping the accuracy level at a very good point will be discussed. To confirm the results of the 3D solver, a number of different gaps in the energy band structure will be compared to the benchmarks.

The inputs to the 3D solver are the physical data about the lattice which is the pseudopotential, the places of the atoms in the lattice, the period of the lattice in each direction which is the same in our cases but is included in the solver for future expansions. The other input data are the number of Fourier coefficients in each direction and the number of wave vector sampling points in each direction.

To start with the first step of the assessment, the fundamentals of the Nearly Free Electron Method, called NFEM hereafter, is reviewed briefly here. In NFEM case, it is assumed that the potential from the lattice is negligible and it only reflects the periodicity and properties of the lattice. So the potentials should

only have a small effect so that the electron feels that it is in a lattice with the properties that are intended for it. It should also be noted that in this method there is only one electron present in the lattice and the effects of the properties and periodicity of the lattice are examined. The quantity of the period of the lattice does not play a role in the calculations as the numbers are not exact and only the shape of the energy band structure which is calculated is of importance in NFEM. To utilize this method in the 3D solver for a diamond lattice, the potentials of the atoms present in the diamond lattice are reduced to be in the order of 10^{-3} to 10^{-5} times of a regular atom like the Si atom so that the electron is nearly free in the lattice and only feels the properties of a diamond lattice and the repetition of the unit cells which reflects the periodicity. In the case presented here, the potentials are chosen to be 10^{-4} times of that of Si atoms. The results presented in [28], which can also be reviewed in figure 2-5a, are generally correct, but are less accurate for the bands with higher energy. For this reason, figures from [80] will be used here as they tend to be more precise, although, as mentioned, the band structure calculated using NFEM in [28] is also present in this thesis in figure 2-5a. The complete energy band structure of a diamond lattice calculated with NFEM is as below:
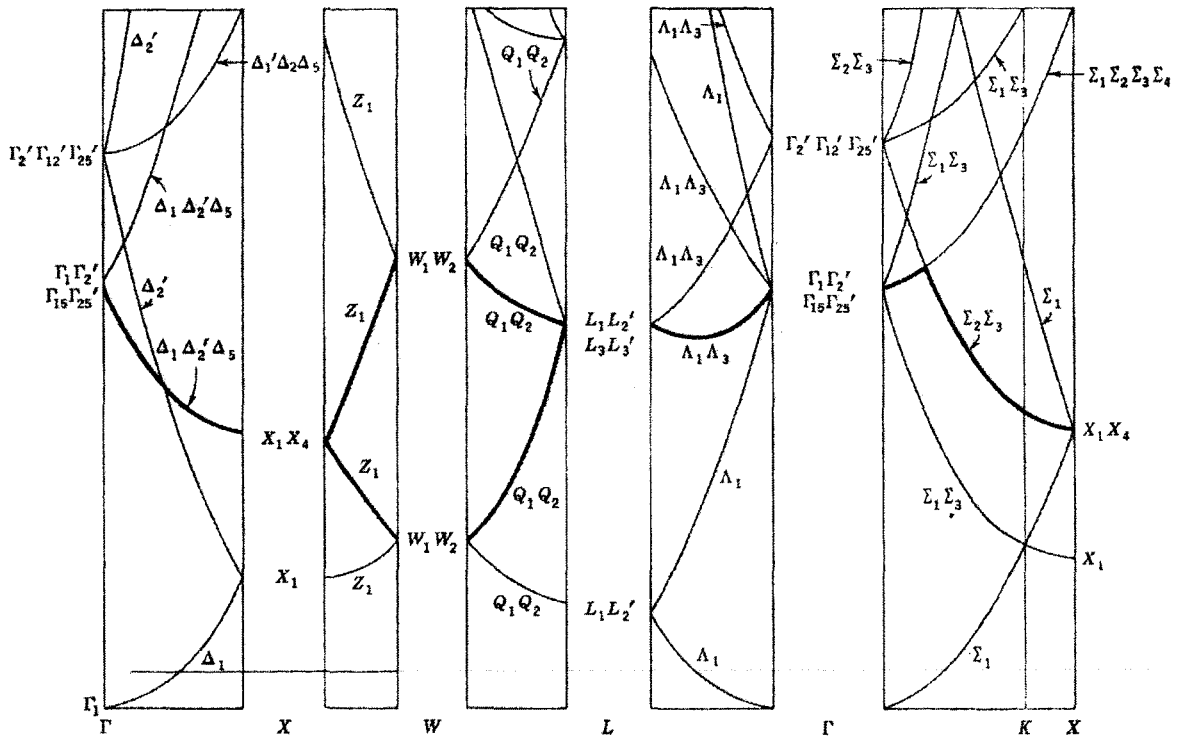
Figure 4-2. NFEM energy band structure of diamond lattice structure [80].

It is important to note that the energy axis (vertical axis) has no quantity on it because the NFEM method does not provide any specifics. It should be noted that the first and fourth column in figure 4-2 are the most important columns as they are the parts that include the band gap and main energy band structure part of most diamond structures. These are the same two columns that appear in figure 2-5a as well. The 3D solver will calculate the same two columns as well. The results of the 3D solver and parts of figure 4-2 are compared in figure 4-3 in the next page. It should be noted that the columns in the benchmark figure in figure 4-3a do not match vertically as they are not computer generated figures and are rather hand-drawn. Looking at each column separately it can be seen

150

that each column is in agreement with its respective column in the calculated results of the 3D solver.

So, as it can be seen, the calculations of the 3D solver are in complete agreement with those of [28] and [80]. So it is shown that, the NFEM method can be implemented with the 3D solver with a minimal data input. For the case that is presented here, there are only eight wave vector sampling points in each direction. As there is no need for iterations and calculations of density function in NFEM, there will be only sixteen wave vector sampling points of concern which accounts for eight in each column that is compared with the results of the benchmarks. The 3D solver calculates the results accurately and efficiently. The NFEM calculations are mostly done to find general information about a lattice type. The energy band structure that is calculated has similarities with all the band structures of the diamond lattice materials that are made of one type of atoms.

Only two Fourier coefficients where used in the calculations because the accuracy of the potential presentation does not play a part and only the fact that there is a potential at the place of each atom plays a role. Ten wave vector sampling points in each direction were used.
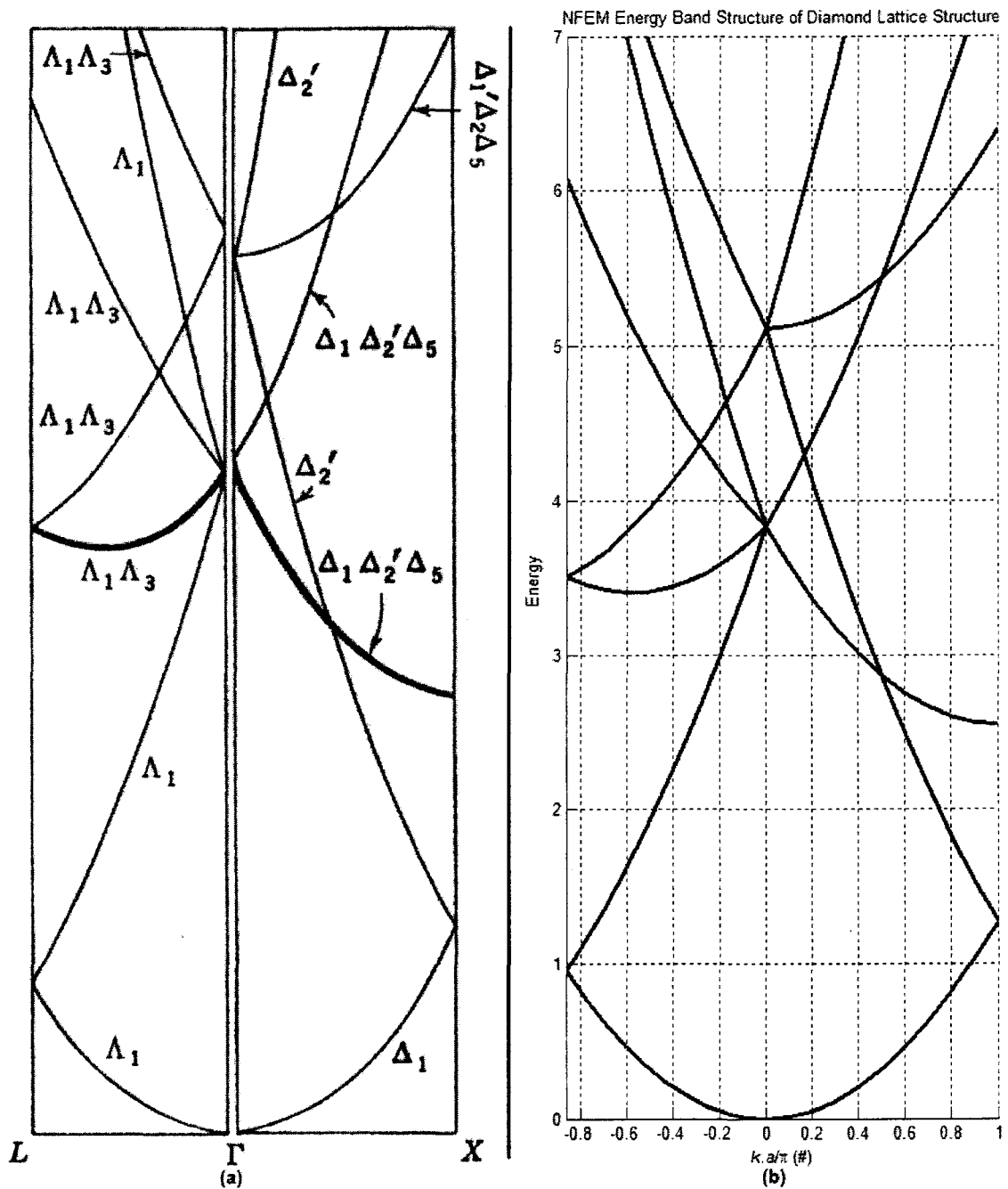
Figure 4-3. (a) NFEM calculations of energy band structure of diamond lattice structure performed in [80] (b) NFEM calculations of energy band structure of diamond lattice structure performed by the 3D Solver. Calculation Time: 1.769s.

As a second step in assessing the 3D solver, the silicon lattice's energy band structure will be calculated. To measure the agreement of the calculated results with the energy band structures obtained in other studies, some of the extreme points and energy gaps in the electronic band structures will be compared.

In contrast with the 1D case and the NFEM calculations of the 3D solver, the results of the calculations of a material's lattice in 3D are almost never exactly the same as any other calculations. This is because of different calculation methods, different starting pseudopotentials, different simplifications that are used and many other differences that have impact on the calculation results.

The goal in this study is to get results that are in the same range as the results of the benchmark results. As it can be seen later, the results of the bookmarks are not the same as each other either. The physical properties of silicon including its lattice period and the pseudopotential introduced in the last parts and the position of the atoms in the silicon cristal are the first part of the inputs to the solver. To calculate the energy band structure of silicon, the number of wave vector sampling points, including zero, that is used in each direction can be seven, nine, or eleven for an optimization of accuracy and efficiency which accounts for 7^3, 9^3, or 11^3 wave vector sampling points in a unit cell. The number of wave vector sampling points in the calculations is ten in each direction (not counting but considering zero). The number of Fourier coefficients is the

most important factor that should be kept to the minimum number that keeps accuracy at a good level while maintaining the efficiency of the 3D solver. In the calculations of silicon electronic band structure, the number of plane waves in each direction that were used was seven including the average or the 0th term. This number accounts for 7^3 Fourier coefficients. As the 0th is not counted (but considered) in this work, it is referred as six Fourier coefficients in each direction. The relative change of the density function in order to assume convergence to the results where set to be $\Delta\rho_{rel} = 0.75\%$. For more accuracy the relative change may be set to a smaller number, but this will lead to a larger number of iterations to get the results. As relative change of the density function becomes smaller the number of iterations for convergence of the results grows rapidly and this fact compromises the efficiency of the 3D solver. As it will be shown later, the 3D solver has a very good accuracy with the relative change of the density function that is set above.

To start assessing the results of the 3D solver in the case of silicon lattice, the benchmark results are shown in figures first and the 3D results are presented after them. The energy band structures will be compared to each other at different X, Γ, and L points which accounts for a total of 12 points in the energy band structure. As a last confirmation the energy band gap of silicon will be compared in the different groups of results. It will be shown that the results obtained by the 3D solver are in the same range as the benchmark results.

Based on the band structure shape and the compared energy values at selected points, it is shown that the 3D solver will lead to correct and accurate results.

The first benchmark is the work which is one of the best works done on silicon and is a commonly cited reference which is done by D. Brust [58]. The energy band structure of silicon calculated by D. Brust is shown in Figure 4-4 as follows. It should be noted that the k-axis in figure 4-4 is not plotted exactly to the proportions as it is a hand drawn figure rather than a computer generated one.

Figure 4-4. The electronic band structure of silicon calculated using EPM by D. Brust in [58].

Another commonly cited reference for silicon energy band structure is the work done by Chelikowsky and Cohen [81]. The energy band structure of silicon is calculated using two similar methods in this reference and the results of both methods used are presented here in figure 4-5 as follows.
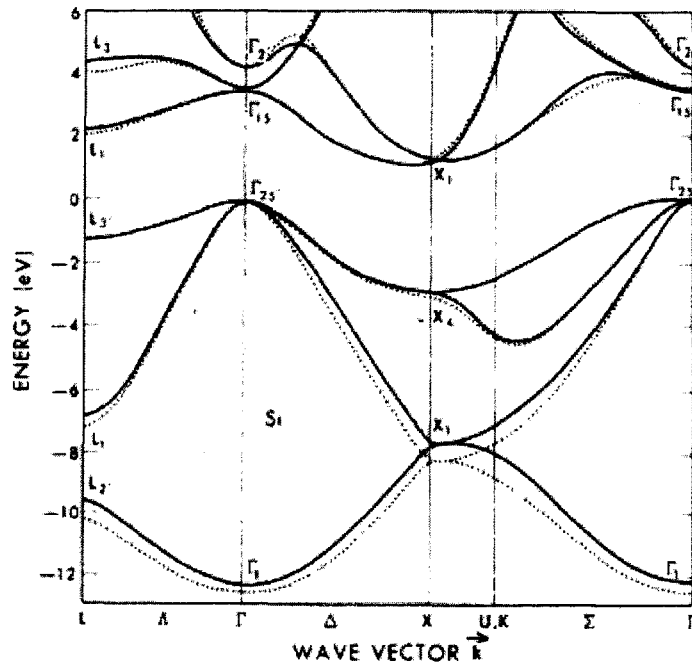
Figure 4-5. The energy band structure of silicon calculated using SCPM with LDA (dotted lines) and Non-Local Density Approximation, NLDA (solid lines) in [81].

The other benchmark data used here is the Ioffe Physico-Technical Institute's database of semiconductor materials' properties [82]. This database does not have a complete picture of the energy band structure of silicon, but it offers useful data about it which will be presented among other data from the last two benchmarks in table (4-1).

The final unit cell's potential energy that is calculated in the program is a 3D potential energy that cannot be shown directly. In order to show the potential energy here, potential energy on $z = 0$ plane is shown at different x and y values. This potential energy can be seen in figure 4-6 as follows:
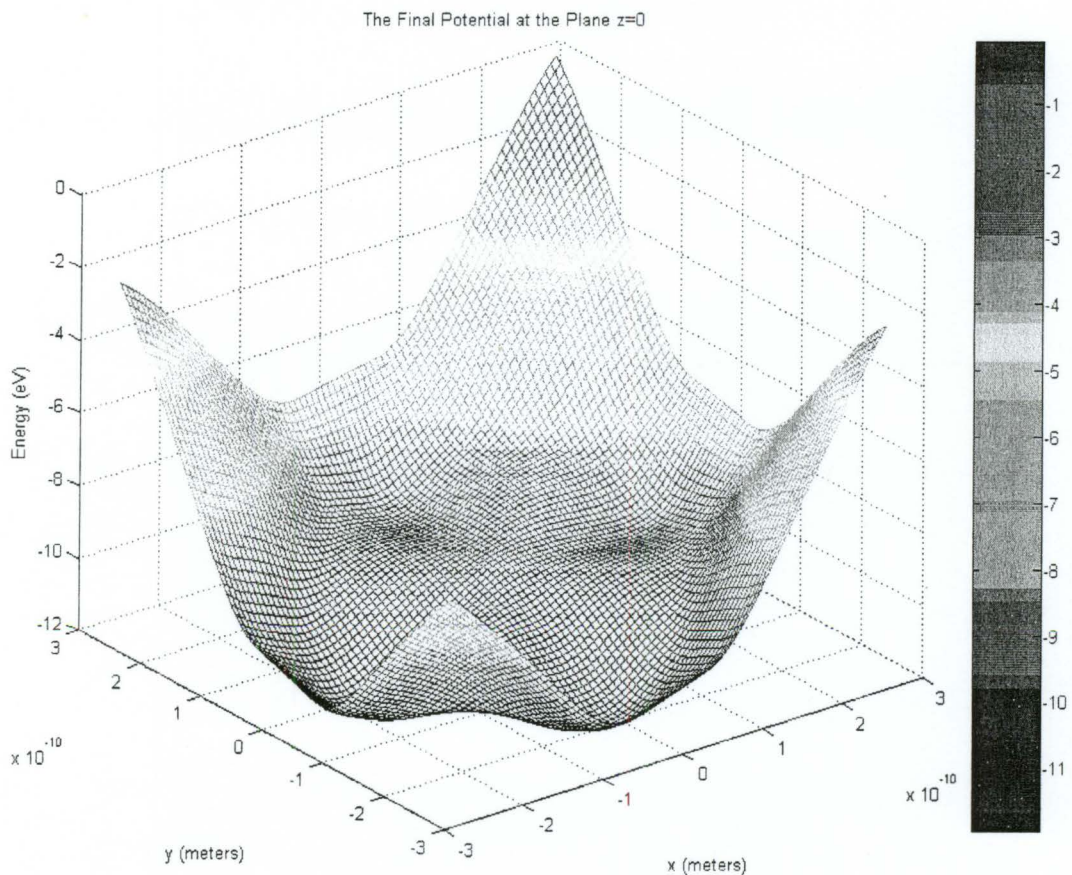
Figure 4-6. The final unit cell's potential energy on $z = 0$ plane.

The results of the calculations of the 3D solver are done in the most important part of the energy band structure of silicon. The part of the band

structure that is calculated using the 3D solver starts from the L point on Λ direction to the Γ point and from the Γ point on Δ direction to the X point. This is only a part of figures 4-4 and 4-5 and does not include all that is shown in those figures. For more information about points and directions in the Brillouin zone the reader is referred to section 2.1.2 of this thesis. The electronic band structure of silicon calculated with 3D solver is presented in figure 4-7.
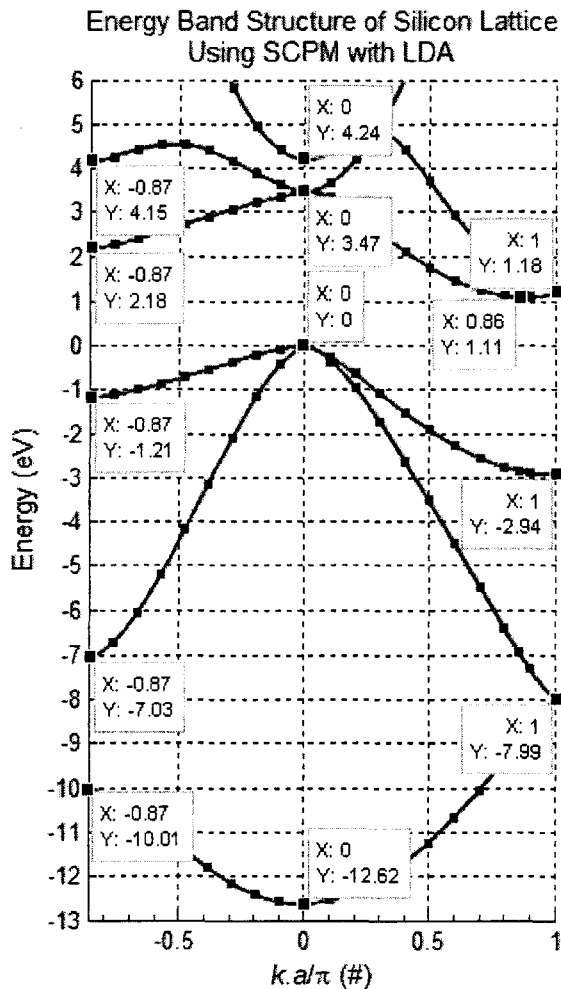
Figure 4-7. Energy band structure of silicon lattice calculated by 3D solver using SPCM with LDA. Calculation Time: 2863.548s.

All the energies that are shown on figure 4-7 are those that will be compared to the benchmark values in table (4-1). The energy gap of silicon which is calculated by 3D solver as $1.11\,eV$, will also be compared to other benchmarks after table (4-5). The comparison of the energy values at all other points are done in table (4-1) as follows:

Brillouin Zone Point	Cohen [81] SCPM-LDA	Cohen [82] SCPM-NLDA	D. Brust EPM [58]	Ioffe [82] Database	3D Solver SCPM-LDA
Γ_1	-12.53	-12.36	-	-	-12.62
$\Gamma_{25'}$	0	0	0	0	0
Γ_{15}	3.43	3.42	3.4	3.4	3.47
$\Gamma_{2'}$	4.17	4.10	4.2	3.8	4.24
$L_{2'}$	-10.17	-9.55	-	-	-10.01
L_1	-7.24	-6.96	-	-	-7.03
$L_{3'}$	-1.22	-1.23	$L_{3'} - L_1$ $= 3.1$	-	-1.21
L_1	2.15	2.23		2.0	2.18
L_3	4.00	4.34	$L_{3'} - L_3 = 5.4$	-	4.15
X_1	-8.27	-7.69	-	-	-7.99
X_4	-2.99	-2.86	$X_1 - X_4$ $= 4.0$	-	-2.94
X_1	1.22	1.17		1.2	1.18

Table 4-1. Comparison of the benchmark results with the results of the 3D solver.

As it can be seen, the results of the 3D solver are in the same range as the benchmark results and in most of the cases it is very close to other results that are presented. As the last measure to assess the 3D solver, the band gap of silicon calculated with 3D solver is compared to benchmarks that have indicated silicon band gap. The references that will be used in this part are [2], [26], and [82]. In [2] the band gap of silicon lattice is mentioned to be $1.11\,eV$. The band gap is also indicated the as the same energy which is $1.11\,eV$ in [26]. However, the silicon band gap is shown as a different amount of $1.12\,eV$ in [82]. The 3D solver calculates the band gap to be $1.11\,eV$. According to the comparisons done above, it can be assessed that the 3D solver is correctly calculating the electronic band structure of silicon. By calculating the electronic band structure of diamond lattice structure with the 3D solver using NFEM and solving the electronic band structure of silicon using SCPM with LDA, the solver is assessed.

4.5 Summary

In this chapter the 3D Electronic Band Structure Solver was discussed. The algorithm of the solver was reviewed and many similarities with the 1D solver algorithm were mentioned. In fact both algorithms are the same except for the number of dimensions. The calculation methods used in the 3D solver have many similarities with the methods used for the 1D solver. The differences with 1D solver's calculation methods were discussed in details. Some similarities were briefly discussed as well. The differences included the OPW Expansion

because of the difference in the number of dimensions, integral calculations, solution method of the eigen value problem, and minor difference in calculations of the density function which was explained in the part designated for Hartree and XC potential calculations.

The 3D solver was then assessed with two different cases. The first case compared the results of the 3D solver in the case of diamond lattice structure solved by NFEM with two benchmarks. Based on the results it was concluded that the 3D solver is in complete agreement with the benchmark results. To make the case stronger for the 3D solver, the silicon lattice was solved and the results were compared to three benchmarks which included 4 set of data about each point in the band structure that was going to be compared. The measure for agreement was to see if the results of the 3D solver in silicon's case are in the same range as other sets of data that are available in the benchmarks. Showing all the data extracted from the 3D solver and comparing them to the other data available in a table, it was shown that all the data from 3D solver are in the same range as other data and most of them are very near to other results. By comparing the band gap of silicon that was calculated with 3D solver with three benchmarks as the last measure for assessment, it was shown that the 3D solver passed all the assessment measures.

Chapter 5: Conclusion and Future Work

5.1 Summary

In this thesis, two solvers were developed to calculate the energy band structure of 1D and 3D crystalline lattices. As a first step, an introduction over the methods used was done. The backgrounds of the research were discussed. After an introduction of the basics needed for the thesis, including quantum mechanics, translational symmetries, and Brillouin zones, different methods that could be used to develop the solver were expressed. Self-Consistent Pseudopotential Method was chosen over the other methods that were introduced. The reasons for this choice were discussed in parts of the thesis. The methods that were discussed were nearly free electron method, the k.p method, the tight-binding method, the empirical pseudopotential method, and the self-consistent pseudopotential method.

In the discussion of self-consistent pseudopotential method, the pseudopotential choices were discussed. The different methods for solving the Schrödinger equation were introduced as well. The local density approximation in calculating the exchange and correlation potential was thoroughly discussed. Some of the applications of the empirical pseudopotential method and the self-consistent pseudopotential method were introduced as a last part of the introduction of methods.

In the next part of this thesis, the 1D crystal electronic band structure solver was explained. The algorithm with which the 1D solver runs was introduced. The calculation methods for different parts of the 1D solver were discussed. It was explained how the orthogonal plane wave expansion can help the solver. The integral calculations method, eigen value problem solution, the Hartree and exchange and correlation potential energies, and the comparison method used to compare the resulting density functionals of different steps of the solver were all discussed. To assess the 1D solver, two analytically solved benchmarks were used. The benchmarks were Kronig-Penney lattices. Through the assessment process the minimum number of input information needed for a good accuracy were found. The less the number of input information, the more speed the solver will have. This information was found to be used later in the 3D solver as in 3D solver the volume of data that the program has as input is very large and our goal in 1D solver is to find out how much of that information is not needed and speed up the process in developing the 3D Solver.

The last part of this thesis was on the 3D solver. In this part, the algorithm of the solver was reviewed again and it was shown that it was quite similar to that of the 1D solver. Instead of going over the calculation methods used in the 3D solver in details, only the differences with the 1D solver were explained in details and the similarities were referred to the 1D solver calculation methods for reference. In the assessment part the minimization of the input data was not performed and the experience from the 1D solver was used for the minimal input

to be fed to the 3D solver. It was shown that with minimal change the solver can perform NFEM as well. The results of the NFEM calculations of the diamond lattice structure were compared with benchmarks and it was confirmed that the 3D solver had calculated the right energy band structure. As a second measure to assess the 3D solver, the silicon energy band structure was calculated and confirmed to be calculated right by using three benchmarks. The 3D solver was confirmed to be an accurate energy band structure calculator for SPCM with LDA and NFEM calculations.

5.2 Suggestions on Future Research Directions

As a guide to the future directions that this thesis may be continued, the following are suggested:

1.   The solver can be expanded to calculate the energy band structure of silicon-germanium alloys. To solve the Si_xGe_{1-x} structure, a statistical study should be done on the placement of the Si and Ge atoms in the lattice structure. An new program should be added to the solver that generates multiple number of Si_xGe_{1-x} unit cells based on the number 'x'. This unit cells should then be joined together to make a main unit cell which can represent the same alloy of SiGe that is under study. The number of unit cells can be eight, twenty seven, sixty four, ...

based on the accuracy of the representation that is needed. This step is an important and necessary step to add because one unit cell may not be enough to represent an alloy exactly in the way it really exists. A table or formula should be generated to calculate the lattice periodicity of each structure based on the number 'x' in the alloy. This expansion of the Solver may need a comprehensive study of statistics. The large number of atoms present in the main cell that is generated may bring additional complexity to the solver.

2.   The solver can be expanded to calculate the energy band structure of many forms of SiC including 3C-SiC, 2H-SiC, 4H-SiC, and 6H-SiC. The program should be expanded to be able to simulate the HCP Lattices. A good pseudopotential for carbon atom should either be found or introduced. A new basis for lattice periods should be developed as the HCP lattice has basic differences with diamond lattice. The hexagonal Miller indices should be utilized for directions in the lattice. The periodicity of the lattice is different for each direction for SiC but the program of the solver has the ability to do the calculations of Fourier series with different periodicities in each direction. Although the unit cells of the different SiC lattices are different,

their band structure's can be calculated using the 3D solver if the mentioned modifications are done to the solver.

3. The Solver may be expanded to support the calculation of the energy band structure of non-periodic structures such as silicon nano-ball imbedded in silicon dioxide, by substituting the Fourier series that are used in the solver with Fourier transform. This substitution cannot be done without preparation that is necessary to utilize the solver for non-periodic structures. Some parts of the main algorithm may have to be changed. In this approach the main cell that is generated has to be the structure that is going to be studied. Because the Fourier transform cannot be utilized directly some form of discrete Fourier transform should be used which is subject to the argument that the solver will then be calculating a periodic structure with a large period and is not really calculating a non-periodic structure. More studies should be conducted about the effect of this calculation method before it is utilized in the Solver.

Bibliography

1. Peter Y. Yu and Manuel Cardona, *Fundamentals of Semiconductors: Physics and Materials Properties*, Springer, 2001, pp. 17-18

2. S. Wang, *Fundamentals of Semiconductor Theory and Device Physics*, Prentice-Hall International Inc., 1989, pp. 113-119 and 232-238

3. E. Fermi, Nuovo Cimento II, 157, (1934)

4. M.L. Cohen, *Intl. J. of Quantum Chem.*, 17, 583-595 (1983)

5. H. Hellman, *J Chem. Phys.*, 3, 61 (1935)

6. J.C. Phillips and L. Kleinman, *Phys. Rev.*, 116, 287 (1959)

7. M.L. Cohen and V. Heine, *Solid State Phys.*, 24, 37 (1970)

8. J. P. Walter and M. L. Cohen, *Phys. Rev. B*, 4, 1877 (1971)

9. L. Kleiman and J. C. Phillips, *Phys. Rev.*, 116, No. 4, 880 (1959)

10. L. Kleiman and J. C. Phillips, *Phys. Rev.*, 117, No. 2, 460 (1960)

11. L. Kleiman and J. C. Phillips, *Phys. Rev.*, 118, No. 5, 1153 (1960)

12. L. C. Allen and A. M. Karo, *Rev. of Modern Phys.*, 32, No. 2, 275 (1960)

13. P. Hohenberg and W. Kohn, *Phys. Rev.*, 136, No. 3B, B864, (1964)

14. W. Kohn and L. J. Sham, *Phys. Rev.*, 140, No. 4A, A1133 (1965)

15. S. Golin, *Phys. Rev.*, 140, No. 3A, A993 (1965)

16. W. A. Goddard, *Phys. Rev.*, 174, No. 3, 659 (1968)

17. P. M. O'Keefe and W. A. Goddard, *Phys. Rev.*, 180, No. 3, 747 (1969)

18. A. B. Kunz and N. O. Lipari, *Phys. Rev. B*, 4, No. 4, 1374 (1971)

19. N. O. Lipari and A. B. Kunz, *Phys. Rev. B*, 4, No. 12, 4639 (1971)

20. A. Redondo, W. A. Goddard and T. C. McGill, *Phys. Rev. B*, 15, No. 10, 5038 (1977)

21. D. R. Hamann, M. Schlüter and C. Chiang, *Phys. Rev. Lett.*, 43, No. 20, 1494 (1979)

22. G. B. Bachelet, D. R. Hamann and M. Schlüter, *Phys. Rev. B*, 26, No. 8, 4199 (1982)

23. G. P. Kerker, *Phys Rev. B*, 23, No. 6, 3082 (1981)

24. M. T. Yin and M. L. Cohen, *Phys. Rev. B*, 25, No. 12, 7403 (1982)

25. D. Vanderbilt, *Phys. Rev. B*, 41, No. 11, 7892 (1990)

26. Ben G. Streetman, *Solid State Electronic Devices*, fifth edition, Prentice Hall, 2000

27. N. W. Ashcroft and N.D. Mermin, *Solid State Physics*, Philadelphia: W.B. Saunders,1976

28. Peter Y. Yu and Manuel Cardona, *Fundamentals of Semiconductors: Physics and Materials Properties*, Springer, 2001, pp. 20-105

29. H. Clark, *Solid State Physics: an introduction to its theory*, "Macmillan" & "St. Martin's Press", 1968

30. A. J. Dekker, *Solid State Physics*, Prentice Hall, 1957

31. Weisstein, Eric W. "Floquet's Theorem.", MathWorld--A Wolfram Web Resource. http://mathworld.wolfram.com/FloquetsTheorem.html

32. C. Kittel, *Introduction to Solid State Physics*, 7th ed., Wiley, New York, 1995, pp. 37

33. E. O. Kane, Band Structure of Indium Antimonide, *J. Phys. Chem. Solids*, 1, 249-261 (1957)

34. S. L. Chuang, *Physics of Optoelectronic Devices*, Wiley, 1995, pp. 124-199

35. M. L. Cohen and J. Chelikowsky, *Electronic Structure and Optical Properties of Semiconductors*, 2nd ed., Springer Ser. Solid State Sci., 1989, Vol. 75, pp. 16-21

36. C. Pisani (Ed.), *Quantum-Mechanical Ab-initio Calculation of the Properties of Crystalline Materials*, Springer, 1996

37. J. A. Appelbaum and D. R. Hamann, *Phys. Rev. B*, 8, No. 4, 1777 (1973)

38. O. K. Andersen, *Phys. Rev. B*, 12, No. 8, 3060 (1975)

39. T. L. Loucks, *Augmented Plane Wave Method*, Benjamin, New York, 1967

40. J. O. Dimmock, *Solid State Physics*, Academic, New York, 1971, Vol. 26

41. J. Korringa, *Physica*, 13, 392 (1947)

42. W. Kohn and N. Rostoker, *Phys. Rev.*, 94, No. 5, 1111 (1954)

43. B. Segall and F. S. Ham, *Methods in Computational Physics*, Academic, New York, 1971, Vol. 8, chap. 7

44. O. K. Andersen and O. Jepsen, *Phisica B*, 91, 317 (1977)

45. L. H Thomas, Proc. Cambridge Philos. Soc., 23, 542 (1927)

46. E. Fermi, Z. Phys., 48, 73 (1928)

47. P. A. M. Dirac, Proc. Cambridge Philos. Soc., 26, 376, (1930)

48. R. G. Parr and W. Yang, *Density Functional Theory of Atoms and Molecules*, Oxford University Press, New York, 1989

49. J. P. Perdew and A. Zunger, *Phys. Rev. B*, 23, No. 10, 5048 (1981)

50. D. Pines, *Elementary Excitations in Solids*, Benjamin, New York, 1963

51. D. M. Ceperley and B. J. Alder, *Phys. Rev. Lett.*, No. 7, 45,566 (1980)

52. L. A. Cole and J. P. Perdew, *Phys. Rev. A*, 25, No. 3, 1265 (1982)

53. C. Lee, W. Yang and R. G. Parr, *Phys. Rev. B*, 37, No. 2, 785 (1988)

54. J. P. Perdew and Y. Wang, *Phys. Rev. B*, 45, No. 23, 13244 (1992)

55. X. Jiang and Z. Gan, *Phys. Rev. B*, 52, No. 19, 14254 (1995)

56. C. Y. Fong and M. L. Cohen, *Phys. Rev. Lett.*, 24, No. 7, 306 (1970)

57. C. Y. Fong and M. L. Cohen, *Phys. Rev. B*, 6, No. 10, 3633 (1972)

58. D. Brust, *Phys. Rev.*, 134, No. 5A, A1337 (1964)

59. J. P. Walter and M. L. Cohen, *Phys. Rev. B*, 5, No. 8, 3101 (1972)

60. P. Friedel, M. S. Hybertsen, and M. Schlüter, *Phys. Rev. B*, 39, No. 11, 7974 (1989)

61. J. P. Walter and M. L. Cohen, *Phys. Rev.*, 183, No. 3, 763 (1969)

62. S. T. Pantelides, D. J. Mickish, and A. B. Kunz, *Phys. Rev. B*, 10, No. 12, 5203 (1974)

63. N. O. Lipari and A. B. Kunz, *Phys. Rev. B*, 3, No. 2, 491 (1971)

64. J. Ihm and J. D. Joannopoulos, *Phys. Rev. B*, 24, No. 8, 4191 (1981)

65. G. P. Srivastava, *Phys. Rev. B*, 25, No. 4, 2815 (1982)

66. H. F. Schaefer and F. E. Harris, *Phys. Rev.*, 170, No. 1, 108 (1968)

67. M. L. Cohen, M. Schlüter, J. R. Chelikowsky, and S. G. Louie, *Phys. Rev. B*, 12, No. 12, 5575 (1975)

68. Wikipedia, "Trapezium Rule", Internet: http://en.wikipedia.org/wiki/Trapezoidal_Rule, Mar. 24th 2008 [May 8th 2008]

69. Wikipedia, "Image:Composite trapezoidal rule illustration.png", Internet: http://en.wikipedia.org/wiki/Image:Composite_trapezoidal_rule_illustration.png, Apr. 29th 2007 [May 8th 2008]

70. J. E. Gentle, *Numerical Linear Algebra for Applications in Statistics*, Berlin, Springer-Verlag, 1998, pp. 93-95

71. J. C. Nash, *Compact Numerical Methods for Computers: Linear Algebra and Function Minimisation*, 2nd ed., Bristol, England, Adam Hilger, 1990, pp. 84-93

72. W. H. Press, B. P. Flannery, S. A. Teukolsky, and W. T. Vetterling, *Numerical Recipes in FORTRAN: The Art of Scientific Computing*, 2nd ed., Cambridge, England, Cambridge University Press, 1992

73. Wikipedia, "Root mean square deviation", Internet: http://en.wikipedia.org/wiki/Root_mean_square_deviation, Mar. 14th 2008 [May 10th 2008]

74. Wikipedia, "Root mean square", Internet: http://en.wikipedia.org/wiki/Root_mean_square, May. 3rd 2008 [May 10th 2008]

75. G. C. Wetsel, Jr., *Am. J. Phys.*, 46, No. 7, 714 (1978)

76. Wikipedia, "QR algorithm", Internet: http://en.wikipedia.org/wiki/QR_algorithm, Jun. 17th 2008 [July 13th 2008]

77. J. G. F. Francis, *The Comp. J., Oxford journals*, 4, No. 3, 265 (1961)

78. J. G. F. Francis, *The Comp. J., Oxford journals*, 4, No. 4, 332 (1962)

79. Vera N. Kublanovskaya, *USSR Comp. Math. And Math. Phys.*, 3, 637 (1961)

80. J. C. Slater, *Quantum Theory of Molecules and Solids*, Vol. 2, McGraw-Hill Book Company, 1965, pp. 250-305

81. J. R. Chelikowsky and M. L. Cohen, *Phys. Rev. B*, 10, No. 12, 5095 (1974)

82. Ioffe Physico-Technical Institute, "NSM Archive – Band Structure and Carrier Concentration of silicon (Si)", Internet: http://www.ioffe.rssi.ru/SVA/NSM/Semicond/Si/bandstr.html, [Aug. 20th 2008]

Appendix A: The Basics of Quantum Mechanics

A.1 Probability and the Uncertainty Principle

The uncertainty principle states that it is impossible to know everything about an event in the atomic scale with absolute precision. So we cannot know the exact values of position, momentum, and energy of a particle at a time. Instead, we can know the expectation values of the mentioned properties as a measurement. We should know that this uncertainty is not a shortcoming of the theory. But it is a major strength of the theory that can look at the facts and describe them as probabilistic events, because there are often very many (usually in the order of 10^{15} or more) particles (e.g. electrons) that participate in a quantum effect. So the position, energy, or any other property of an electron cannot be described without a particular uncertainty. This particular uncertainty is described by Heisenberg uncertainty principle as below [26].

The uncertainty involved in the measurement of the position and momentum of a particle are related by the following equation:

$$(\Delta x)(\Delta p_x) \geq \hbar \tag{A-1}$$

Similarly, the energy measurement uncertainty is related to the uncertainty in the time of the energy measurement:

$$(\Delta E)(\Delta t) \geq \hbar \tag{A-2}$$

The limitations that are exposed to the measurements of position, energy, momentum and time tell us that for example, we cannot have position and

momentum of a particle very exact at the same time and there should be some inaccuracy in them. In fact the Plank's constant (h) is a rather small number (6.63 × 10^{-34} J-s), so the inaccuracy in the measurement of position and momentum of a large and heavy thing like a stone is not of any importance. On the other side, if we do the same measurements for a small particle like an electron, the uncertainty principle will be a serious limitation to it.

We can interpret this fact as we cannot have the certain position of a particle, e.g. electron, but we can have the probability of finding the particle in a position. So it can be inferred that quantum mechanics gives us a probability density function for a particle in a given environment so that we can calculate the particle's properties such as position, momentum, or energy from this function. If we have the probability density function of $P(x)$ in a 1D problem, we can find the probability of finding the particle anywhere we want. For example the probability of finding the particle between x and $x+dx$ is $P(x)dx$. Because we will surely find the particle somewhere in the space, the probability of finding it over the space should be unity.

$$\int_{-\infty}^{\infty} P(x)dx = 1 \qquad\qquad (A\text{-}3)$$

If $P(x)$ is chosen properly. So equation (A-3) is normalizing the function $P(x)$. (Since the integral equals unity).

To know the expectation value of any function of x, we have to multiply that by $P(x)$ and integrate over the space. So the expectation value (average value) of $f(x)$ will be:

$$< f(x) >= \int_{-\infty}^{\infty} f(x)P(x)dx \qquad \text{(A-4a)}$$

When the probability density function is not normalized, equation (A-4a) will be modified like below:

$$< f(x) >= \frac{\int_{-\infty}^{\infty} f(x)P(x)dx}{\int_{-\infty}^{\infty} P(x)dx} \qquad \text{(A-4b)}$$

A.2 Derivation of Schrödinger Equation

Different methods are developed to derive the Schrödinger equation by applying the quantum mechanics basics to classical mechanics equations. The way that is presented here is a simple method. In this method we consider a few postulates to derive the wave equation from them, with the help of a classical mechanics equation. We then accept the developed equation is accurate as it is a justification to the postulates. The basic postulates are as follows:

1. Any particle in a physical system is described by a wave function $\Psi(x, y, z, t)$. The wave function and its space derivative are continuous, finite, and single valued.

2. Any of the quantities of the particles are described as a quantum operator that operates on the wave function to give us the required results. These quantum operators has nothing to do with the real world and do not have a direct physical meaning. The operators are shown in table (1-1).

3. To find the probability of finding a particle with wave function Ψ in the volume $dxdydz$, one should find $\Psi^*\Psi dxdydz$. It should be noted that the product $\Psi^*\Psi$ should be normalized according to Eq. (A-3) so we will have: [26]

$$\int_{-\infty}^{\infty} \Psi^*\Psi dxdydz = 1 \qquad\qquad (A\text{-}5)$$

To find the average value of any wanted variable about the particle, $<Q>$, we have to know the quantum mechanics operator of the variable, Q_{op}, to calculate its expected value from the integral below:

$$<Q> = \int_{-\infty}^{\infty} \Psi^* Q_{op} \Psi dxdydz \qquad\qquad (A\text{-}6)$$

Classical variable	Quantum operator
X	X
$f(x)$	$f(x)$
$p(x)$	$(\dfrac{\hbar}{i})\dfrac{\partial}{\partial x}$
E	$(-\dfrac{\hbar}{i})\dfrac{\partial}{\partial t}$

Table A-1. A list of quantum operators used instead of classical variables in quantum mechanics. The table is true for the other two directions if we change x to y or z.

In wave mechanics, as soon as the wave function, Ψ, is found for the particle, we can calculate any desired property of the particle like its average position, energy, and momentum. So the most important part of any problem in quantum mechanics is to find the wave function for the given particle and environment. From the third postulate we can find out that the probability density function is nothing but $\Psi^*\Psi$, or $|\Psi|^2$.

The energy preservation in the classical mechanics will be used here to derive the Schrödinger equation. The equation for energy preservation in the classical mechanics is:

Kinetic energy + potential energy = total energy

$$\frac{1}{2m}p^2 + V = E \tag{A-7}$$

We always use the operator form of the variables in quantum mechanics. So for a 1D space equation (A-7) becomes

$$(\frac{-\hbar^2}{2m})\frac{\partial^2 \Psi(x,t)}{\partial x^2} + V(x)\Psi(x,t) = (\frac{-\hbar}{i})\frac{\partial \Psi(x,t)}{\partial t} \tag{A-8}$$

Equation (2-8) is the one-dimensional time-dependent Schrödinger equation. The equation in three dimensions is

$$(-\frac{\hbar^2}{2m})\nabla^2 \Psi + V\Psi = (-\frac{\hbar}{i})\frac{\partial \Psi}{\partial t} \tag{A-9a}$$

where $\nabla^2 \Psi$ is

$$\nabla^2 \Psi = \frac{\partial^2 \Psi}{\partial x^2} + \frac{\partial^2 \Psi}{\partial y^2} + \frac{\partial^2 \Psi}{\partial z^2} \tag{A-9b}$$

Appendix B: Derivation of Equation (2-40)

The general Schrödinger equation is as follows:

$$[-\frac{\hbar^2}{2m}\nabla^2 + V(r)]\psi_{nk}(r) = E_{nk}\psi_{nk}(r) \tag{B-1}$$

Because we are in the periodic potential of a crystalline lattice, we can use the Bloch theorem:

$$\psi_{nk}(r) = e^{ik\cdot r}u_{nk}(r) \tag{B-2}$$

We will substitute (B-2) in (B-1) and derive equation (B-3) which is the same as equation (2-40) and is as follows:

$$(\frac{p^2}{2m} + \frac{\hbar k.p}{m} + \frac{\hbar^2 k^2}{2m} + V)u_{nk} = E_{nk}u_{nk} \tag{B-3}$$

In the first step of substituting, equation (B-1) will change to the following:

$$[-\frac{\hbar^2}{2m}\nabla^2 + V(r)]e^{ik\cdot r}u_{nk}(r) = E_{nk}e^{ik\cdot r}u_{nk}(r) \tag{B-4}$$

Multiplying the terms in the left-hand side, we will have:

$$-\frac{\hbar^2}{2m}\nabla^2[e^{ik\cdot r}u_{nk}(r)] + V(r)e^{ik\cdot r}u_{nk}(r) = E_{nk}e^{ik\cdot r}u_{nk}(r) \tag{B-5}$$

To continue we have to calculate $\nabla^2[e^{ik\cdot r}u_{nk}(r)]$ first. To do so we will do the calculations in two steps and we will calculate $\nabla \cdot \{\nabla[e^{ik\cdot r}u_{nk}(r)]\}$. For the inside terms we will have:

$$\nabla[e^{ik\cdot r}u_{nk}(r)] = ike^{ik\cdot r}u_{nk}(r) + e^{ik\cdot r}\nabla u_{nk}(r) \tag{B-6}$$

Now we can continue to the next calculation, because:

$$\nabla \cdot \{\nabla[e^{ik \cdot r} u_{nk}(r)]\} = \nabla \cdot \{ik e^{ik \cdot r} u_{nk}(r) + e^{ik \cdot r} \nabla u_{nk}(r)\} \qquad \text{(B-7)}$$

So we will have:

$$\nabla^2[e^{ik \cdot r} u_{nk}(r)] = (ik)^2 e^{ik \cdot r} u_{nk}(r) + 2ik e^{ik \cdot r} \nabla u_{nk}(r) + e^{ik \cdot r} \nabla^2 u_{nk}(r)$$

As it is known the operator for momentum, p, in quantum mechanics is

$p = \dfrac{\hbar}{i} \nabla$. Substituting in equation (A-5) we will have:

$$(\frac{p^2}{2m} + \frac{\hbar k.p}{m} + \frac{\hbar^2 k^2}{2m} + V)u_{nk} = E_{nk} u_{nk} \qquad \text{(B-8)}$$

Which is equation (2-40). Thus it is shown that substituting (2-39) in equation (2-38) will result in equation (2-40).

Appendix C: The Solver Programs

%1D ELECTRONIC BAND STRUCTURE SOLVER

```
clc;
close all;
clear all;

Number_of_Terms=20
Num_of_Steps=20

tic
```

% THE OBJECTIVE OF THIS PROGRAM IS TO FIND THE BAND DIAGRAM OF KRONIG
% PENNEY LATTICE USING THE PSUEDOPOTENTIAL METHOD. THE PROGRAM WILL BE
% CONSISTED OF THE FOLLOWING PARTS:

% FIRST PART: ENTERING THE BASIC PHYSICAL PROPERTIES OF THE LATTICE AS
% CONSTANTS.

% SECOND PART: TO INTRODUCE THE PSEUDOPOTENTIAL THAT WE ARE GOING TO START
% OUR ITERATION WITH.

% THIRD PART: IN THIS PART WE HAVE TO SOLVE THE SCHRODINGER EQUATION FOR
% THE BULK MATERIAL. THE PREFERRED WAY TO SOLVE THIS EQUATION IS TO USE THE
% BLOCH THEOREM AND SOLVE ONLY FOR ONE CELL. TO SOLVE FOR THE CELL WE WILL
% TRY THE PLANE WAVE EXPANTION METHOD TO SOLVE THE SCHRODINGER EQUATION.

% FORTH PART: WE WILL FIND THE CHARGE DENSITY FUNCTION USING THE WAVE
% FUNCTION THAT WE HAVE FOUND IN THE LAST PART.

```
% FIFTH PART: THE POISON EQUATION WILL BE SOLVED USING THE
CHARGE DENSITY
% FUNCTION.

% WE SHALL ITERATE BETWEEN PART THREE TO PART FIVE UNTIL WE
HAVE THE BEST
% PSUEDOPOTENTIAL WITH A GOOD LEVEL OF ACCURACY.

%%%%%%%%%%%%%%%%%%%%%%%%%%%%%%%%%%%%%%%%%%
% FIRST PART


global a EPSILON_R ee z EPSILON_0


a=2.2e-10;          %LATTICE CONSTANT
EPSILON_0=8.854e-12;  %ELECTRICAL PERMITTIVITY OF FREE SPACE--
S^4A^2/m^3Kg

ee = 1.6e-19;       %ELECTRIC CHARGE UNIT

h_bar = 1.056e-34    %PLANK'S CONSTANT-- m^2Kg/S
m0 = 9.11e-31;      %ELECTRON'S MASS


%%%%%%%%%%%%%%%%%%%%%%%%%%%%%%%%%%%%%%%%%%
% SECOND PART
% THE PSEUDOPOTENTIAL FUNCTION IS IN v_pp_final.m AND HERE WE TRY
TO FIND THE
% FOURIER SERIES OF THE v_pp_final FUNCTION.

step_y=a/2000
y=-a/2:step_y:a/2;
%figure(1)
%grid on
%plot(y,v_pp_final(y));

len_y=length(y);
int=1;
%Number_of_Terms=20

c_l=zeros(1,2*Number_of_Terms+1);

for l=-Number_of_Terms:Number_of_Terms
   for intemp= 1:len_y-1
```

```
        c_l(l+Number_of_Terms+1)=c_l(l+Number_of_Terms+1)+...
          ((v_pp_final(y(intemp)))*exp(-i*(2*pi*l/a)*y(intemp))+...
          v_pp_final(y(intemp+1))*...
          exp(-i*(2*pi*l/a)*y(intemp+1)))/2)*step_y;
    end
end


c_l=(1/a).*c_l;

%figure(2)
%grid on
%plot([-Number_of_Terms:Number_of_Terms],real(c_l),'*');


%%%%%%%%%%%%%%%%%%%%%%%%%%%%%%%%%%%%%%%%%
% THIRD PART
% THE SCHRODINGER EQUATION IS SOLVED ANALYTHICALLY AND THE
RESULTS ARE A
% SET OF ALGEBRIC EQUATIONS WHICH HAVE TO BE SOLVED AND THE
SOLUTION TO
% THEM WILL BE USED TO PRODUCE THE RESULTS OF THE SCHRODINGER
EQUATION.
% THE METHOD THAT IS USED ANALYTHICALLY TO SIMPLIFY THE
SCHRODINGER
% EQUATION IS PLANE WAVE EXPANSION METHOD.

% ACCORDING TO THE ANALYTICAL ALGEBRIC EQUATIONS WE FIRST TRY
TO GENERATE
% THE RIGHT HAND SIDE MATRIX WHICH WILL BE MULTIPLIED BY THE
COEFFICIENTS
% VECTOR OF WAVE FUNCTION.


Mxrght=zeros(Number_of_Terms+1);

for rw=1:Number_of_Terms+1
    for clmn=1:Number_of_Terms+1
        Mxrght(rw,clmn)=c_l(rw+Number_of_Terms+1-clmn);
    end
end
```

```
% ACCORDING TO THE ANALYTICAL ALGEBRIC EQUATIONS WE WILL
MAKE THE LEFT
% HAND SIDE MATRIX. THE MATRIX WILL BE A DIAGONAL MATRIX.

%Num_of_Steps=20
step_k=pi/((Num_of_Steps/2)*a);
aa=zeros(Number_of_Terms+1,Num_of_Steps+1);
evec=zeros(Number_of_Terms+1,Number_of_Terms+1,Num_of_Steps+1)

for k=-pi/a:step_k:pi/a
    FastMx=Mxrght;
    for rw=1:Number_of_Terms+1
        FastMx(rw,rw)=FastMx(rw,rw)+(h_bar^2/(2*m0))*((2*pi*(rw-
(Number_of_Terms/2+1))/a)+k)^2;
    end

[evec(:,Number_of_Terms+1,Num_of_Steps+1),aa(:,round(k/step_k)+Num_of_Steps/2+
1)]=eig(FastMx);
end

%FOURTH PART AND FIFTH PART

oldro=zeros(1,2*Number_of_Terms+1);
oldro(1)=1;
newro=zeros(1,2*Number_of_Terms+1);

while (relative(oldro,newro)>.005)

    oldro=newro;
    newro=0;
    evcnum=0;

    for Kx=(-pi/a):step_k:(pi/a)
        %This part generates the eigen
        %vectors. no info about eigen
        %values needed at this time.
        %EigVals used here only for
        %avoiding errors. it will be used
        %later for band structure ploting.

        rw=0;
        FastMx=Mxrght;
        evcnum=evcnum+1;
```

```
    for Lcntr=-Number_of_Terms:Number_of_Terms    %Calculating the wave
functions

        rw=rw+1;
        Mxrght(rw,rw)=Mxrght(rw,rw)+...
            HbM*Kx*(4*pi*Lcntr/a+Kx);

    end

    [evec(:,:,EigVecsNum),aa]=eig(Mxrght);

    end
end
end



for evcnum=1:(Num_of_Steps+1)   %Calculating the new
    for vselect=1:MxSize         %density function
        smallro=0;
        SingleVec=evec(:,vselect,evcnum);
        for LL=-Number_of_Terms:Number_of_Terms
            for ll=-Number_of_Terms:Number_of_Terms

                smallro(LL)=smallro(LL)+...
                    SingleVec((ll+Number_of_Terms))*...
                    conj(SingleVec((ll-LL));
            end
        end
    end
    newro=newro+smallro;
end


c_l_T=c_l+c_hartree(NewDen)+c_xc(NewDen);


rw=0;
%Row number reset to 0 for the
%total general matrix generation

for LL=-Number_of_Terms:Number_of_Terms
    %This loop generates the matrix
    %from the total fourier coefficients
```

184

```
    rw=rw+1;
    clmn=0;
    for ll=-L_Flag:L_Flag

        clmn=clmn+1;

        Mxrght(rw,clmn)=c_1_T(LL-ll+Number_of_Terms+1);

    end
end


end



% Plotting


vbandnum=0;
vflag=0;

while (vbandnum<(Number_of_Terms+1)) & (vflag==0)
    vbandnum=vbandnum+1;
    vbandtester=0;
    for jk=1:(Num_of_Steps+1)
        vbandtester=vbandtester+aa(vbandnum,jk);
    end
    if vbandtester>0
        vbandnum=vbandnum-1;
        vflag=1;
    end
end


figure(3)
hold on
grid on
set(gcf,'position',[50,100,850,600]) %[500,100,420,620])%
xlabel('\itk.a\rm/\pi (#)','fontsize',11)
ylabel('Energy (eV)','fontsize',11)
```

185

```
title({['Energy Band Structure of Kronig-Penney Lattice No. 2 Using
'];[int2str(Number_of_Terms), ' Fourier Coefficients and ',int2str(Num_of_Steps),' \itk
Sampling Points']},'fontsize',11)


aa=aa./(1.6e-19);
step_kk=step_k*a/pi;
kk=[-1:step_kk:1];

for tempnum=1:vbandnum+1
plot(kk,aa(tempnum,:),'s-','MarkerSize',4,'MarkerFaceColor','b')
end

toc

%%%%%%%%%%%%%%%%%%%%%%%%%%%%%%%%%%%%%%%%%%

function vpp = v_pp(x)

global a EPSILON_R ee z EPSILON_0

tempnum1 = a/2;
tempnum2 = tempnum1/1.1; %a/100;
const = (z * ee^2)/(4*pi*EPSILON_0);

LL=length(x);

for dd = 1:LL
   if (x(dd)>=-tempnum1) & (x(dd)<-tempnum2)
      %vpp(dd) = -const/abs(x(dd));
      vpp(dd)=0;
   elseif (x(dd)>=-tempnum2) & (x(dd)<=tempnum2)
      %vpp(dd)=(1.5*const/tempnum2^5)*x(dd)^4-(2.5*const/tempnum2^3)*x(dd)^2;
      vpp(dd) = -100*1.6e-19;
   elseif (x(dd)<=tempnum1) & (x(dd)>tempnum2)
      %vpp(dd) = -const/x(dd);
      vpp(dd)=0;
   else
      vpp(dd)=0;
   end
end

%%%%%%%%%%%%%%%%%%%%%%%%%%%%%%%%%%%%%%%%%%
```

```
function vppfinal = v_pp_final(x)

global a EPSILON_R ee z EPSILON_0

LLL=length(x);

for ddd = 1:LLL

    %vppfinal(ddd) = v_pp(x(ddd)-a/10) + v_pp(x(ddd)+a/10) + v_pp(x(ddd)+ a/7);
    vppfinal(ddd)=v_pp(x(ddd));

end

%%%%%%%%%%%%%%%%%%%%%%%%%%%%%%%%%%%%%%%%%%

function rel = relative(new,old)

x1=old.-new;
dif=0;
old2=0;
for iii=1:length(old)
    dif=dif+x1(i)^2;
    old2=old2+old(i)^2;
end

rel=sqrt(dif/old2);

end

%%%%%%%%%%%%%%%%%%%%%%%%%%%%%%%%%%%%%%%%%%


%3D Crystal Electronic Band Structure Solver

%The main function of this program at this point is to calculate the energy
%band structure of the bulk silicon. there are provisions in the program to
%make the unit cell's of simple cubic, BCC, FCC, and diamond lattice
%structures, however, the pseudopotential chosen in this program has not
%been proven to be effective for all materials although it might work for
%them. the pseudopotential and the lattice constants as well as other
%individual physical properties are set to be those of silicon. the
%program's inputs are the physical properties of silicon, the no. fourier
%coefficients to be used, and the number of wave vector sampling points.
%although the number of divisions in the unit cell for integral
```

187

%calculations is changable it is recomanded that this number is set so that
%the accuracy of the integrals are not affected. this number should be
%chosen based on the lattice constant and rate of change of the potentials
%that are present in the first step. This number is set to be near the
%minimum number that keeps the suitable accuracy levels for silicon. this
%number can be changed if any other material is going to be analysed using
%this solver. the plotting part is also a part that is designed for diamond
%materials and should be changed if any other material with a non-diamond
%lattice is going to be analized.

```
clc;
close all;
clear all;




%%%%%%%%%%%%%%%%%%%%%%%%%%%%%%%%%%%%%%%%%%%%
% CONSTANTS

disp('****************************************************************');
disp('****************************************************************');

tic

global PPRad const CoEff1 CoEff2 a b c


a = 5.431e-10;              %LATTICE CONSTANT
b = 5.431e-10;              %LATTICE CONSTANT
c = 5.431e-10;              %LATTICE CONSTANT

disp('a=b=c=');disp(a);

EPSILON_0=8.854e-12;            %ELECTRICAL PERMITTIVITY
                   %OF FREE SPACE-- S^4A^2/m^3Kg
EPSILON_R = 11.7;           %Silicon DIELECTRIC CONSTANT-- #


ee = 1.6e-19;              %ELECTRIC CHARGE UNIT
zz = 4;                 %SILCON ATOMIC NUMBER-core electrons - #
```

```
h_bar = 1.056e-34;              %PLANK'S CONSTANT-- m^2Kg/S
m0 = 9.11e-31;                  %ELECTRON'S MASS


const = (zz * ee^2)/(4*pi*EPSILON_0);   %Constant used for potential energy
PPRad = ((a+b+c)/3)/2.5;        %Cut-off radius
CoEff1=(1.5*const/PPRad^5);         %Core pseudopotential Coefficients
CoEff2=(2.5*const/PPRad^3);         %Core pseudopotential Coefficients
HbM=(h_bar^2)/(2*m0);           %h_bar^2 over 2m0


MODE=1                      % MODE=1 IS DIAMOND
                           % MODE=2 IS FCC
                           % MODE=3 IS BCC
                           % MODE=4 IS SIMPLE CUBIC



%%%%%%%%%%%%%%%%%%%%%%%%%%%%%%%%%%%%%%%%%%%%%


Num_of_Terms=6              %No. of Fourier coefficients, not
                           %including the 0th term


C_Devider=30;              %No. Divisions of space for integrating

STEPX=a/C_Devider;
XA=-a/2:STEPX:a/2;

STEPY=b/C_Devider;
YA=-b/2:STEPY:b/2;

STEPZ=c/C_Devider;
ZA=-c/2:STEPZ:c/2;

[XB,YB,ZB]=meshgrid(XA,YA,ZA);      %Creating the space using meshgrid


ALPHA=zeros(2*Num_of_Terms+1,2*Num_of_Terms+1,2*Num_of_Terms+1);
                   %ALPHA: the array to keep the
                   %fourier coefficients in.
VPP_Mx=v_pp_final_3D(XB,YB,ZB,MODE);    %the descrete final VPP in the space
```

```
for SL=-Num_of_Terms:Num_of_Terms      %This loops calculate the coefficients
    for SM=-Num_of_Terms:Num_of_Terms
        for SN=-Num_of_Terms:Num_of_Terms

        F_INTEGRAL=VPP_Mx .* exp(-i*2*pi*(SL*XB/a+SM*YB/b+SN*ZB/c));

        ALPHA(SL+Num_of_Terms+1,SM+Num_of_Terms+1,...
            SN+Num_of_Terms+1)=sum(sum(sum(F_INTEGRAL)));
                        %Sum uses the CPU powers and does
                        %not add up the numbers one by one
                        %instead it does the maximum
                        %additions possible with the
                        %present CPU at the same time

        end
    end
end


ALPHA=ALPHA/(C_Devider^3);         %the final amounts of the
                        %coefficients are found here
                        %instead of the divisions being
                        %done one by one they are done
                        %based on the powers of the present
                        %CPU because they are done in
                        %matrix format

clear F_INTEGRAL                %the data that is not needed is
                        %deleted for added free memory
                        %and increased efficiency.



%%%%%%%%%%%%%%%%%%%%%%%%%%%%%%%%%%%%%%%%%%%
%%%% Making the matrix for eigenvalue problem


MxSize=(Num_of_Terms+1)^3;         %Column and row size of the matrix
Mx1=zeros(MxSize);                %Starting up the general matrix
                        %which will be later modified
                        %for each k point

L_Flag=Num_of_Terms/2;
```

```
M_Flag=Num_of_Terms/2;
N_Flag=Num_of_Terms/2;


rw=0;                           %Row number reset to 0 for the
                                %general matrix generation

for LL=-L_Flag:L_Flag           %This loop generates the matrix
   for MM=-M_Flag:M_Flag            %from the fourier coefficients
     for NN=-N_Flag:N_Flag
       rw=rw+1;
       clmn=0;
       for ll=-L_Flag:L_Flag
          for mm=-M_Flag:M_Flag
             for nn=-N_Flag:N_Flag

             clmn=clmn+1;

             Mx1(rw,clmn)=ALPHA(LL-ll+Num_of_Terms+1,...
                MM-mm+Num_of_Terms+1,NN-nn+Num_of_Terms+1);

             end
          end
       end

     end
   end
end


%%%%%%%%%%%%%%%%%%%%%%%%%%%%%%%%%%%%%%%%%%%%%%%%
%%%% Making the matrices for eigenvalue problems


Num_of_K_Steps=10;              %the number of k sampling points
                                %in each direction.
STEP_Kx=(2*pi/a)/Num_of_K_Steps;      %Step size in X direction
STEP_Ky=(2*pi/b)/Num_of_K_Steps;      %Step size in Y direction
STEP_Kz=(2*pi/c)/Num_of_K_Steps;      %Step size in Z direction


L_Flag=Num_of_Terms/2;          %Flags for the loop
M_Flag=Num_of_Terms/2;          %Flags for the loop
N_Flag=Num_of_Terms/2;          %Flags for the loop
```

```
rw=0;                      %Row number set to zero

for Lcntr=-L_Flag:L_Flag        %adding a common part to the
   for Mcntr=-M_Flag:M_Flag         %general matrix before starting to
      for Ncntr=-N_Flag:N_Flag      %generate each single matrix for
                       %eigen value problem
         rw=rw+1;

         Mx1(rw,rw)=Mx1(rw,rw)+...
            HbM*((4*pi^2)*((Lcntr/a)^2+(Mcntr/b)^2+(Ncntr/c)^2));

      end
   end
end


%%%%%%%%%%%%%%%%%%%%%%%%%%%%%%%%%%%%%%%%%%%%%%%%%
%%%% convergance loop

OldDen=zeros(1,2* Num_of_Terms+1);
OldDen(1)=1;
NewDen=zeros(1,2* Num_of_Terms+1);

while (RELERR(NewDen,OldDen)>.0075)


EigVecs=zeros(MxSize,MxSize,(Num_of_K_Steps+1)^3);
EigVals=zeros(MxSize,MxSize);
EigVecsNum=0;

for Kx=(-pi/a):STEP_Kx:(pi/a)       %This part generates the eigen
   for Ky=(-pi/a)):STEP_Ky:(pi/a)      %vectors. no info about eigen
      for Kz=(-pi/a)):STEP_Kz:(pi/a) %values needed at this time.
                     %EigVals used here only for
                     %avoiding errors. it will be used
                     %later for band structure ploting.

         rw=0;
         LastMx=Mx1;
         EigVecsNum=EigVecsNum+1;

         for Lcntr=-L_Flag:L_Flag   %Calculating the wave functions
```

192

```
            for Mcntr=-M_Flag:M_Flag
                for Ncntr=-N_Flag:N_Flag

                    rw=rw+1;
                    LastMx(rw,rw)=LastMx(rw,rw)+...
                        HbM*Kx*(4*pi*Lcntr/a+Kx)+...
                        HbM*Ky*(4*pi*Mcntr/a+Ky)+...
                        HbM*Kz*(4*pi*Ncntr/a+Kz);


                end
            end
        end


        [EigVecs(:,:,EigVecsNum),EigVals]=eig(LastMx);


    end
  end
end


OldDen=NewDen;
NewDen=0;

for EigVecsNum=1:(Num_of_K_Steps+1)^3   %Calculating the new
    for VecSelector=1:MxSize          %density function
        SingleDen=0;
        SingleVec=EigVecs(:,VecSelector,EigVecsNum);
        for LL=-Num_of_Terms:Num_of_Terms
            for MM=-Num_of_Terms:Num_of_Terms
                for NN=-Num_of_Terms:Num_of_Terms
                    for ll=-Num_of_Terms:Num_of_Terms
                        for mm=-Num_of_Terms:Num_of_Terms
                            for nn=-Num_of_Terms:Num_of_Terms
                                SingleDen(LL,MM,NN)=SingleDen(LL,MM,NN)+...
                                    SingleVec((ll+Num_of_Terms)*...
                                    Num_of_Terms^2+(mm+Num_of_Terms)*...
                                    Num_of_Terms+(ll+Num_of_Terms)+1)*...
                                    conj(SingleVec((ll-LL)*...
                                    Num_of_Terms^2+(mm-MM)*...
                                    Num_of_Terms+(nn-NN)+1));
                            end
                        end
                    end
                end
            end
        end
```

```
                NewDen=NewDen+SingleDen;
            end
        end
    end


ALPHA_T=ALPHA+V_Hart(NewDen)+V_xc(NewDen);



L_Flag=Num_of_Terms/2;
M_Flag=Num_of_Terms/2;
N_Flag=Num_of_Terms/2;



rw=0;                        %Row number reset to 0 for the
                             %total general matrix generation

for LL=-L_Flag:L_Flag            %This loop generates the matrix
    for MM=-M_Flag:M_Flag            %from the total fourier coefficients
        for NN=-N_Flag:N_Flag
            rw=rw+1;
            clmn=0;
            for ll=-L_Flag:L_Flag
                for mm=-M_Flag:M_Flag
                    for nn=-N_Flag:N_Flag

                        clmn=clmn+1;

                        Mx1(rw,clmn)=ALPHA_T(LL-ll+Num_of_Terms+1,...
                            MM-mm+Num_of_Terms+1,NN-nn+Num_of_Terms+1);


                    end
                end
            end

        end
    end
end


end
```

```
% for Kx=0:STEP_Kx:(pi/a)
%    rw=0;
%    LastMx=Mx1;
%    SolNum=SolNum+1;
%    for Lcntr=-L_Flag:L_Flag
%       for Mcntr=-M_Flag:M_Flag
%          for Ncntr=-N_Flag:N_Flag
%             rw=rw+1;
%             LastMx(rw,rw)=LastMx(rw,rw)+HbM*Kx*(4*pi*Lcntr/b+Kx);
%          end
%       end
%    end
%    SolMx(:,SolNum)=eig(LastMx);
% end

% for Kz=(-pi/a):STEP_Kz:(pi/a)
%    rw=0;
%    LastMx=Mx1;
%    SolNum=SolNum+1;
%    for Lcntr=-L_Flag:L_Flag
%       for Mcntr=-M_Flag:M_Flag
%          for Ncntr=-N_Flag:N_Flag
%             rw=rw+1;
%             LastMx(rw,rw)=LastMx(rw,rw)+HbM*Kz*(4*pi*Ncntr/c+Kz);
%          end
%       end
%    end
%    SolMx(:,SolNum)=eig(LastMx);
% end


%%%%%%%%%%%%%%%%%%

%%%%%%%%%%%%%%%%%%%%%%%%%%%%%%%%%%%%%%%%%%%%%%%
%%%% Plotting the Band Structure


% the plotting is done by going over the symmetry points on symmetrical
% directions. the eigen value problems are solved one last time in order to
% get the eigen values which are the energy band structure of the bulk
% silicon. there is no need for eigen vectors in this part of the
% calculations.
```

```
SolMx1=zeros(MxSize,Num_of_K_Steps/2+1);
SolMx2=zeros(MxSize,Num_of_K_Steps/2+1);
SolMx3=zeros(MxSize,Num_of_K_Steps/2+1);
SolMx4=zeros(MxSize,Num_of_K_Steps/2+1);
SolMx5=zeros(MxSize,Num_of_K_Steps/2+1);
SolMx6=zeros(MxSize,Num_of_K_Steps/2+1);
SolMx7=zeros(MxSize,Num_of_K_Steps/2+1);

SolNum=0;


for Kx=(-pi/(2*a)):STEP_Kx/2:0
   rw=0;
   LastMx=Mx1;
   SolNum=SolNum+1;
   for Lcntr=-L_Flag:L_Flag
      for Mcntr=-M_Flag:M_Flag
         for Ncntr=-N_Flag:N_Flag
            rw=rw+1;
            LastMx(rw,rw)=LastMx(rw,rw)+HbM*Kx*(4*pi*Lcntr/a+Kx)+...
               HbM*Kx*(4*pi*Mcntr/a+Kx)+HbM*Kx*(4*pi*Ncntr/a+Kx);
         end
      end
   end
   SolMx1(:,SolNum)=eig(LastMx);
end

SolNum=0;

for Kx=0:STEP_Kx:(pi/a)
   rw=0;
   LastMx=Mx1;
   SolNum=SolNum+1;
   for Lcntr=-L_Flag:L_Flag
      for Mcntr=-M_Flag:M_Flag
         for Ncntr=-N_Flag:N_Flag
            rw=rw+1;
            LastMx(rw,rw)=LastMx(rw,rw)+HbM*Kx*(4*pi*Lcntr/b+Kx);
         end
      end
   end
   SolMx2(:,SolNum)=eig(LastMx);
end
```

196

```
SolNum=0;

for Kx=(-pi/a):STEP_Kx/2:(-pi/(2*a))
   rw=0;
   LastMx=Mx1;
   SolNum=SolNum+1;
   for Lcntr=-L_Flag:L_Flag
      for Mcntr=-M_Flag:M_Flag
         for Ncntr=-N_Flag:N_Flag
            rw=rw+1;
            LastMx(rw,rw)=LastMx(rw,rw)+HbM*Kx*(4*pi*Lcntr/a+Kx)+...
               HbM*Kx*(4*pi*Mcntr/a+Kx)+HbM*Kx*(4*pi*Ncntr/a+Kx);
         end
      end
   end
   SolMx3(:,SolNum)=eig(LastMx);
end

SolNum=0;

for Kx=(3*pi/(2*a)):-STEP_Kx/2:(pi/a)
   rw=0;
   LastMx=Mx1;
   SolNum=SolNum+1;
   for Lcntr=-L_Flag:L_Flag
      for Mcntr=-M_Flag:M_Flag
         for Ncntr=-N_Flag:N_Flag
            rw=rw+1;
            LastMx(rw,rw)=LastMx(rw,rw)+HbM*Kx*(4*pi*Lcntr/a+Kx)+...
               HbM*((2*pi/a)-Kx)*(4*pi*Mcntr/a+((2*pi/a)-Kx))+...
               HbM*((2*pi/a)-Kx)*(4*pi*Ncntr/a+((2*pi/a)-Kx));
         end
      end
   end
   SolMx4(:,SolNum)=eig(LastMx);
end

SolNum=0;

for Kx=(3*pi/(2*a)):STEP_Kx/2:(2*pi/a)
   rw=0;
   LastMx=Mx1;
   SolNum=SolNum+1;
   for Lcntr=-L_Flag:L_Flag
```

```
       for Mcntr=-M_Flag:M_Flag
          for Ncntr=-N_Flag:N_Flag
             rw=rw+1;
             LastMx(rw,rw)=LastMx(rw,rw)+HbM*Kx*(4*pi*Lcntr/a+Kx)+...
                HbM*((2*pi/a)-Kx)*(4*pi*Mcntr/a+((2*pi/a)-Kx))+...
                HbM*((2*pi/a)-Kx)*(4*pi*Ncntr/a+((2*pi/a)-Kx));
          end
       end
    end
    SolMx5(:,SolNum)=eig(LastMx);
end

SolNum=0;

for Kx=(pi/a):-STEP_Kx:0
   rw=0;
   LastMx=Mx1;
   SolNum=SolNum+1;
   for Lcntr=-L_Flag:L_Flag
      for Mcntr=-M_Flag:M_Flag
          for Ncntr=-N_Flag:N_Flag
             rw=rw+1;
             LastMx(rw,rw)=LastMx(rw,rw)+HbM*Kx*(4*pi*Lcntr/a+Kx)+...
                HbM*(pi/a)*(4*pi*Mcntr/a+(pi/a))+...
                HbM*(pi/a)*(4*pi*Ncntr/a+(pi/a));
          end
       end
    end
    SolMx6(:,SolNum)=eig(LastMx);
end

SolNum=0;

for Kx=(2*pi/a):STEP_Kx:(3*pi/a)
   rw=0;
   LastMx=Mx1;
   SolNum=SolNum+1;
   for Lcntr=-L_Flag:L_Flag
      for Mcntr=-M_Flag:M_Flag
          for Ncntr=-N_Flag:N_Flag
             rw=rw+1;
             LastMx(rw,rw)=LastMx(rw,rw)+HbM*Kx*(4*pi*Lcntr/b+Kx);
          end
       end
```

198

```matlab
        end
    SolMx7(:,SolNum)=eig(LastMx);
end



%%%%%%%%%%%%%%%%%%%%%

SolMx1=SolMx1./ee;
SolMx2=SolMx2./ee;
SolMx3=SolMx3./ee;
SolMx4=SolMx4./ee;
SolMx5=SolMx5./ee;
SolMx6=SolMx6./ee;
SolMx7=SolMx7./ee;

STEP_Kx_pi=STEP_Kx/(pi/a);
radical=.75^.5
figure()
hold on
grid on


for tempnum=1:1
    plot(...
        [-radical:STEP_Kx_pi*radical:0],SolMx1(1,[1:Num_of_K_Steps/2+1]),...
        [0:STEP_Kx_pi:1],SolMx2(1,[1:Num_of_K_Steps/2+1]),...
        [0:STEP_Kx_pi:1],SolMx2(2,[1:Num_of_K_Steps/2+1]),...
        [0:STEP_Kx_pi:1],SolMx2(3,[1:Num_of_K_Steps/2+1]),...
        [-radical:STEP_Kx_pi*radical:0],SolMx3(1,[Num_of_K_Steps/2+1:-1:1]),...
        [-radical:STEP_Kx_pi*radical:0],SolMx3(8,[Num_of_K_Steps/2+1:-1:1]),...
        [-radical:STEP_Kx_pi*radical:0],SolMx4(2,[1:Num_of_K_Steps/2+1]),...
        [-radical:STEP_Kx_pi*radical:0],SolMx4(5,[1:Num_of_K_Steps/2+1]),...
        [-radical:STEP_Kx_pi*radical:0],SolMx5(2,[1:Num_of_K_Steps/2+1]),...
        [-6*STEP_Kx_pi*radical:STEP_Kx_pi*radical:0],SolMx5(5,[5:11]),...
        [0:STEP_Kx_pi:1],SolMx6(1,[1:Num_of_K_Steps/2+1]),...
        [0:STEP_Kx_pi:1],SolMx6(5,[1:Num_of_K_Steps/2+1]),...
        [0:STEP_Kx_pi:1],SolMx7(6,[1:Num_of_K_Steps/2+1]));

end


%%%%%%%%%%%%%%%%%%%%%%%%%%%%%%%%%%%%%%%%%%%%%
function vpp = v_pp_3D(x,y,z)
```

```
global PPRad const CoEff1 CoEff2


rr=(x.^2+y.^2+z.^2).^(0.5);

vpp=-const./rr;

vpp(rr<PPRad)=(CoEff1.*rr(rr<PPRad).^4-CoEff2.*rr(rr<PPRad).^2);

%vpp=rr-1e-16-rr;

% if rr>PPRad
%    vpp=-const/rr;
% else
%    vpp=CoEff1*rr.^4-CoEff2*rr.^2;
% end
%%%%%%%%%%%%%%%%%%%%%%%%%%%%%%%%%%%%%%%%%%%%%%%
function vppfinal = v_pp_final_3D(x,y,z,mode)

global a b c

% MODE=1 IS DIAMOND
% MODE=2 IS FCC
% MODE=3 IS BCC
% MODE=4 IS SIMPLE CUBIC

%vppfinal can be any function of v_pp_3D
if mode==1

%     vppfinal=v_pp_3D(x-a/8,y-b/8,z-c/8)+v_pp_3D(x+a/8,y+b/8,z+c/8)+...
%        v_pp_3D(x-a/8+a,y-b/8,z-c/8)+v_pp_3D(x+a/8+a,y+b/8,z+c/8)+...
%        v_pp_3D(x-a/8-a,y-b/8,z-c/8)+v_pp_3D(x+a/8-a,y+b/8,z+c/8)+...
%        v_pp_3D(x-a/8,y-b/8+b,z-c/8)+v_pp_3D(x+a/8,y+b/8+b,z+c/8)+...
%        v_pp_3D(x-a/8,y-b/8-b,z-c/8)+v_pp_3D(x+a/8,y+b/8-b,z+c/8)+...
%        v_pp_3D(x-a/8+a,y-b/8+b,z-c/8)+v_pp_3D(x+a/8+a,y+b/8+b,z+c/8)+...
%        v_pp_3D(x-a/8-a,y-b/8+b,z-c/8)+v_pp_3D(x+a/8-a,y+b/8+b,z+c/8)+...
%        v_pp_3D(x-a/8-a,y-b/8-b,z-c/8)+v_pp_3D(x+a/8-a,y+b/8-b,z+c/8)+...
%        v_pp_3D(x-a/8+a,y-b/8-b,z-c/8)+v_pp_3D(x+a/8+a,y+b/8-b,z+c/8)+...
%        v_pp_3D(x-a/8+a/2,y-b/8+b/2,z-c/8)+v_pp_3D(x+a/8+a/2,y+b/8+b/2,z+c/8)+...
%        v_pp_3D(x-a/8-a/2,y-b/8+b/2,z-c/8)+v_pp_3D(x+a/8-a/2,y+b/8+b/2,z+c/8)+...
%        v_pp_3D(x-a/8-a/2,y-b/8-b/2,z-c/8)+v_pp_3D(x+a/8-a/2,y+b/8-b/2,z+c/8)+...
%        v_pp_3D(x-a/8+a/2,y-b/8-b/2,z-c/8)+v_pp_3D(x+a/8+a/2,y+b/8-b/2,z+c/8)+...
%        v_pp_3D(x-a/8,y-b/8,z-c/8+c)+v_pp_3D(x+a/8,y+b/8,z+c/8+c)+...
```

```
%        v_pp_3D(x-a/8+a,y-b/8,z-c/8+c)+v_pp_3D(x+a/8+a,y+b/8,z+c/8+c)+...
%        v_pp_3D(x-a/8-a,y-b/8,z-c/8+c)+v_pp_3D(x+a/8-a,y+b/8,z+c/8+c)+...
%        v_pp_3D(x-a/8,y-b/8+b,z-c/8+c)+v_pp_3D(x+a/8,y+b/8+b,z+c/8+c)+...
%        v_pp_3D(x-a/8,y-b/8-b,z-c/8+c)+v_pp_3D(x+a/8,y+b/8-b,z+c/8+c)+...
%        v_pp_3D(x-a/8+a,y-b/8+b,z-c/8+c)+v_pp_3D(x+a/8+a,y+b/8+b,z+c/8+c)+...
%        v_pp_3D(x-a/8-a,y-b/8+b,z-c/8+c)+v_pp_3D(x+a/8-a,y+b/8+b,z+c/8+c)+...
%        v_pp_3D(x-a/8-a,y-b/8-b,z-c/8+c)+v_pp_3D(x+a/8-a,y+b/8-b,z+c/8+c)+...
%        v_pp_3D(x-a/8+a,y-b/8-b,z-c/8+c)+v_pp_3D(x+a/8+a,y+b/8-b,z+c/8+c)+...
%        v_pp_3D(x-a/8+a/2,y-b/8+b/2,z-
c/8+c)+v_pp_3D(x+a/8+a/2,y+b/8+b/2,z+c/8+c)+...
%        v_pp_3D(x-a/8-a/2,y-b/8+b/2,z-c/8+c)+v_pp_3D(x+a/8-
a/2,y+b/8+b/2,z+c/8+c)+...
%        v_pp_3D(x-a/8-a/2,y-b/8-b/2,z-c/8+c)+v_pp_3D(x+a/8-a/2,y+b/8-
b/2,z+c/8+c)+...
%        v_pp_3D(x-a/8+a/2,y-b/8-b/2,z-c/8+c)+v_pp_3D(x+a/8+a/2,y+b/8-
b/2,z+c/8+c)+...
%        v_pp_3D(x-a/8,y-b/8,z-c/8-c)+v_pp_3D(x+a/8,y+b/8,z+c/8-c)+...
%        v_pp_3D(x-a/8+a,y-b/8,z-c/8-c)+v_pp_3D(x+a/8+a,y+b/8,z+c/8-c)+...
%        v_pp_3D(x-a/8-a,y-b/8,z-c/8-c)+v_pp_3D(x+a/8-a,y+b/8,z+c/8-c)+...
%        v_pp_3D(x-a/8,y-b/8+b,z-c/8-c)+v_pp_3D(x+a/8,y+b/8+b,z+c/8-c)+...
%        v_pp_3D(x-a/8,y-b/8-b,z-c/8-c)+v_pp_3D(x+a/8,y+b/8-b,z+c/8-c)+...
%        v_pp_3D(x-a/8+a,y-b/8+b,z-c/8-c)+v_pp_3D(x+a/8+a,y+b/8+b,z+c/8-c)+...
%        v_pp_3D(x-a/8-a,y-b/8+b,z-c/8-c)+v_pp_3D(x+a/8-a,y+b/8+b,z+c/8-c)+...
%        v_pp_3D(x-a/8-a,y-b/8-b,z-c/8-c)+v_pp_3D(x+a/8-a,y+b/8-b,z+c/8-c)+...
%        v_pp_3D(x-a/8+a,y-b/8-b,z-c/8-c)+v_pp_3D(x+a/8+a,y+b/8-b,z+c/8-c)+...
%        v_pp_3D(x-a/8+a/2,y-b/8+b/2,z-c/8-c)+v_pp_3D(x+a/8+a/2,y+b/8+b/2,z+c/8-
c)+...
%        v_pp_3D(x-a/8-a/2,y-b/8+b/2,z-c/8-c)+v_pp_3D(x+a/8-a/2,y+b/8+b/2,z+c/8-
c)+...
%        v_pp_3D(x-a/8-a/2,y-b/8-b/2,z-c/8-c)+v_pp_3D(x+a/8-a/2,y+b/8-b/2,z+c/8-c)+...
%        v_pp_3D(x-a/8+a/2,y-b/8-b/2,z-c/8-c)+v_pp_3D(x+a/8+a/2,y+b/8-b/2,z+c/8-
c)+...
%        v_pp_3D(x-a/8+a/2,y-b/8,z-c/8+c/2)+v_pp_3D(x+a/8+a/2,y+b/8,z+c/8+c/2)+...
%        v_pp_3D(x-a/8-a/2,y-b/8,z-c/8+c/2)+v_pp_3D(x+a/8-a/2,y+b/8,z+c/8+c/2)+...
%        v_pp_3D(x-a/8,y-b/8+b/2,z-c/8+c/2)+v_pp_3D(x+a/8,y+b/8+b/2,z+c/8+c/2)+...
%        v_pp_3D(x-a/8,y-b/8-b/2,z-c/8+c/2)+v_pp_3D(x+a/8,y+b/8-b/2,z+c/8+c/2)+...
%        v_pp_3D(x-a/8+a/2,y-b/8+b,z-
c/8+c/2)+v_pp_3D(x+a/8+a/2,y+b/8+b,z+c/8+c/2)+...
%        v_pp_3D(x-a/8-a/2,y-b/8+b,z-c/8+c/2)+v_pp_3D(x+a/8-
a/2,y+b/8+b,z+c/8+c/2)+...
%        v_pp_3D(x-a/8-a/2,y-b/8-b,z-c/8+c/2)+v_pp_3D(x+a/8-a/2,y+b/8-
b,z+c/8+c/2)+...
%        v_pp_3D(x-a/8+a/2,y-b/8-b,z-c/8+c/2)+v_pp_3D(x+a/8+a/2,y+b/8-
b,z+c/8+c/2)+...
```

201

```
%       v_pp_3D(x-a/8+a,y-b/8+b/2,z-
c/8+c/2)+v_pp_3D(x+a/8+a,y+b/8+b/2,z+c/8+c/2)+...
%       v_pp_3D(x-a/8-a,y-b/8+b/2,z-c/8+c/2)+v_pp_3D(x+a/8-
a,y+b/8+b/2,z+c/8+c/2)+...
%       v_pp_3D(x-a/8-a,y-b/8-b/2,z-c/8+c/2)+v_pp_3D(x+a/8-a,y+b/8-
b/2,z+c/8+c/2)+...
%       v_pp_3D(x-a/8+a,y-b/8-b/2,z-c/8+c/2)+v_pp_3D(x+a/8+a,y+b/8-
b/2,z+c/8+c/2)+...
%       v_pp_3D(x-a/8+a/2,y-b/8,z-c/8-c/2)+v_pp_3D(x+a/8+a/2,y+b/8,z+c/8-c/2)+...
%       v_pp_3D(x-a/8-a/2,y-b/8,z-c/8-c/2)+v_pp_3D(x+a/8-a/2,y+b/8,z+c/8-c/2)+...
%       v_pp_3D(x-a/8,y-b/8+b/2,z-c/8-c/2)+v_pp_3D(x+a/8,y+b/8+b/2,z+c/8-c/2)+...
%       v_pp_3D(x-a/8,y-b/8-b/2,z-c/8-c/2)+v_pp_3D(x+a/8,y+b/8-b/2,z+c/8-c/2)+...
%       v_pp_3D(x-a/8+a/2,y-b/8+b,z-c/8-c/2)+v_pp_3D(x+a/8+a/2,y+b/8+b,z+c/8-
c/2)+...
%       v_pp_3D(x-a/8-a/2,y-b/8+b,z-c/8-c/2)+v_pp_3D(x+a/8-a/2,y+b/8+b,z+c/8-
c/2)+...
%       v_pp_3D(x-a/8-a/2,y-b/8-b,z-c/8-c/2)+v_pp_3D(x+a/8-a/2,y+b/8-b,z+c/8-c/2)+...
%       v_pp_3D(x-a/8+a/2,y-b/8-b,z-c/8-c/2)+v_pp_3D(x+a/8+a/2,y+b/8-b,z+c/8-
c/2)+...
%       v_pp_3D(x-a/8+a,y-b/8+b/2,z-c/8-c/2)+v_pp_3D(x+a/8+a,y+b/8+b/2,z+c/8-
c/2)+...
%       v_pp_3D(x-a/8-a,y-b/8+b/2,z-c/8-c/2)+v_pp_3D(x+a/8-a,y+b/8+b/2,z+c/8-
c/2)+...
%       v_pp_3D(x-a/8-a,y-b/8-b/2,z-c/8-c/2)+v_pp_3D(x+a/8-a,y+b/8-b/2,z+c/8-c/2)+...
%       v_pp_3D(x-a/8+a,y-b/8-b/2,z-c/8-c/2)+v_pp_3D(x+a/8+a,y+b/8-b/2,z+c/8-c/2);



vppfinal=v_pp_3D(x,y,z)+...
    v_pp_3D(x+a/2,y+b/2,z)+v_pp_3D(x+a/2,y-b/2,z)+...
    v_pp_3D(x-a/2,y+b/2,z)+v_pp_3D(x-a/2,y-b/2,z)+...
    v_pp_3D(x+a/2,y,z+c/2)+v_pp_3D(x,y+b/2,z+c/2)+...
    v_pp_3D(x-a/2,y,z+c/2)+v_pp_3D(x,y-b/2,z+c/2)+...
    v_pp_3D(x+a/2,y,z-c/2)+v_pp_3D(x,y+b/2,z-c/2)+...
    v_pp_3D(x-a/2,y,z-c/2)+v_pp_3D(x,y-b/2,z-c/2)+...
    v_pp_3D(x+a/4,y+b/4,z+c/4)+...
    v_pp_3D(x+a/4+a/2,y+b/4+b/2,z+c/4)+v_pp_3D(x+a/4+a/2,y+b/4-b/2,z+c/4)+...
    v_pp_3D(x+a/4-a/2,y+b/4+b/2,z+c/4)+v_pp_3D(x+a/4-a/2,y+b/4-b/2,z+c/4)+...
    v_pp_3D(x+a/4+a/2,y+b/4,z+c/4+c/2)+v_pp_3D(x+a/4,y+b/4+b/2,z+c/4+c/2)+...
    v_pp_3D(x+a/4-a/2,y+b/4,z+c/4+c/2)+v_pp_3D(x+a/4,y+b/4-b/2,z+c/4+c/2)+...
    v_pp_3D(x+a/4+a/2,y+b/4,z+c/4-c/2)+v_pp_3D(x+a/4,y+b/4+b/2,z+c/4-c/2)+...
```

202

```
                v_pp_3D(x+a/4-a/2,y+b/4,z+c/4-c/2)+v_pp_3D(x+a/4,y+b/4-b/2,z+c/4-c/2);


  elseif mode==2
    vppfinal=v_pp_3D(x,y,z)+...
        v_pp_3D(x+a/2,y+b/2,z)+v_pp_3D(x+a/2,y-b/2,z)+...
        v_pp_3D(x-a/2,y+b/2,z)+v_pp_3D(x-a/2,y-b/2,z)+...
        v_pp_3D(x+a/2,y,z+c/2)+v_pp_3D(x,y+b/2,z+c/2)+...
        v_pp_3D(x-a/2,y,z+c/2)+v_pp_3D(x,y-b/2,z+c/2)+...
        v_pp_3D(x+a/2,y,z-c/2)+v_pp_3D(x,y+b/2,z-c/2)+...
        v_pp_3D(x-a/2,y,z-c/2)+v_pp_3D(x,y-b/2,z-c/2);
  elseif mode==3
    vppfinal=v_pp_3D(x,y,z)+...
        v_pp_3D(x+a/2,y+b/2,z+c/2)+v_pp_3D(x-a/2,y+b/2,z+c/2)+...
        v_pp_3D(x+a/2,y-b/2,z+c/2)+v_pp_3D(x-a/2,y-b/2,z+c/2)+...
        v_pp_3D(x+a/2,y+b/2,z-c/2)+v_pp_3D(x-a/2,y+b/2,z-c/2)+...
        v_pp_3D(x+a/2,y-b/2,z-c/2)+v_pp_3D(x-a/2,y-b/2,z-c/2);
  elseif mode==4
    vppfinal=v_pp_3D(x,y,z)+v_pp_3D(x+a,y,z)+...
        v_pp_3D(x,y+b,z)+v_pp_3D(x,y,z+c)+...
        v_pp_3D(x-a,y,z)+v_pp_3D(x,y-b,z)+...
        v_pp_3D(x,y,z-c);
end


%%%%%%%%%%%%%%%%%%%%%%%%%%%%%%%%%%%%%%%%%%%%%%%%


function relerr = RELERR(new,old)

x1=old.-new;
DIFSUM=0;
ALLSUM=0;
for iii=1:length(old)
  DIFSUM=DIFSUM+x1(i)^2;
  ALLSUM=ALLSUM+old(i)^2;
end

relerr=sqrt(DIFSUM/ALLSUM);

end


%%%%%%%%%%%%%%%%%%%%%%%%%%%%%%%%%%%%%%%%%%%%%%%%
```